TRACKING THE RESPONSE OF HYDROCARBON-DEGRADING MICROORGANISMS TO ENVIRONMENTAL FORCINGS

by

TITO DAVID PEÑA MONTENEGRO

(Under the Direction of Samantha B. Joye and Jonathan Arnold)

ABSTRACT

In April 2010, the Deepwater Horizon caused a large magnitude perturbation on native microbial communities across the huge range of fragile marine ecosystems located in the Gulf of Mexico. This study explored perturbations on microbial communities across a range of habitats similar to those impacted by the Deepwater Horizon spill. Our assessment utilized bioinformatics approaches taking advantage of coupled -omic datasets and publicly available information. Specifically, we developed and applied the concept of Differentially Expressed Meta pangenome to describe species-specific responses of microbial drivers to chemical exposure. This technique provided insight into contrasting strategies to respond performed by *Colwellia* and *Marinobacter*. Further inspection of microbial responses to oil-dispersant perturbations involved the application of RNA:DNA ratios (LRD score). This approach showed potential niche adaptations based on the carbon source, replication, and biosynthesis rates, especially for large carbon-degraders and methylovores. Finally, we explore the perturbations in a preconditioned microcosm allowing us to compare the variability of the microbial communities and expected functional fingerprint.

INDEX WORDS: Chemical Dispersant; Corexit 9500A; *Colwellia*; *Marinobacter*, Deepwater Horizon; DEM-pangenome

TRACKING THE RESPONSE OF HYDROCARBON-DEGRADING MICROORGANISMS TO ENVIRONMENTAL FORCINGS

by

TITO DAVID PEÑA MONTENEGRO

BSc, Universidad de los Andes, Colombia, 2010

BSc, Universidad de los Andes, Colombia, 2012

MSc, Universidad de los Andes, Colombia, 2013

A Dissertation Submitted to the Graduate Faculty of The University of Georgia in Partial Fulfillment of the Requirements for the Degree

DOCTOR OF PHILOSOPHY

ATHENS, GEORGIA

2021

TRACKING THE RESPONSE OF HYDROCARBON-DEGRADING MICROORGANISMS TO ENVIRONMENTAL FORCINGS

TITO DAVID PEÑA MONTENEGRO

Major Professor:	Samantha B. Joye
Co-Major Professor:	Jonathan Arnold
Committee:	A. Murat Eren
	William B. Whitman
	Heinz-Bernd Schüttler

Electronic Version Approved:

Ron Walcott
Dean of the Graduate School
The University of Georgia
May 2021

DEDICATION

To God, for his infinite love.

A ti, Santísima Virgen María por acompañarme a cada instante.

A ti, Abuelita. Siempre te extraño.

To my husband, Andrew. Love of my life.

A mi familia, pilares de mi vida. Gracias mamita Yaneth. Gracias hermanitos Aurita y Alex. Gracias Guillermo, por su amor paternal. Gracias, tías Tere y Elita. Gracias a todos aquellos amigos que también son *mi familia*. Maru, Mari, Leynar, El Grupito, Enmanuel. Los llevo siempre en mi corazón.

To Ramisito, Sachita, Leito, Junior, Zeus… I promise to continue working for a better life for all dogs, cats, and living beings in this beautiful home called Earth.

To the memory of those who couldn't finish their dissertations.

To the memory of those who couldn't see their dream come true.

To the forgotten children in the mountains and streets of Colombia. I promise to continue working for a life in peace, justice, and dignity that you deserve.

.

.

IT'S COLOMBIA, NOT COLUMBIA.

☆ ☿ ♂ ☾ ♄ ♀ ☆

ACKNOWLEDGEMENTS

I express deep gratitude to my advisors Dr. Samantha “Mandy” Joye and Dr. Jonathan Arnold. I want to thank the continuous support of my committee members, Dr. Joye’s Research Group, Dr. Arnold’s Research Group, Institute of Bioinformatics, and the Department of Marine Sciences for their support and insight.

Dr. Murat “Meren” Eren, and the Meren Lab, I am deeply grateful for the countless times you helped me during my research.

Dr. Sara Kleindienst, Cathrine Shepard, and every member involved in the research projects. Your time and effort were essential for our projects.

Thank you, Dr. Guangchao Zhuang, Dr. Jason Westrich, Dr. Mary-Kate Rogener, Sarah Harrison, Rachael Storo, Andy Montgomery, and those who helped me through my time in the lab. I enjoyed working with you.

Thanks to The Carpentries node at UGA for the experience I acquired as a Data Scientist and as a Teacher.

Thanks to the *Sociedad de Doctores e Investigadores de Colombia* (Society of Doctors and Researchers of Colombia). I am grateful to be one of your *co*-founders, and I hope to continue working together for a better future for Colombian Scientists throughout the world.

TABLE OF CONTENTS

CHAPTER 1

INTRODUCTION

The Gulf of Mexico (hereafter referred to as "The Gulf") is a 1.6 million km^2 ocean basin bordered by the United States, Mexico, and Cuba in which marine species are under threats of overfishing, habitat loss, and pollution (Adams, Hernandez, and Cato, 2004). Salt marshes, mangrove forests, oyster reefs, seagrasses, barrier islands, corals, pelagic *Sargassum* clusters, hydrocarbon seeps, and chemosynthetic communities are some of the ecologically important habitats found in the Gulf ecosystem (Love, Baldera, Yeung, and Robbins, 2013). However, the spatial distribution and intensity of threats across these habitats can vary extensively given the disparity of conservation efforts of the involved governmental jurisdictions (Strongin et al., 2020). Activities such as industrial drilling and dredging can permanently change habitats due to the release of trapped chemicals and gasses into the environment as well as changes in the seabed topography (Jetz, Wilcove, and Dobson, 2007). Compared to the Caribbean, industrial development in the Gulf is more severe, and the oil and gas industry has had a major influence on ecosystem modifications (Turner and Rabalais, 2019).

Although pollution in the Gulf is comparable to measurements reported in the Western Atlantic and the Greater Caribbean (Hyland et al., 2003; Jambeck et al., 2015), petrochemical disasters is only one of the threats that impose danger to the Gulf ecosystem. The discharge of nutrients and agrochemicals from the Mississippi River is a major source of pollution for the Gulf, which leads to frequent large-scale eutrophication events and anoxic zones in the northern

Gulf (Mitsch et al., 2001). The effects of these hypoxic events on the marine communities are not completely clear, but reported increases in net surface productivity and deficiencies in benthic oxygen levels can significantly alter species composition and ecosystem function (Davis, 2017).

Large scale, automated fisheries are another threat in Gulf. Currently, high-value species as groupers, snappers, and tunas are legally targeted since the prescription of the Magnuson-Stevens Act. Since then, nearly 90% of all United States managed fisheries had been maintained at sustainable levels, although concerns remain, including barriers to full reporting, poor administrative practices, and corruption (Strongin et al., 2020). In fact, overfishing and illegal fishing are still happening even in marine protected areas (Mangin et al., 2018; Pala, Zhang, Zhuang, and Allen, 2018). Since 1983, the United States-Mexico Fisheries Cooperation program has promoted communication and cooperation efforts to protect endangered species, management, and enforcement of guidelines for commercial and recreational fishing activities. However, further steps are needed in this aspect, especially considering the changing political environments and associated policies (Strongin et al., 2020). In addition, extensive coastal developments and shoreline modification continue to impact species dependent on sensitive, near-shore environments, such as seagrass and estuarine habitats. Species in these habitats may be experiencing more severe impacts from habitat loss compared to outside of the Gulf (Archambault, Rivot, Savina, and Le Pape, 2018; Waycott et al., 2009). With more than 50 million people living along the Gulf coastline, near-shore habitats are often the most severely degraded (Halpern et al., 2008).

As described above, the Gulf is constantly under multiple threats that may lead to severe and irreversible habitat degradation. Anthropogenic activities can introduce petroleum into the

environment at high rates, on the scale of 1.6×10^7 L day^{-1}, or much higher rates when a major oil spill occurs (Reddy et al., 2012). In 2010, the Deepwater Horizon (DWH) drilling platform sank, and the riser pump was severed, releasing $9.94 \times 10^8 - 1.11 \times 10^9$ L of oil from the Macondo well into the northern Gulf of Mexico (S. B. Joye, 2015; McNutt et al., 2012). The well was finally capped in July 2010, accounting for at least 102,000 dead birds across 93 species, 15,000 reported cases of other deceased wildlife, 94.7 million to 1.6 billion dollar loss to the Gulf's commercial fishing industry (Bureau of Ocean Energy Management, 2016; US Fish and Wildlife Service, 2011), 84 days of the uncontrolled blowout, and 5,000,000 barrels of oil released to the Gulf (S. B. Joye, 2015). During the emergency, a fraction of hydrocarbons (including CH_4) was subsequently dissolved and dispersed throughout the Gulf via physical mixing in deepwater plumes (Reddy et al., 2012).

Unfortunately, the DWH event is a tale of two spills. To facilitate the degradation of the oil discharged into the Gulf, approximately 8 million L of dispersant were applied at the wellhead and to surface waters (Kujawinski et al., 2011). The majority of dispersant application (56%) was applied to affected surface areas with aircrafts and vessels, while the remaining volume (44%) was applied directly at the discharging wellhead at 1500 m with a remotely operated vehicle (CRRC, RPI, and NOAA, 2012). Incubation experiments evaluated the effect of oil and dispersants on microbial community composition by the application of oil-amended water accommodated fractions (WAFs), chemically enhanced (i.e., chemically dispersed oil) WAFs (CEWAFs). Biochemical measurements overtime for these microcosms have provided preliminary insights into the effects of these amendments on the microbial communities and on their capabilities to tolerate and degrade oil (Singer et al., 2000).

Kleindienst et al. (2015) conducted microcosms experiments to achieve comparable chemical exposure levels of those observed at the DWH plume using water collected from 1178 m depth at the natural seep site GC600 in the Gulf. Their study revealed that dispersant application negatively impacted the microbial community's ability to degrade oil. After one week, incubations performed and incubated at 5°C led to an increase in *Colwellia* abundance from 1% to 26-43% in CEWAF (± nutrients) and in Corexit-only treatments (Kleindienst et al., 2015). A single amplified genome (SAG) of *Colwellia* isolated from a DWH plume indicated genes for denitrification and a capability to degrade gaseous and aromatic hydrocarbons (Mason, Han, Woyke, and Jansson, 2014). *Colwellia* species isolated from deepwater plumes were able to assimilate ethane, propane, and benzene, as evidenced by ^{13}C label incorporation experiments (Redmond and Valentine, 2012). Kleindienst et al. (2015) also determined that the WAF amendment treatment showed an increased abundance of *Marinobacter* from 2% to 42%, and in *Cycloclasticus* from 12% to 23% (Kleindienst et al., 2015). *Marinobacter* can degrade linear and branched aliphatic compounds, as well as polycyclic aromatics (Dombrowski et al., 2016).

Similar studies have reported isolates from oil-exposed beach samples with strain-specific response to oil, dispersed oil, and dispersant treatments, where notably *Marinobacter* was almost entirely inhibited after exposure to environmentally relevant dispersant concentrations (1 to 10 mg/L) (Hamdan and Fulmer, 2011; Kleindienst et al., 2015; Overholt et al., 2016). However, other studies showed different diversity shifts in microbial communities for similar experimental conditions (Techtmann et al., 2017). Whether changes in the microbial community composition and resulting community function are due to toxicity of the dispersant and/or dispersed oil, or if the shift instead results from competition between heterotrophs exposed to different carbon sources, has remained unclear (Kleindienst et al., 2015).

Comparing these studies, microbial degraders were present in very small numbers in uncontaminated Gulf environments until a significant growth was observed upon the influx of oil and other pollutants. With their ability to utilize hydrocarbon as energy source, the rare biosphere became quickly abundant colonizers accounting up to 90% of the community (Karthikeyan et al., 2019; Kleindienst et al., 2016). Similarly, native populations that typically dominated healthy Gulf ecosystems declined in abundance after the DWH spill and even remained altered for at least a year (Huettel et al., 2018; Newell et al., 2014). Most of these observations could not be documented by culture-dependent methods. Therefore, omics methods revealed keystone species that should be targeted for future studies (Joye and Kostka, 2020). Alongside the sampling scheme in the Kleindienst et al. (2015) experiment, RNA extractions were obtained and processed (Peña-Montenegro et al., 2020). This dataset provided an extraordinary opportunity to determine species-specific responses at transcriptome level given environmental perturbations. **Chapter 2** covers the transcriptomic analysis from the perspective of Differentially Expressed Metapangenomes (DEMpangenomes). This work aimed to identify functional aspects that are remarkably unique and linked to the core and accessory pangenome of two of the most important microbial drivers of this experiment, *Colwellia* and *Marinobacter*. This approach is fundamentally important to understand species-specific adaptation of the rare biosphere to environmental perturbations.

Metatranscriptomic and other -omic analyses have allowed the discovery of new microbial drivers in oil-contaminated marine environments. Similarly, new genes have been assigned to hydrocarbon degradation metabolic pathways (Joye and Kostka, 2020). For instance, major known classes of microbes (e.g., *Bacteroidetes*) have been found to exhibit a previously unknown potential for hydrocarbon biodegradation (Liu and Liu, 2013). Kleindienst et al. (2015)

experiment provided 16S rRNA gene sequencing data paired to a metatranscriptomic library. These datasets provided a unique opportunity to identify cooperative microbial communities that would be overlooked by examining only individual expression profiles or population diversity markers alone (Mason et al., 2012). In **Chapter 3**, the repertoire of responses of the entire community to the exposure of oil and dispersants is analyzed through the estimation of biological activity rates by linking expression and replication signals. This approach allowed us to identify fast and slow responders to the perturbations in the environment. Finally, by inspecting role-dependent taxonomic groups, we identified the association of selective transcriptional signatures of megaviruses, suggesting their potential regulatory role.

The time of application and sampling during the microcosm experiments is a factor that could have influenced the metatranscriptomic and the biochemical fingerprint of the microbial communities, as it will be described in chapters 2 and 3, as well as noted previously (Kleindienst et al., 2015; Peña-Montenegro et al., 2020). However, microbial communities at the time of the DWH spill could have been disproportionately affected across the spatial distribution of dispersants over the oil slick and their vicinities. For instance, plume-affected sites exhibited significantly reduced diversity compared to surrounding, unaffected sites (Hazen et al., 2010; Kleindienst et al., 2016; Valentine et al., 2010).

To assess the influence of site-specific exposure of Corexit 9500A on microbial communities for Gulf surface water samples, Shepard (2019) carried out preconditioning experiments that revealed nutrient-dependent trends of bacterial production and potential hydrocarbon oxidation rates. 16S rRNA gene sequencing data was also generated along with the Shepard experiment. Further inspection of 16S community composition generated a meta-functional snapshot of the microbial community, as shown in **Chapter 4**.

Overarching conclusions of this dissertation are presented in **Chapter 5**, as well as considerations for future research.

1.1 References

Adams, C. M., Hernandez, E., and Cato, J. C. (2004). The economic significance of the Gulf of Mexico related to population, income, employment, minerals, fisheries and shipping. *Ocean & Coastal Management*, *47*(11–12), 565–580. https://doi.org/10.1016/j.ocecoaman.2004.12.002

Archambault, B., Rivot, E., Savina, M., and Le Pape, O. (2018). Using a spatially structured life cycle model to assess the influence of multiple stressors on an exploited coastal-nursery-dependent population. *Estuarine, Coastal and Shelf Science, 201*, 95–104. https://doi.org/10.1016/j.ecss.2015.12.009

Bureau of Ocean Energy Management. (2016). *2016 Update of Occurrence Rates for Offshore Oil Spills.* Retrieved from https://www.bsee.gov/sites/bsee.gov/files/osrr-oil-spill-response-research/1086aa.pdf

CRRC, RPI, and NOAA. (2012). *The Future of Dispersant Use in Oil Spill Response Initiative.* Retrieved from https://crrc.unh.edu/sites/crrc.unh.edu/files/media/docs/Workshops/dispersant_future_11/Dispersant_Initiative_FINALREPORT.pdf

Davis, J. E. (2017). Booms, Blooms, and Doom: The Life of the Gulf of Mexico Dead Zone. *Alabama Review*, *70*(2), 156–170. https://doi.org/10.1353/ala.2017.0011

Dombrowski, N., Donaho, J. A., Gutierrez, T., Seitz, K. W., Teske, A. P., and Baker, B. J. (2016). Reconstructing metabolic pathways of hydrocarbon-degrading bacteria from the

Deepwater Horizon oil spill. *Nature Microbiology*, 16057. https://doi.org/10.1038/nmicrobiol.2016.57

Halpern, B. S., Walbridge, S., Selkoe, K. A., Kappel, C. V., Micheli, F., D'Agrosa, C., … Watson, R. (2008). A Global Map of Human Impact on Marine Ecosystems. *Science*, *319*(5865), 948–952. https://doi.org/10.1126/science.1149345

Hamdan, L., and Fulmer, P. (2011). Effects of COREXIT® EC9500A on bacteria from a beach oiled by the Deepwater Horizon spill. *Aquatic Microbial Ecology*, *63*(2), 101–109. https://doi.org/10.3354/ame01482

Hazen, T. C., Dubinsky, E. A., DeSantis, T. Z., Andersen, G. L., Piceno, Y. M., Singh, N., … Mason, O. U. (2010). Deep-sea oil plume enriches indigenous oil-degrading Bacteria. *Science*, *330*(6001), 204–208. https://doi.org/10.1126/science.1195979

Huettel, M., Overholt, W. A., Kostka, J. E., Hagan, C., Kaba, J., Wells, Wm. B., and Dudley, S. (2018). Degradation of Deepwater Horizon oil buried in a Florida beach influenced by tidal pumping. *Marine Pollution Bulletin*, *126*, 488–500. https://doi.org/10.1016/j.marpolbul.2017.10.061

Hyland, J. L., Balthis, W. L., Engle, V. D., Long, E. R., Paul, J. F., Summers, J. K., and Van Dolah, R. F. (2003). Incidence of Stress in Benthic Communities Along the U.S. Atlantic and Gulf of Mexico Coasts within Different Ranges of Sediment Contamination from Chemical Mixtures. In B. D. Melzian, V. Engle, M. McAlister, S. Sandhu, and L. K. Eads (Eds.), *Coastal Monitoring through Partnerships* (pp. 149–161). Dordrecht: Springer Netherlands. https://doi.org/10.1007/978-94-017-0299-7_14

Jambeck, J. R., Geyer, R., Wilcox, C., Siegler, T. R., Perryman, M., Andrady, A., … Law, K. L. (2015). Plastic waste inputs from land into the ocean. *Science*, *347*(6223), 768–771. https://doi.org/10.1126/science.1260352

Jetz, W., Wilcove, D. S., and Dobson, A. P. (2007). Projected Impacts of Climate and Land-Use Change on the Global Diversity of Birds. *PLoS Biology*, *5*(6), e157. https://doi.org/10.1371/journal.pbio.0050157

Joye, S. B. (2015). Deepwater Horizon, 5 years on. *Science*, *349*(6248), 592–593. https://doi.org/10.1126/science.aab4133

Joye, S., and Kostka, J. E. (2020). *Microbial Genomics of the Global Ocean System: Report on an American Academy of Microbiology (Academy), The American Geophysical Union (AGU), and The Gulf of Mexico Research Initiative (GoMRI) Colloquium held on 9 and 10 April 2019*. American Society for Microbiology. https://doi.org/10.1128/AAMCol.Apr.2019

Karthikeyan, S., Rodriguez-R, L. M., Heritier-Robbins, P., Kim, M., Overholt, W. A., Gaby, J. C., … Konstantinidis, K. T. (2019). "Candidatus *Macondimonas diazotrophica*", a novel gammaproteobacterial genus dominating crude-oil-contaminated coastal sediments. *The ISME Journal*, *13*(8), 2129–2134. https://doi.org/10.1038/s41396-019-0400-5

Kleindienst, S., Grim, S., Sogin, M., Bracco, A., Crespo-Medina, M., and Joye, S. B. (2016). Diverse, rare microbial taxa responded to the Deepwater Horizon deep-sea hydrocarbon plume. *The ISME Journal*, *10*(2), 400–415. https://doi.org/10.1038/ismej.2015.121

Kleindienst, S., Seidel, M., Ziervogel, K., Grim, S., Loftis, K., Harrison, S., … Joye, S. B. (2015). Chemical dispersants can suppress the activity of natural oil-degrading

microorganisms. *Proceedings of the National Academy of Sciences*, *112*(48), 14900–14905. https://doi.org/10.1073/pnas.1507380112

Kujawinski, E. B., Kido Soule, M. C., Valentine, D. L., Boysen, A. K., Longnecker, K., and Redmond, M. C. (2011). Fate of Dispersants Associated with the Deepwater Horizon Oil Spill. *Environmental Science & Technology*, *45*(4), 1298–1306. https://doi.org/10.1021/es103838p

Liu, Z., and Liu, J. (2013). Evaluating bacterial community structures in oil collected from the sea surface and sediment in the northern Gulf of Mexico after the *Deepwater Horizon* oil spill. *MicrobiologyOpen*, *2*(3), 492–504. https://doi.org/10.1002/mbo3.89

Love, M., Baldera, A., Yeung, C., and Robbins, C. (2013). *The Gulf of Mexico Ecosystem: A Coastal and Marine Atlas*. Ocean Conservancy.

Mangin, T., Cisneros-Mata, M. Á., Bone, J., Costello, C., Gaines, S. D., McDonald, G., … Zapata, P. (2018). The cost of management delay: The case for reforming Mexican fisheries sooner rather than later. *Marine Policy*, *88*, 1–10. https://doi.org/10.1016/j.marpol.2017.10.042

Mason, O. U., Han, J., Woyke, T., and Jansson, J. K. (2014). Single-cell genomics reveals features of a *Colwellia* species that was dominant during the Deepwater Horizon oil spill. *Frontiers in Microbiology*, *5*. https://doi.org/10.3389/fmicb.2014.00332

Mason, O. U., Hazen, T. C., Borglin, S., Chain, P. S. G., Dubinsky, E. A., Fortney, J. L., … Jansson, J. K. (2012). Metagenome, metatranscriptome and single-cell sequencing reveal microbial response to Deepwater Horizon oil spill. *The ISME Journal*, *6*(9), 1715–1727. https://doi.org/10.1038/ismej.2012.59

McNutt, M. K., Camilli, R., Crone, T. J., Guthrie, G. D., Hsieh, P. A., Ryerson, T. B., … Shaffer, F. (2012). Review of flow rate estimates of the Deepwater Horizon oil spill. *Proceedings of the National Academy of Sciences*, *109*(50), 20260–20267. https://doi.org/10.1073/pnas.1112139108

Mitsch, W. J., Day, J. W., Wendell Gilliam, J., Groffman, P. M., Hey, D. L., Randall, G. W., and Wang, N. (2001). Reducing Nitrogen Loading to the Gulf of Mexico from the Mississippi River Basin: Strategies to Counter a Persistent Ecological Problem. *BioScience*, *51*(5), 373. https://doi.org/10.1641/0006-3568(2001)051[0373:RNLTTG]2.0.CO;2

Newell, S. E., Eveillard, D., McCarthy, M. J., Gardner, W. S., Liu, Z., and Ward, B. B. (2014). A shift in the archaeal nitrifier community in response to natural and anthropogenic disturbances in the northern Gulf of Mexico: Archaeal nitrifier community shift in the Gulf of Mexico. *Environmental Microbiology Reports*, *6*(1), 106–112. https://doi.org/10.1111/1758-2229.12114

Overholt, W. A., Marks, K. P., Romero, I. C., Hollander, D. J., Snell, T. W., and Kostka, J. E. (2016). Hydrocarbon-Degrading Bacteria Exhibit a Species-Specific Response to Dispersed Oil while Moderating Ecotoxicity. *Applied and Environmental Microbiology*, *82*(2), 518–527. https://doi.org/10.1128/AEM.02379-15

Pala, A., Zhang, J., Zhuang, J., and Allen, N. (2018). Behavior Analysis of Illegal Fishing in the Gulf of Mexico. *Journal of Homeland Security and Emergency Management*, *15*(1), 20160017. https://doi.org/10.1515/jhsem-2016-0017

Peña-Montenegro, T. D., Kleindienst, S., Allen, A. E., Eren, A. M., McCrow, J. P., Sánchez-Calderón, J. D., … Joye, S. B. (2020). Colwellia *and* Marinobacter *metapangenomes*

reveal species-specific responses to oil and dispersant exposure in deepsea microbial communities [Preprint]. Microbiology. https://doi.org/10.1101/2020.09.28.317438

Reddy, C. M., Arey, J. S., Seewald, J. S., Sylva, S. P., Lemkau, K. L., Nelson, R. K., … Camilli, R. (2012). Composition and fate of gas and oil released to the water column during the Deepwater Horizon oil spill. *Proceedings of the National Academy of Sciences, 109*(50), 20229–20234. https://doi.org/10.1073/pnas.1101242108

Redmond, M. C., and Valentine, D. L. (2012). Natural gas and temperature structured a microbial community response to the Deepwater Horizon oil spill. *Proceedings of the National Academy of Sciences, 109*(50), 20292–20297. https://doi.org/10.1073/pnas.1108756108

Shepard, C. G. (2019). *Nutrient availability modulates the effects of Corexit 9500A on oil biodegradation* (University of Georgia). University of Georgia, Athens, GA, USA. Retrieved from https://getd.libs.uga.edu/pdfs/shepard_cathrine_g_201908_ms.pdf

Singer, M. M., Aurand, D., Bragin, G. E., Clark, J. R., Coelho, G. M., Sowby, M. L., and Tjeerdema, R. S. (2000). Standardization of the Preparation and Quantitation of Water-accommodated Fractions of Petroleum for Toxicity Testing. *Marine Pollution Bulletin, 40*(11), 1007–1016. https://doi.org/10.1016/S0025-326X(00)00045-X

Strongin, K., Polidoro, B., Linardich, C., Ralph, G., Saul, S., and Carpenter, K. (2020). Translating globally threatened marine species information into regional guidance for the Gulf of Mexico. *Global Ecology and Conservation, 23*, e01010. https://doi.org/10.1016/j.gecco.2020.e01010

Techtmann, S. M., Zhuang, M., Campo, P., Holder, E., Elk, M., Hazen, T. C., … Santo Domingo, J. W. (2017). Corexit 9500 enhances oil biodegradation and changes active

bacterial community structure of oil-enriched microcosms. *Applied and Environmental Microbiology, 83*(10), e03462-16, e03462-16. https://doi.org/10.1128/AEM.03462-16

Turner, R. E., and Rabalais, N. N. (2019). The Gulf of Mexico. In *World Seas: An Environmental Evaluation* (pp. 445–464). Elsevier. https://doi.org/10.1016/B978-0-12-805068-2.00022-X

US Fish and Wildlife Service. (2011). *Deepwater Horizon Response Consolidated Fish and Wildlife Collection Report.* Retrieved from https://fws.gov/home/dhoilspill/pdfs/ConsolidatedWildlifeTable041711.pdf

Valentine, D. L., Kessler, J. D., Redmond, M. C., Mendes, S. D., Heintz, M. B., Farwell, C., … Villanueva, C. J. (2010). Propane respiration jump-starts microbial response to a deep oil spill. *Science, 330*(6001), 208–211. https://doi.org/10.1126/science.1196830

Waycott, M., Duarte, C. M., Carruthers, T. J. B., Orth, R. J., Dennison, W. C., Olyarnik, S., … Williams, S. L. (2009). Accelerating loss of seagrasses across the globe threatens coastal ecosystems. *Proceedings of the National Academy of Sciences, 106*(30), 12377–12381. https://doi.org/10.1073/pnas.0905620106

CHAPTER 2

SPECIES-SPECIFIC RESPONSES OF MARINE BACTERIA TO ENVIRONMENTAL PERTURBATION [1]

[1] Peña-Montenegro TD, Kleindienst S, Allen AE, Eren AM, McCrow JP, Sánchez-Calderón JD, Arnold J, Joye SB. To be submitted to *Science*

2.1 Abstract

Environmental perturbations alter the structure and function of microbial communities. Oil spills are a perturbation that requires active measures, like synthetic dispersant application, to minimize impacts. We merged metatranscriptomic libraries with pangenomes to generate **D**ifferentially **E**xpressed **M**etatranscriptomic pangenomes (DEM-pangenomes) for two hydrocarbon degraders to identify species-specific responses to oil and dispersant exposure. The *Colwellia* DEM-pangenome illustrated activation of genes involved in the core and accessory genome, suggesting an opportunistic strategy. *Marinobacter* responded to oil exposure alone; its DEM-pangenome reflected stimulation of mainly accessory genes involved in carbon and lipid metabolism, chemotaxis, and a type IV secretion system. These findings highlight treatment-dependent responses in the metabolism of key microorganisms to perturbations and underscore the utility of the DEM-pangenome approach for assessing and revealing the mechanisms of microbial community response to environmental perturbation.

One-Sentence Summary: Gene expression mapped onto pangenomes show species-specific responses to environmental triggers in microbial populations.

2.2 Main document

The ocean is the Earth's oldest and most dynamic habitat. Ocean microbes form the base of the food web and moderate key ecosystem services (*1*, *2*). They produce half of the Earth's oxygen each year, they sequester carbon via the primary fixation of inorganic carbon into biomass, they modulate global biogeochemical cycles, and they transform and detoxify pollutants (*3*). Marine microbial populations are taxonomically and functionally diverse (*4*). The low abundance "rare biosphere" accounts for a majority of phylogenetic diversity in microbial populations (*5*, *6*) and represents a tremendous repository of metabolic functionality (*7*). Disturbance influences microbial community structure and function in ways that impact the ecosystem services microorganisms provide. Understanding how microbial communities respond to disturbance is a key question in microbial ecology that impacts global ocean biogeochemistry (*8*). Identifying why certain taxa respond to disturbance more effectively than others is a key step towards achieving predictability of the functional capacity of microbial populations and the ecosystem dynamics they mediate.

Oil spills are a frequent perturbation to marine environments, yet much remains to be learned about how these perturbations alter oceanic microbial communities (*9*). We utilized data generated during a laboratory simulation of an oil spill (*10*) to explore how key members of the microbial "rare biosphere" responded to different environmental conditions (***Supplementary Materials***). In April 2010, a catastrophic explosion on the Deepwater Horizon (DWH) drilling rig ultimately sank the platform and initiated an uncontrolled discharge of 4.9 million barrels of crude oil into the Gulf of Mexico over 84 days. A major response measure to the oil spill was the application of seven million liters of synthetic dispersants (Corexit EC9500A and EC9527A) to surface oil slicks and to the discharging wellhead at 1500 m depth (*11*, *12*). Dispersant

application enhanced oil droplet formation and aqueous phase solubilization of oil and aimed to stimulate biodegradation. But, dispersants had negative effects on microbial communities (*10, 13, 14*). A more comprehensive understanding of how dispersants impact microbial populations will advance the understanding of how microbial populations respond to disturbance in general.

We assessed the response of key oil-degrading taxa to dispersant and/or oil exposure in lab microcosms and found that patterns of ecological succession in the lab experiments mirrored those observed in the deepwater oil plumes during the DWH incident (*15–17*), offering powerful insight to the underlying mechanisms of the microbial reaction. Indigenous hydrocarbon degraders occupy the rare biosphere of Gulf waters (*7*) and are primed to respond to hydrocarbon inputs from natural or anthropogenic sources (*9*). Seven weeks after the discharge began, the dominant Oceanospirillales communities shifted to a community dominated by *Cycloclasticus* and *Colwellia* (*18–20*). *Colwellia* is a genus of psychrophilic marine bacteria (*21*) isolated from the Puerto Rico Trench. *Colwellia* spp. responded rapidly *in situ* during the DWH incident (*20, 22*) and in experiments with controlled additions of oil/dispersed oil (*10, 20, 23*). *Marinobacter*, first described in 1992 (*24*), colonizes a broad range of marine habitats (*25*) and is considered a biogeochemical "opportunitroph" (*26*). *Marinobacter* strains degraded alkanes (*27*) and polycyclic aromatic hydrocarbons (PAH) under anoxic conditions during the DWH incident (*28*). Chemical dispersants can inhibit *Marinobacter* sp. (*10, 13, 14, 29*). Recently, Rughöft et al. showed reduced growth and hydrocarbon biodegradation in starved cultures of *Marinobacter* sp. TT1 following Corexit EC9500A exposure, suggesting that nutritional status poises its response to environmental perturbation (*30*). The ecological fitness of *Marinobacter* and *Colwellia*, and other microorganisms, influences their response to environmental perturbation.

Microbial populations underpin biogeochemical cycles across Earth's ecosystem, mediating key processes with global consequences. Perturbation-driven compositional changes in microbial communities can alter their functionality, thus impacting processes at the ecosystem level (*31*). The understanding needed to predict the trajectory and speed of recovery of baseline microbial communities and the strategies they mediate is lacking at present. We used the transcriptional signatures to investigate the ecological role of niche partitioning for *Colwellia* and *Marinobacter* by assessing differentially expressed genes in the context of pangenomes. We refer to the mapping of differentially expressed signals from the metatranscriptome to the pangenome as the "DEM-pangenome" (see *Supplementary Materials*). The DEM-pangenome approach offers a way to begin to identify how and why individual species respond to perturbation in specific ways to promote an unprecedented understanding of ecological disturbance.

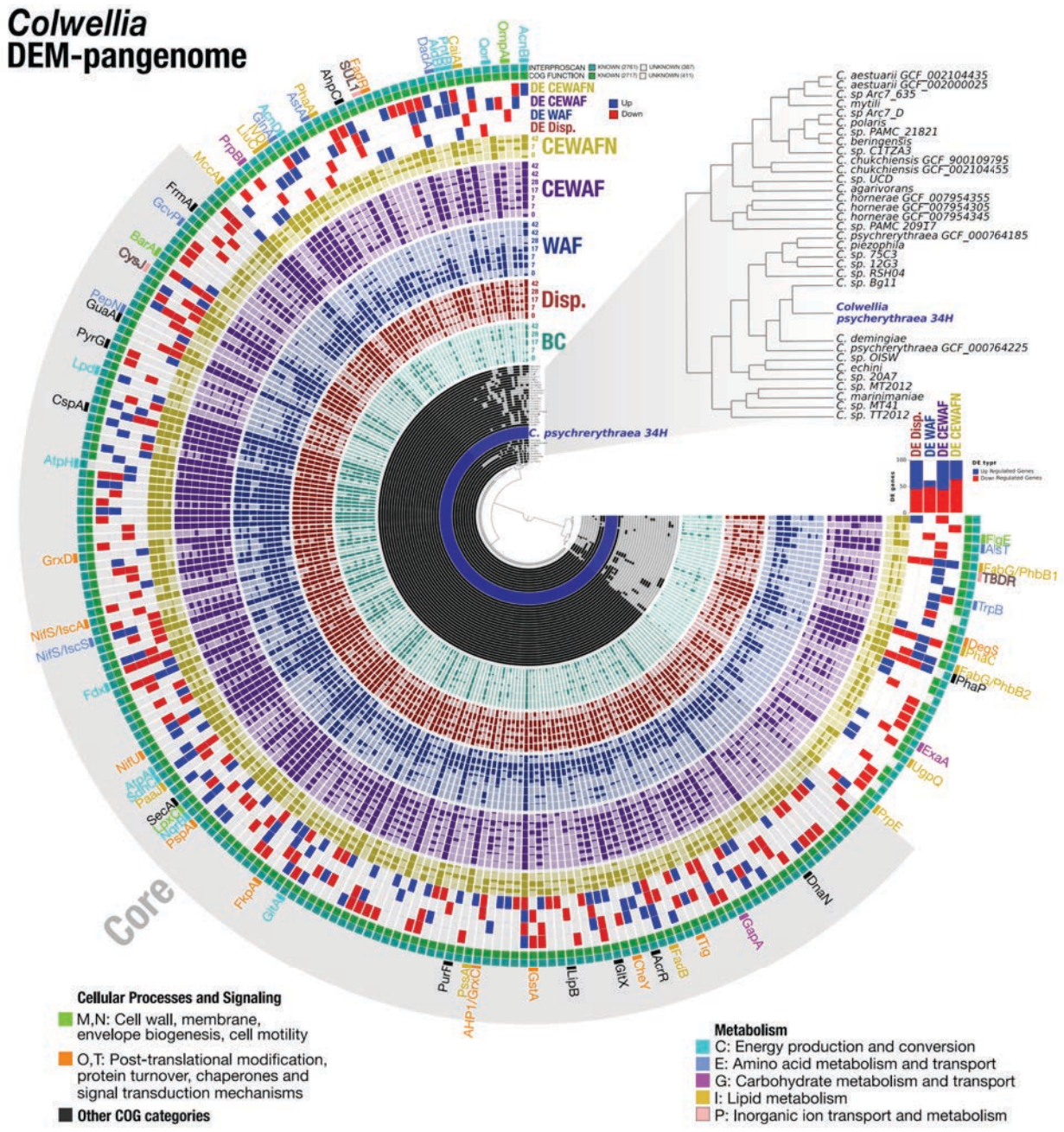
Colwellia
DEM-pangenome
INTERPROSCAN KNOWN (2761) UNKNOWN (387)
COG FUNCTION KNOWN (2717) UNKNOWN (411)
DE CEWAFN
DE CEWAF
DE WAF
DE Disp.
Up
Down
CEWAFN
CEWAF
WAF
Disp.
BC
C. psychrerythraea 34H
C. aestuarii GCF_002104435
C. aestuarii GCF_002000025
C. sp Arc7_635
C. mytili
C. sp Arc7_D
C. polaris
C. sp. PAMC_21821
C. beringensis
C. sp. C1TZA3
C. chukchiensis GCF_900109795
C. chukchiensis GCF_002104455
C. sp. UCD
C. agarivorans
C. hornerae GCF_007954355
C. hornerae GCF_007954305
C. hornerae GCF_007954345
C. sp. PAMC_20917
C. psychrerythraea GCF_000764185
C. piezophila
C. sp. 75C3
C. sp. 12G3
C. sp. RSH04
C. sp. Bg11
Colwellia psycherythraea 34H
C. demingiae
C. psychrerythraea GCF_000764225
C. sp. OISW
C. echini
C. sp. 20A7
C. sp. MT2012
C. marinimaniae
C. sp. MT41
C. sp. TT2012
DE Disp.
DE WAF
DE CEWAF
DE CEWAFN
DE type
Up Regulated Genes
Down Regulated Genes
DE genes
Core
Cellular Processes and Signaling
M,N: Cell wall, membrane, envelope biogenesis, cell motility
O,T: Post-translational modification, protein turnover, chaperones and signal transduction mechanisms
Other COG categories
Metabolism
C: Energy production and conversion
E: Amino acid metabolism and transport
G: Carbohydrate metabolism and transport
I: Lipid metabolism
P: Inorganic ion transport and metabolism

Figure 2.1. Gene detection of metatranscriptomic reads in the context of the core and accessory metapangenome in *Colwellia*. The 33 inner layers show the presence-absence of 225 gene clusters with 6,646 genes identified in 33 *Colwellia* genomes. An expanded dendrogram of the reference genomes based on the distribution of gene clusters using Euclidian distance and ward clustering is shown in the top-right. *Colwellia psycherythraea* 34H (highlighted in blue) was the reference genome that recruited the largest fraction of transcriptomic reads among *Colwellia* genomes. Gene detection profiles of metatranscriptomic reads recruited by *C. psycherythraea* 34H are sorted and color-coded by the corresponding experimental treatment: Biotic Control (BC), Dispersants (Disp.), WAF, CEWAF, and CEWAFN. Time is expressed in days. The next four layers show the presence-absence of differentially expressed (DE) genes with respect to the biotic control treatment are shown in blue (upregulation) and red (downregulation). A stacked bar diagram on the right describes the DE genes counts across treatments following the color code for each of the treatments. The next two layers represent the gene clusters in which at least one gene was functionally annotated with InterproScan or COGs. Finally, the outermost layer shows the protein family name assigned to the DE gene on the corresponding cluster. Protein family names are color-coded by COG categories, as shown in the bottom legends. A detailed description of these DE genes is shown in Supplementary Data 1.

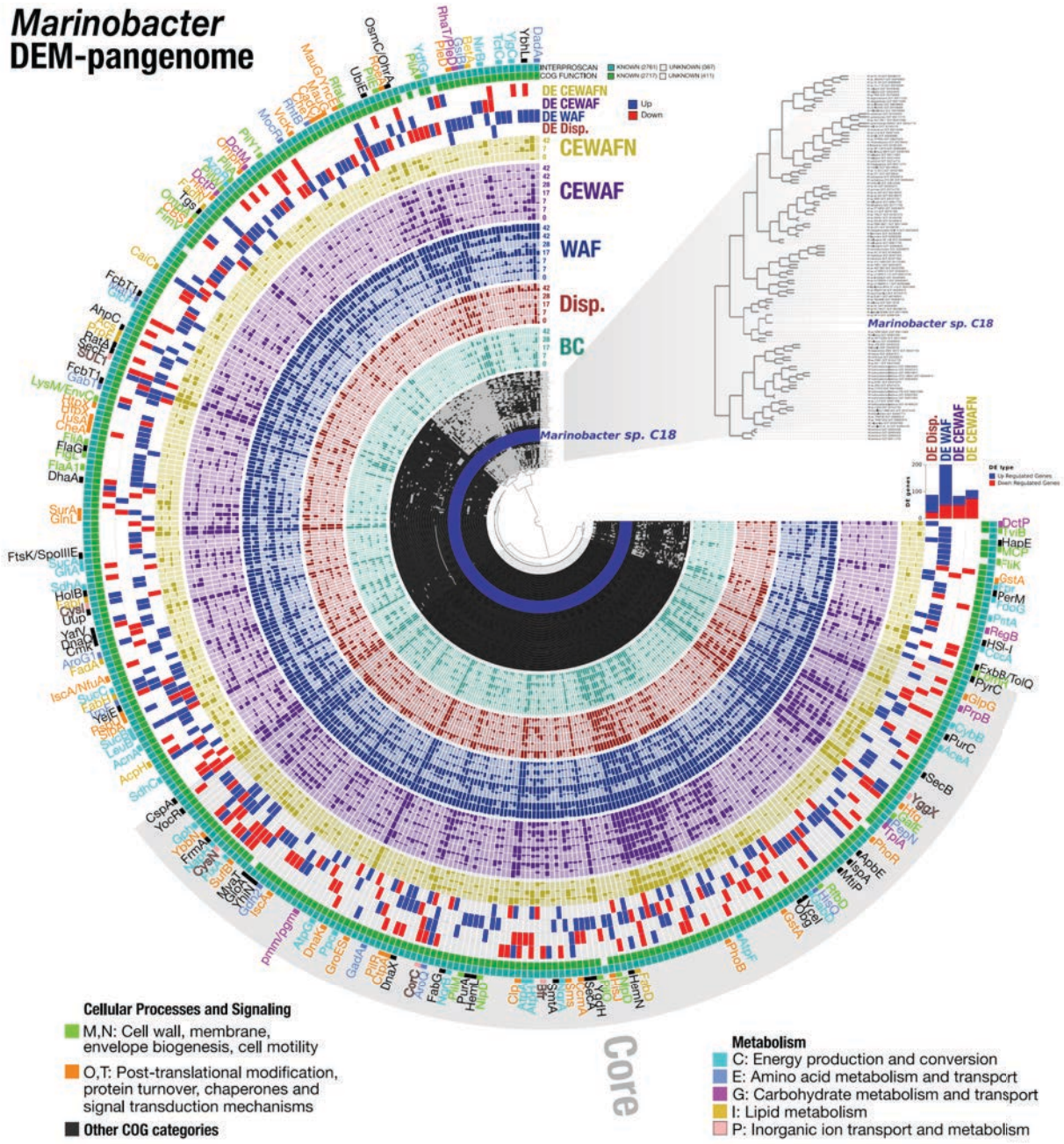
Marinobacter
DEM-pangenome
INTERPROSCAN
COG FUNCTION
KNOWN (2761)
KNOWN (2717)
UNKNOWN (567)
UNKNOWN (611)
DE CEWAFN
DE CEWAF
DE WAF
DE Disp.
Up
Down
CEWAFN
CEWAF
WAF
Disp.
BC
Marinobacter sp. C18
Marinobacter sp. C18
DE Disp.
DE WAF
DE CEWAF
DE CEWAFN
DE type
Up Regulated Genes
Down Regulated Genes
DE genes
Cellular Processes and Signaling
M,N: Cell wall, membrane, envelope biogenesis, cell motility
O,T: Post-translational modification, protein turnover, chaperones and signal transduction mechanisms
Other COG categories
Core
Metabolism
C: Energy production and conversion
E: Amino acid metabolism and transport
G: Carbohydrate metabolism and transport
I: Lipid metabolism
P: Inorganic ion transport and metabolism

Figure 2.2. Gene detection of metatranscriptomic reads in the context of the core and accessory metapangenome in *Marinobacter*. The 113 inner layers show the presence-absence of 342 gene clusters with 35,909 genes identified in 113 *Marinobacter* genomes. An expanded dendrogram of the reference genomes based on the distribution of gene clusters using Euclidian distance and ward clustering is shown in the top-right. *Marinobacter* sp. C18 (highlighted in blue) was the reference genome that recruited the largest fraction of transcriptomic reads among *Marinobacter* genomes. Gene detection profiles of metatranscriptomic reads recruited by *Marinobacter* sp. C18 are sorted and color-coded by the corresponding experimental treatment: Biotic Control (BC), Dispersants (Disp.), WAF, CEWAF, and CEWAFN. Time is expressed in days. The next four layers show the presence-absence of differentially expressed (DE) genes with respect to the biotic control treatment are shown in blue (upregulation) and red (down-regulation). A stacked bar diagram on the right describes the DE genes counts across treatments following the color code for each of the treatments. The next two layers represent the gene clusters in which at least one gene was functionally annotated with InterproScan or COGs. Finally, the outermost layer shows the protein family name assigned to the DE gene on the corresponding cluster. Protein family names are color-coded by COG categories, as shown in the bottom legends. A detailed description of these DE genes is shown in Supplementary Data 1.

Kleindienst et al. (4) documented differences of *Colwellia* and *Marinobacter* abundance in response to different cocktails of organic carbon (*32*, *Supplementary Materials*). This study aimed to discover the underlying mechanisms by assessing differentially expressed (DE) genes in pangenomes. We identified the best reference genome for *Colwellia* and *Marinobacter* and mapped metatranscriptomic libraries to all available complete genomes (NCBI) for these microorganisms (*Supplementary Materials*). The oil-only treatment showed the largest amount of DE genes for *Marinobacter* and the smallest amount of DE genes for *Colwellia* (red and blue histograms in Figures 2.1 and 2.2). In contrast, for *Colwellia*, the largest fraction of DE genes was observed in dispersant-amended treatments*;* the smallest fraction of DE genes for *Marinobacter* occurred in dispersant-amended treatments*.* The distribution of upregulated genes ranged from 37 to 179 for *Marinobacter*; and from 12 to 55 for *Colwellia.* In contrast, the distribution of downregulated genes ranged from 29 to 89 for *Marinobacter*; and from 44 to 63 for *Colwellia*.

To identify species-level functional traits that corresponded to treatment regimes, we co-investigated the abundance, activity, and the gene pool of *Colwellia* and *Marinobacter* populations in the environment. For this, we extended the workflow implemented in Anvi'o for metapangenomics (*33*, *34*) with metatranscriptomics, referred to as the 'DEM-pangenome', and grouped gene clusters that contained at least one DE gene for downstream analyses (Figures 2.1 and 2.2). By merging pangenomics, metagenomics, and metatranscriptomics in the same framework, the DEM-pangenomes reveal the *in situ* relative abundance and activity of environmental populations while exposing the metabolic determinants of environmental response to perturbation.

The *Colwellia* DEM-pangenome (Figure 2.1) included 6,646 gene calls across 225 gene clusters. Gene clusters were grouped into two bins based on their occurrence across genomes: (1) core gene clusters (*n*=155 or 68%), which reflect clusters found in all genomes, and (2) accessory gene clusters (*n*=70 or 31.4%) which reflect clusters found in only a subset of genomes. Most of the gene clusters contained DE genes with functional annotation from InterproScan (*n*=100%) and COGs (*n*=97.3%). The *Marinobacter* DEM-pangenome (Figure 2.2) included 35,909 gene calls across 342 gene clusters. For these organisms, 156 (45.6%) and 186 (54.4%) gene clusters were associated with the core and accessory DEM-pangenome, respectively. Most of the gene clusters contained DE genes with functional annotation from InterproScan (*n*=100%) and COGs (*n*=97.4%).

Colwellia exhibited a robust transcriptomic response in the core DEM-pangenome (Figure 2.1, Supplementary Data 1). Oxidative phosphorylation, energy, and carbohydrate metabolism categories, including genes for components of the TCA cycle, were upregulated in the CEWAF±nutrient treatments (Supplementary Materials). Stress response and folding catalysts genes were also upregulated in the CEWAF treatment. Additional genes related to fatty acid biosynthesis were up-expressed in the CEWAF+nutrient treatment. About 27.3% of upregulated genes in the core DEM-pangenome of *Colwellia* were assigned to the COG categories J, K, and L, associated with genetic information processing (*i.e.*, translation, RNA degradation, replication, and DNA repair), suggesting a rapid response in growth and stress moderation to dispersants. A sub-set of functions in the core DEM-pangenome of *Colwellia* were upregulated in the dispersants-only treatment, reflecting a response only to the carbon components from Corexit, not oil (Figure 2.1, Supplementary Data 1, Supplementary Materials).

The upregulated genes included membrane precursors, two-component sensing systems, and transferases.

The presence of additional nutrients stimulated specific biosynthetic pathways that clustered in *Colwellia*'s accessory DEM-pangenome (Figure 2.1, Supplementary Data 2.1, Supplementary Materials). Upregulated genes in this treatment included those involved in the synthesis of polyhydroxybutyrate, the most common polyhydroxyalkanoate, the largest known group of natural polyesters, and genes required for fatty acid degradation (*35*). Genes encoding for a tryptophan halogenase, which produces a precursor used in the biosynthesis of pyrrolnitrin, an antibiotic, as well as genes involved in membrane transport (Ton-B Dependent Receptor) were upregulated as well. Altogether, these results indicate sophisticated, niche-specific responses for *Colwellia* at the genus level.

Upregulated genes in the accessory DEM-pangenome of *Marinobacter* in the WAF treatment (Figure 2.2, Supplementary Data 2.1, Supplementary Materials) included essential genes involved in carbon and lipid metabolism, stress response genes, amino acid metabolism, and chloroalkane and chloroalkene degradation genes. The latter genes may reflect the metabolism of intermediates of chlorinated aromatics metabolism (*36*). Genes involved in triacylglycerol and wax biosynthesis, sensor kinases, and type IV pilus assembly were also upregulated.

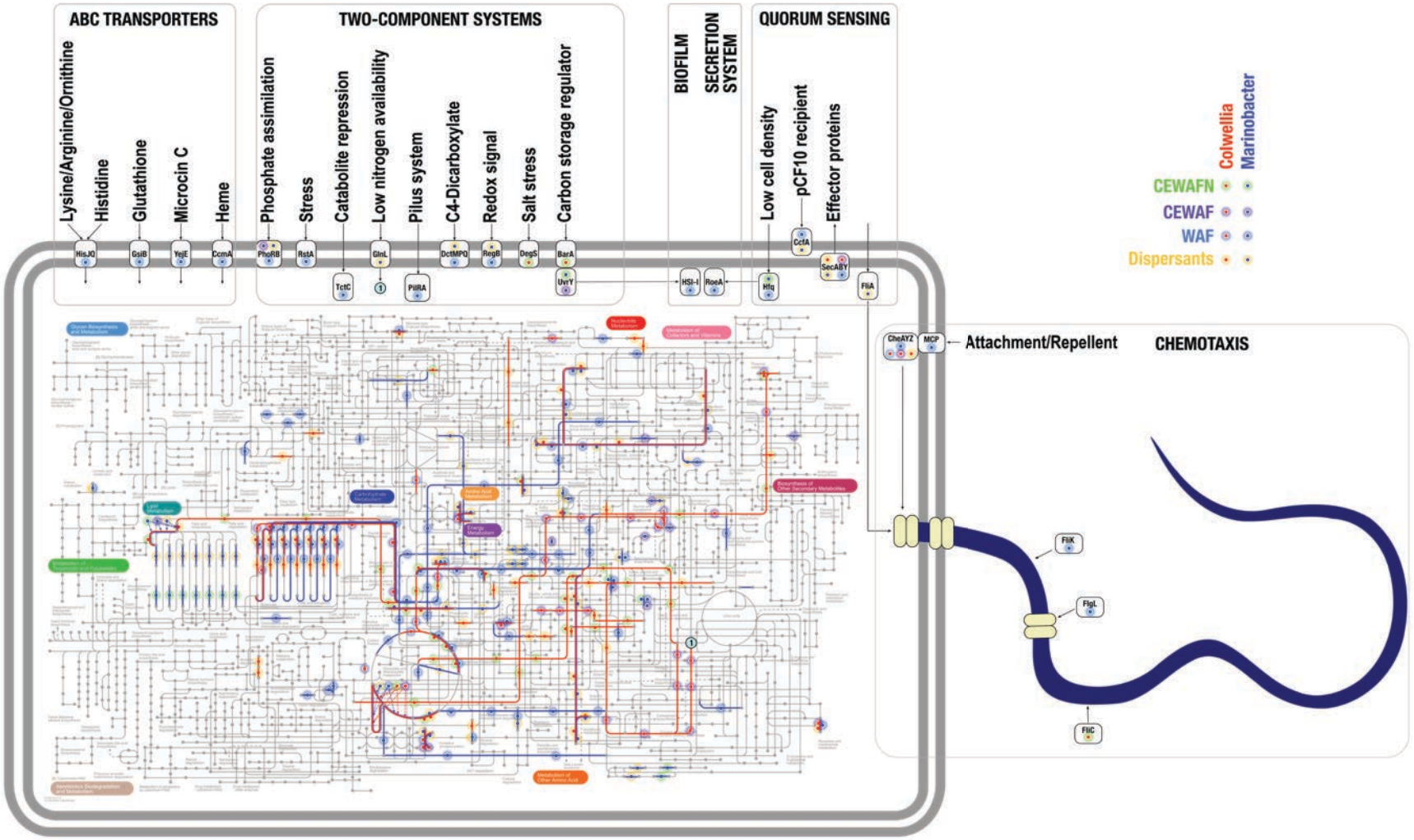
ABC TRANSPORTERS
Lysine/Arginine/Ornithine
Histidine
Glutathione
Microcin C
Heme
HisJQ
GsiB
YejE
CcmA
TWO-COMPONENT SYSTEMS
Phosphate assimilation
Stress
Catabolite repression
Low nitrogen availability
Pilus system
C4-Dicarboxylate
Redox signal
Salt stress
Carbon storage regulator
PhoRB
RstA
TctC
GlnL
PilRA
DctMPQ
RegB
DegS
BarA
UvrY
BIOFILM
SECRETION SYSTEM
HSI-I
RoeA
QUORUM SENSING
Low cell density
pCF10 recipient
Effector proteins
Hfq
CcfA
SecABY
FliA
Colwellia
Marinobacter
CEWAFN
CEWAF
WAF
Dispersants
CheAYZ
MCP
Attachment/Repellent
CHEMOTAXIS
FliK
FlgL
FliC

Figure 2.3. Upregulation of metabolic pathways under dispersants, WAF, CEWAF, and CEWAF+nutrients exposure in *Colwellia psycherythraea* 34H and *Marinobacter* sp. C18. Lines and dots in red and blue indicate upregulated reactions or components in *Colwellia psycherythraea* 34H and *Marinobacter* sp. C18, respectively. Pathway visualization was generated using the iPath 3 module based on KEGG orthology numbers. An interactive version of the metabolic map is available at https://pathways.embl.de/ipath3.cgi?s=xqvYg5kHHCsxGqWy8yJ

The core of the *Marinobacter* DEM-pangenome comprised a large group of housekeeping genes and a large group of genes in COG categories J, K, and L. Upregulation of fatty acid biosynthesis (CEWAF+nutrient) and [Fe-S] cluster assembly genes, possibly involved in nitrogen metabolism (**Figure 2.2**, *37*), were upregulated in the dispersants-only treatment. The core and accessory DEM-pangenome of *Marinobacter* overlapped functionally in the upregulation of processes involving changes and maintenance of the membrane as well as the type IV pilus assembly genes, which were both upregulated in the WAF treatment. These patterns indicated very specific adaptations of *Marinobacter* sp. C18 to oil exposure.

To compare the architecture of metabolic reaction pathways that were upregulated across the treatments, we mapped KEGG orthology numbers into the iPath 3 module (*38*) (**Figure 2.3**). Fatty acid biosynthesis routes from acetate to medium-chain fatty acyl-CoA molecules were upregulated for *Marinobacter* (in the WAF treatment) and *Colwellia* (in the dispersants treatment). Additionally, routes involving the TCA cycle, conversion of pyruvate and acetaldehyde to citrate, and concomitant biosynthesis of L-alanine via transamination of glyoxylate, occurred in *Marinobacter* in the WAF treatment, and *Colwellia* in the CEWAF+nutrient treatment. Additional overlapping upregulated reactions between *Colwellia* and *Marinobacter* occurred in oxidative phosphorylation routes and in purine metabolism.

Colwellia signatures in the DEM-pangenomes indicated opportunistic behavior in response to the chemical exposure regime and time. Dispersed oil treatments led to co-clustering of the expression of isocitrate lyase, TBDR, and propionate-CoA ligase, probably involved in the acquisition of substrates and downstream processing via Glyoxylate Cycle. These components followed unique trends over time, suggesting different functional interactions in the WAF versus dispersant-amended treatments. Unique trends among treatments are supported by the Bray-

Curtis PERMANOVA test that showed significant interaction terms dispersant × time, oil × time and dispersant × oil × time and the observed shift of time-dependent trends of pathways in dispersants-only versus CEWAF±nutrient treatments (Peña-Montenegro et al. parallel submission). In addition, *Colwellia* DE genes varied across the dispersants-only and CEWAF ± nutrients treatments in distinct patterns. For instance, the derepression of the *fadR* regulator was not observed in the dispersants-only treatment, suggesting a WAF-dependent activation of fatty acid degradation. Also, nutrient-dependent expression shifts were observed in genes involved in carbon and energy metabolism (*i.e.*, *aldB, acnBD, phbB1B2*). Most importantly, a large proportion of the *Colwellia* transcriptomic responses were associated with the core DEM-pangenome, reflecting an opportunistic response at the genus level (**Figure 2.1**).

The response of *Marinobacter* matched the profile of a well-adapted oil degrader. *Marinobacter* was more transcriptionally active in the first week of the experiment (Supplementary Figure S2.2**,** Peña-Montenegro et al. mBio), consistent with patterns of a responsive oil biodegrader (*10*). Under WAF exposure, *Marinobacter* sp. C18 upregulated transcription of β-oxidation genes (*fadA, acnA, dctMP*), likely indicating increased hydrocarbon degradation activity (*39*). While the microcosms remained aerobic during the experiment, aggregates formed, and the accumulation of nitrite in concert with decreased nitrate suggests that anaerobic metabolism (*i.e.*, nitrate reduction) occurred in aggregates, where local oxygen depletion could have occurred (*10*). Additionally, a wide variety of DE genes in *Marinobacter* were involved in interactions with its environment, such as chemotaxis genes (*cheAY, mcp*), flagellar genes (*flaA1GL, fliK*), and genes for type IV pilus assembly (*pilAWR, fimV*). These observations are consistent with the description of extracellular events and/or aggregate formation linked to hydrocarbon degradation (*40–42*). The majority of these WAF-specific

responses were adaptations at the species level, *i.e.*, generated by accessory DEM-pangenome of *M.* sp. C18, rather than at the genus level, *i.e.*, generated by core DEM-pangenome of *Marinobacter* (**Figure 2.2**). Marinobacter is thus uniquely suited and well-adapted to respond swiftly and efficiently to oil-only exposures in its environment.

Nutrient availability may limit a microorganism's ability to respond to substrate enrichment or allow a microorganism to accelerate its metabolic response and/or tolerate otherwise stressful conditions. The application of oil, dispersants, and nutrients – *i.e.*, the CEWAF+nutrient treatment – shifted the upregulation map for *Colwellia* and *Marinobacter* across treatments and over time (**Figure 2.3**). The WAF treatment was associated with a diverse and complex response in *Marinobacter* involving chemotaxis, membrane two-component sensors, ABC transporters, secretion systems, quorum sensing components, chloroalkane and chloroalkene routes, butyrate, propionate and glutamate assimilation, downstream biosynthesis, and metabolism of nucleotides, as well as cofactors and vitamins. In contrast, *Colwellia* exhibited striking changes in the reaction map, including utilization of glutamine for the biosynthesis of inosine, a precursor for adenosine and nucleotides, consumption of L-glutamate for the biosynthesis of heme cofactors, possibly involved in the biosynthesis of P450 cytochromes, and nitrogen metabolism via transcription of [Fe-S] cluster assembly proteins in the WAF treatment. On the other hand, in the CEWAF+nutrient treatment, *Colwellia* showed upregulation for the biosynthesis of glycerophospholipids, and the metabolism of amino acids, suggesting cell membrane and chaperone maintenance to combat chemical stress. Although the response of *Marinobacter* and *Colwellia* were similar in the CEWAF+nutrient treatment with regard to fatty acid biosynthesis, *Marinobacter* showed specific upregulation of carbon-storage

regulators, cell density sensors, and molybdenum cofactor biosynthesis. This similar response indicates that nutrients improved the fitness of *Marinobacter* in the presence of dispersant.

The DEM-pangenome approach provides valuable insight into the complex interactions between the microbial communities and their surrounding environment that occur in response to perturbation and confirms the hypothesis of Goyal (2018) that accessory genome components promote response and adaptability in microbial populations (*43*). A complex suite of responses in *Colwellia* and *Marinobacter* DEM-pangenomes revealed unique aspects of their metabolic capabilities that explained treatment-specific abundance. *Colwellia* exhibited an opportunistic response to organic carbon enrichment, while *Marinobacter* displayed a well-tuned response to oil pollution. Genomic and transcriptomic plasticity promoted the success of one versus the other across the treatment regime and underscores the role of generalist vs. specialist components of marine microbiomes, revealing how and why specific organisms respond to particular conditions through the employment of metabolic cassettes associated with core versus accessory pangenomes.

Most of the WAF-associated responses in *Marinobacter* arose from species-level responses, illustrating that distinct ecotypes thrived under oil-infused conditions. In contrast, for *Colwellia*, both core and accessory DEM-pangenome showed transcriptomic signals, mostly in response to dispersant addition. *Colwellia* and *Marinobacter* in dispersant-amended and WAF-amended treatments, respectively, exhibited functional responses that followed different treatment- and time-dependent trajectories along with the metabolic map (**Figure 2.3**). The DEM-pangenomic data underscores the fact that the decrease of *Marinobacter* in dispersant treatments stems from metabolic impairment – dispersants inhibited *Marionbacter's* metabolism and decreased its abundance. In contrast, dispersants stimulated *Colwellia's* metabolism and

promoted its growth and biomass accumulation. These data reveal that specific-specific drivers give rise to community-level responses to perturbation and provide a blueprint for assessing microbial responses to environmental perturbation across Earth's ecosystems.

2.3 Supplementary Materials

Supplementary Methods – Microcosm experiment and RNASeq sequencing

The procedures and protocols for the original experiment are presented by Kleindienst et al. (2015), Seidel et al. (2015), and Peña-Montenegro (2021, parallel submission). Briefly, Kleindienst et al. (*10*) simulated environmental conditions in the oil-rich 1,100 m deep water plume that formed during the Deepwater Horizon spill. Their experiment tracked the impacts of oil-only (supplied as a water-accommodated fraction, "WAF"), synthetic dispersant (Corexit 9500; "dispersant-only"), oil-Corexit mixtures (chemically enhanced water-accommodated fraction, CEWAF), and CEWAF with nutrients (CEWAF+nutrient) additions to naturally-occurring microbial populations present in deepwater collected from a natural seep site in the Gulf of Mexico (Green Canyon lease block 600, e.g., GC600). The Kleindienst experiment was designed to reveal the impact of distinct exposure regimes representing infusions of organic carbon from oil, synthetic dispersant, or oil and synthetic dispersant on microbial community evolution and activity over time. Exposure to different organic carbon regimes is known to drive diverging patterns of microbial community composition and activity (*44*). Kleindienst et al. (*10*) observed that exposure to synthetic dispersant alone did not enhance heterotrophic microbial activity or hydrocarbon oxidation rates (*10*)**,** but it did increase *Colwellia* abundance. In contrast, exposure to oil, but not synthetic dispersant, increased abundance of *Marinobacter* and hydrocarbon oxidation rates. Here, we significantly advance the findings of Kleindienst et al.

(*10*) by interpreting metatranscriptomic data from their experiment. RNAseq library preparation, sequencing, and further data processing details are described in Peña-Montenegro et al. (parallel submission).

Supplementary Methods – DEM-pangenome workflow

To explore ecological implications of DE genes in the context of the *Colwellia* and *Marinobacter* DEM-pangenomes. The workflow is shown in Supplementary Figure S2.3 and summarized in the following steps.

A) *Pangenomic analysis: Colwellia* and *Marinobacter* pangenomes were generated by following (*34*) and http://merenlab.org/2016/11/08/pangenomics-v2/ using all available complete genomes in NCBI of *Colwellia* (n=33) and *Marinobacter* (n=113). Briefly, we generated Anvi'o genome storage databases using the program anvi-gen-genomes-storage for each of the reference genomes. Then, we used the program anvi-pan-genome with default settings.

B) *Metatranscriptomic profiling:* Metatranscriptomic libraries were aligned to all available complete genomes in NCBI of *Colwellia* (n=33) and *Marinobacter* (n=113). *Colwellia psychrerythraea* 34H and *Marinobacter* sp. C18 were selected as reference genomes given their largest mapping scores (i.e., average mapping counts and average mapping rates). Metatranscriptomic mapping coverage was included as additional layers to the pangenome using the program anvi-import-misc-data.

C) *Differential Expression (DE) analysis:* DE analysis followed a previous workflow (*15*) with minor adaptations (Peña-Montenegro et al., parallel submission). SAM files were sorted and indexed into BAM files. Gene expression was contrasted for each treatment with respect to the biotic control. Profiles were normalized across all samples using the regularized logarithm transformation. Then, statistical inference was performed using the negative binomial

Wald test with Cook's distance to control for outliers. Those genes with an adjusted p-value < 0.05 (using the Benjamini-Hochberg method) were classified as DE genes.

D) *DE overlay and split-binning:* Additional layers, including the detection of DE genes in gene clusters, were included in the metapangenome using the program anvi-import-misc-data. We visualized the DEM- pangenome using the program anvi-display-pan. For better visualization, gene clusters without DE genes were removed by using the split-binning capabilities of the Anvi'o platform (33). The outcome of these steps is defined as DEM-pangenome. See the Code availability section for details in the workflow.

Results from the broader metatranscriptomic assessment are presented by Peña-Montenegro et al. (mBio, companion manuscript provided). Briefly, metatranscriptomic libraries (n=27) ranged in size from 4.6 to 18.75 million reads, with a mean of 10.58 million reads per sample with an average read length of 97 bp. Roughly 3.1 million reads per library were annotated at the functional level (Supplementary Results, Supplementary Figure S2.1). Further analysis on a functional or taxonomic level used normalized mRNA read counts assigned to known functions or taxa, respectively (Supplementary Data 1).

Mapping counts and mapping reads for all of the recruited reads are shown in Supplementary Data 1. Genomic references with the largest mapping recruitment were ~6.0 million reads for *Colwellia psychrerythraea* 34H; and ~1.7 million reads for *Marinobacter* sp. C18. We performed a DE analysis to identify the collection of genes that showed a significant change in expression levels compared to the biotic control. Mapping counts profiles recruited by the reference genomes were used as input to perform the DE analysis. Distinct profiles of total numbers of DE genes were observed between *Colwellia* and *Marinobacter.*

Supplementary Results

For *Colwellia*, examples of genes involved in oxidative phosphorylation, energy, and carbohydrate metabolism categories that were upregulated in CEWAF±nutrient treatments included the succinate dehydrogenase ***sdhC*** gene (Supplementary Data 1) local_id: C_CORE_137, C_CORE_138), the ATPase ***atpA*** gene (C_CORE_141), the 2-oxoglutarate dehydrogenase complex dihydrolipoamide dehydrogenase ***lpd*** gene (C_CORE_211) and the respiratory NADH-quinone reductase ***nqrB*** gene (C_CORE_129, C_CORE_130). Similarly, the ***sucC*** gene encoding for the succinyl-CoA synthetase β subunit (C_CORE_162, C_CORE_163) component of the TCA cycle was upregulated in the CEWAF ±nutrients treatment. Examples of upregulation of genes related to stress response genes include the cold shock protein gene ***cspA*** (C_CORE_203) and the FK506-binding protein (FKBP) gene ***tig*** (C_CORE_33). The ***accC*** gene encoding for acetyl-CoA carboxylase (C_CORE_37) and the β-acetoacetyl synthase ***fabY*** gene (C_CORE_17), which are involved in fatty acid biosynthesis, were upregulated in CEWAF+nutrient treatments.

Examples of genes that were upregulated in response to dispersants only (not oil) included the phosphatidylserine synthase ***pssA*** gene and the UDP-3-O-acyl-GlcNAc deacetylase ***lpxC*** gene (C_CORE_131), the two-component sensor histidine kinase ***barA*** gene (C_CORE_235), the NADPH-sulfite reductase ***cysJ*** gene (C_CORE_230), the 2Fe-2S ferredoxin ***fdx*** gene (C_CORE_157), the FKBP type peptidyl-prolyl cis-trans isomerase ***fkpA*** gene (C_CORE_114) and the amidophosphoribosyl transferase ***purF*** gene (C_CORE_78).

Upregulated DE genes in the CEWAF±nutrient treatments included the 3-ketoacyl-CoA ***phaA*** gene (C_ACC_65) and the polyhydroxyalkanoate synthase ***phaC*** gene (C_ACC_20) and the ***fadR*** repressor (C_ACC_74). Additional upregulated genes in this treatment included the 2-

methylcitrate dehydratase *acnD* gene (C_ACC_61), the aconitate hydratase *acnB* gene (C_ACC_100), and the aldehyde dehydrogenase *aldB* involved in propionate metabolism. Similarly, the granule-associated protein phasin *phaP* gene (C_ACC_28), the acetoacetyl-CoA reductase *phbB1* (C_ACC_07), and *phbB2* genes (C_ACC_25), which are involved in the biosynthesis of polyhydroxybutyrate. Genes CPS_3734 (encodes for a tryptophan halogenase (C_ACC_14)), and CPS_3737, encoding for a Ton-B dependent receptor (C_ACC_11), were upregulated in the CEWAF treatment. The CPS_3734 is located downstream of a SapC-like S layer protein gene in the *C. psychrerythraea* 34H genome (C_ACC_16).

For *Marinobacter*, upregulated genes in the accessory DEM-pangenome involved in carbon and lipid metabolism included aconitate hydratase *acnA* gene (M_ACC_46), the C4-dicarboxylate transporter genes *dctM* (M_ACC_193), *dctP* (M_ACC_186), the acetyl-CoA acyltransferase *fadA* (M_ACC_74), the formate dehydrogenase gene *fdoG* (M_ACC_16), the 4-aminobutyrate aminotransferase *gabT* gene (M_ACC_129), and glycolate oxidase *glcF* gene (M_ACC_154). Additional upregulation included stress response (alkyl peroxiredoxin *ahpC* gene (M_ACC_149), amino acid metabolism (the D-amino-acid dehydrogenase *dadA* gene (M_ACC_261)), and chloroalkane and chloroalkene degradation genes (the haloalkane dehalogenase *dhaA* gene (M_ACC_112)). Upregulated genes related to sensor kinases included *cheA* (M_ACC_121), *cheY* (M_ACC_210), the methyl-accepting chemotaxis *mcp* gene (M_ACC_06), the polysaccharide biosynthesis gene *flaA1* (M_ACC_115), the flagellar protein gene *flaG* (M_ACC_118), the flagellar hook-associated genes *flgL* (M_ACC_117), *fliK* (M_ACC_08), the type IV pilus assembly genes *pilA* (M_ACC_190), *pilW* (M_ACC_187), *fimV* (M_ACC_174), and the *ompR* regulator (M_ACC_192).

Upregulated genes in the core DEM-pangenome of *Marinobacter* included those involved in fatty acid biosynthesis (gene ***fabD,*** M_CORE_105), [Fe-S] cluster assembly genes (***iscA*** (M_CORE_195) and ***sufB*** (M_CORE_206)). For *Marinobacter*, there was functional overlap of core and accessory DEM-pangenome with regard to changes and maintenance of the membrane, ***i.e.,*** the secretory protein genes ***secA*** (M_CORE_118), which upregulated in the CEWAF treatment, and ***secB*** (M_CORE_22), which was upregulated in the dispersants-only treatment. The type IV pilus assembly genes ***pilM*** (M_CORE_148) and ***pilO*** (M_CORE_115) and type IV pilus assembly regulator ***pilR*** (M_CORE_171) were both upregulated in the WAF treatment.

Nutrient availability can affect how microbes respond to environmental stressors. To identify pathway perturbations in metatranscriptomic signals over time, we fitted a set of linear models using normalized mapped transcript counts per pathway and per treatment as a function of time. Each fitting procedure aimed to identify the model with the best fit (*i.e.*, greatest correlation coefficient R^2) by comparing a first-order linear model with (1) a slope greater than 1.88 as increasing linear (IL), (2) a slope below -1.88 as decreasing linear (DL), (3) and constant (CL) in between; (4) a positive skewed lognormal model to shape early peaks (EP) in the transcriptional distribution; (5) a negative skewed lognormal model to shape late peaks (LP); and 6) a U-shaped (U) second-order linear model. Best fitting models for each pathway and treatment are shown in Supplementary Figure S2.2.

The dispersants-only and the CEWAF + nutrients treatments were mostly associated with U and EP trends, respectively (**Supplementary Results, Supplementary Figure S2.1**). This change in the dynamic of transcriptional time trends was also supported by a paired Pearson χ^2 test. The test aimed to identify statistical differences between the biotic control and the amended

samples. All of the treatments were significantly different from the biotic control (p-value < 0.0001), except the CEWAF treatment (p-value = 0.1592). Further examination in a logistic fitting model indicated that dispersants (p-value = 0.0051), WAF (p-value < 0.0001) and nutrients (p-value < 0.0001) explained the variability of the transcriptional time trend profiles in the experiment.

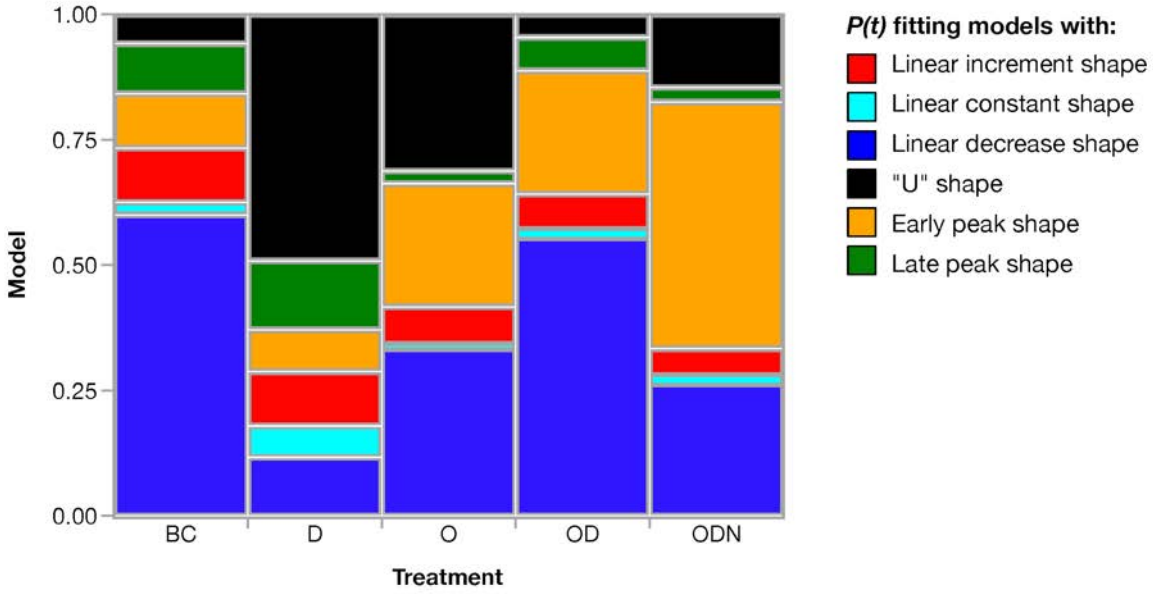

Supplementary Figure S2.1. Proportion of time-dependent expression (*P(t)*) fitting models across the experimental treatments in the K2015 metatranscriptomic data set. Color code matches the distribution of fitting models shown in Supplementary Figure S2.2

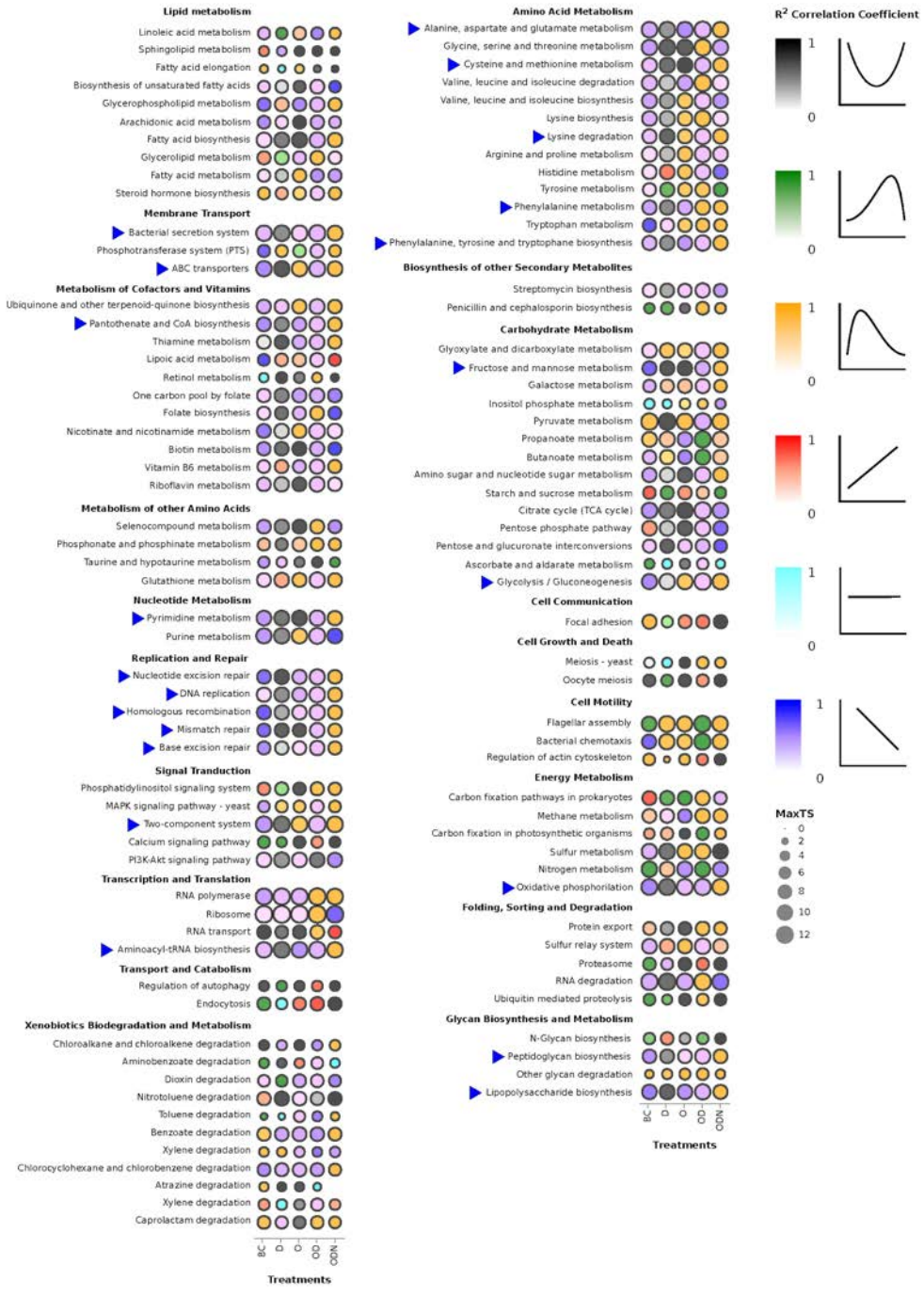
Lipid metabolism
Linoleic acid metabolism
Sphingolipid metabolism
Fatty acid elongation
Biosynthesis of unsaturated fatty acids
Glycerophospholipid metabolism
Arachidonic acid metabolism
Fatty acid biosynthesis
Glycerolipid metabolism
Fatty acid metabolism
Steroid hormone biosynthesis
Membrane Transport
Bacterial secretion system
Phosphotransferase system (PTS)
ABC transporters
Metabolism of Cofactors and Vitamins
Ubiquinone and other terpenoid-quinone biosynthesis
Pantothenate and CoA biosynthesis
Thiamine metabolism
Lipoic acid metabolism
Retinol metabolism
One carbon pool by folate
Folate biosynthesis
Nicotinate and nicotinamide metabolism
Biotin metabolism
Vitamin B6 metabolism
Riboflavin metabolism
Metabolism of other Amino Acids
Selenocompound metabolism
Phosphonate and phosphinate metabolism
Taurine and hypotaurine metabolism
Glutathione metabolism
Nucleotide Metabolism
Pyrimidine metabolism
Purine metabolism
Replication and Repair
Nucleotide excision repair
DNA replication
Homologous recombination
Mismatch repair
Base excision repair
Signal Tranduction
Phosphatidylinositol signaling system
MAPK signaling pathway - yeast
Two-component system
Calcium signaling pathway
PI3K-Akt signaling pathway
Transcription and Translation
RNA polymerase
Ribosome
RNA transport
Aminoacyl-tRNA biosynthesis
Transport and Catabolism
Regulation of autophagy
Endocytosis
Xenobiotics Biodegradation and Metabolism
Chloroalkane and chloroalkene degradation
Aminobenzoate degradation
Dioxin degradation
Nitrotoluene degradation
Toluene degradation
Benzoate degradation
Xylene degradation
Chlorocyclohexane and chlorobenzene degradation
Atrazine degradation
Xylene degradation
Caprolactam degradation
BC
D
O
OD
ODN
Treatments
Amino Acid Metabolism
Alanine, aspartate and glutamate metabolism
Glycine, serine and threonine metabolism
Cysteine and methionine metabolism
Valine, leucine and isoleucine degradation
Valine, leucine and isoleucine biosynthesis
Lysine biosynthesis
Lysine degradation
Arginine and proline metabolism
Histidine metabolism
Tyrosine metabolism
Phenylalanine metabolism
Tryptophan metabolism
Phenylalanine, tyrosine and tryptophane biosynthesis
Biosynthesis of other Secondary Metabolites
Streptomycin biosynthesis
Penicillin and cephalosporin biosynthesis
Carbohydrate Metabolism
Glyoxylate and dicarboxylate metabolism
Fructose and mannose metabolism
Galactose metabolism
Inositol phosphate metabolism
Pyruvate metabolism
Propanoate metabolism
Butanoate metabolism
Amino sugar and nucleotide sugar metabolism
Starch and sucrose metabolism
Citrate cycle (TCA cycle)
Pentose phosphate pathway
Pentose and glucuronate interconversions
Ascorbate and aldarate metabolism
Glycolysis / Gluconeogenesis
Cell Communication
Focal adhesion
Cell Growth and Death
Meiosis - yeast
Oocyte meiosis
Cell Motility
Flagellar assembly
Bacterial chemotaxis
Regulation of actin cytoskeleton
Energy Metabolism
Carbon fixation pathways in prokaryotes
Methane metabolism
Carbon fixation in photosynthetic organisms
Sulfur metabolism
Nitrogen metabolism
Oxidative phosphorilation
Folding, Sorting and Degradation
Protein export
Sulfur relay system
Proteasome
RNA degradation
Ubiquitin mediated proteolysis
Glycan Biosynthesis and Metabolism
N-Glycan biosynthesis
Peptidoglycan biosynthesis
Other glycan degradation
Lipopolysaccharide biosynthesis
BC
D
O
OD
ODN
Treatments
R2 Correlation Coefficient
1
0
MaxTS
0
2
4
6
8
10
12

Supplementary Figure S2.2. Fitting models for each pathway and treatment aiming for the greatest correlation coefficient R^2. Dot sizes are proportional to the largest normalized transcriptomic signal (MaxTS) at a given pathway and treatment. Color scale is matching the assigned best-fitting model among the tested models from top to bottom: U-shaped (U) second-order linear model in black, negatively skewed lognormal model to shape a late peak in green, positively skewed lognormal model to shape an early peak (EP) in golden, first-order increasing linear model (slope>1.88) in red, first-order constant linear model (|slope|≤1.88) in cyan, and first-order decreasing linear (DL) model (slope<-1.88) in blue. Blue triangles indicate those pathways that followed a DL trend in the biotic control, a U trend in the dispersant-only treatment, and an EP trend in the CEWAF+n treatment.

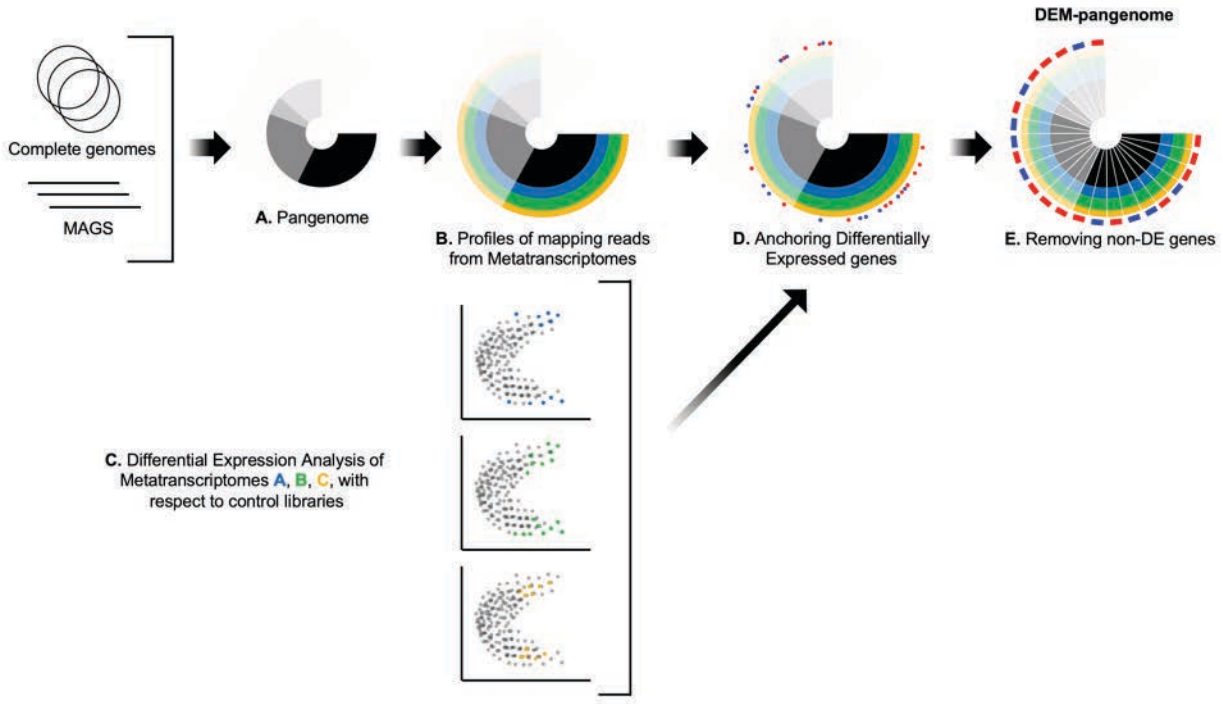

Supplementary Figure S2.3. DEM-pangenome workflow. A) Complete genomes and metagenomic assembled genomes (MAGs) were used to perform pangenomic analysis as described in (*34*). **B)** Metatranscriptomic libraries were mapped to every genome in the pangenomic. The genome with the largest mapping recovery was set as a reference for metatranscriptomic profiling. **C)** Metatranscriptomic libraries are processed for Differentially Expressed (DE) analysis as described in (*15*). **D)** DE genes were labeled as an additional feature for each DE contrast test. Blue and red dots indicate up- and down-regulated genes. **E)** To improve the visualization and further processing of the figure, gene clusters without DE genes were removed by using the split-binning capabilities of the Anvi'o platform (*33*).

2.3 References

1. A. Z. Worden, M. J. Follows, S. J. Giovannoni, S. Wilken, A. E. Zimmerman, P. J. Keeling, Rethinking the marine carbon cycle: Factoring in the multifarious lifestyles of microbes. *Science*. **347**, 1257594–1257594 (2015).

2. M. A. Moran, The global ocean microbiome. *Science*. **350**, aac8455–aac8455 (2015).

3. S. Sunagawa, L. P. Coelho, S. Chaffron, J. R. Kultima, K. Labadie, G. Salazar, B. Djahanschiri, G. Zeller, D. R. Mende, A. Alberti, F. M. Cornejo-Castillo, P. I. Costea, C. Cruaud, F. d'Ovidio, S. Engelen, I. Ferrera, J. M. Gasol, L. Guidi, F. Hildebrand, F. Kokoszka, C. Lepoivre, G. Lima-Mendez, J. Poulain, B. T. Poulos, M. Royo-Llonch, H. Sarmento, S. Vieira-Silva, C. Dimier, M. Picheral, S. Searson, S. Kandels-Lewis, Tara Oceans coordinators, C. Bowler, C. de Vargas, G. Gorsky, N. Grimsley, P. Hingamp, D. Iudicone, O. Jaillon, F. Not, H. Ogata, S. Pesant, S. Speich, L. Stemmann, M. B. Sullivan, J. Weissenbach, P. Wincker, E. Karsenti, J. Raes, S. G. Acinas, P. Bork, E. Boss, C. Bowler, M. Follows, L. Karp-Boss, U. Krzic, E. G. Reynaud, C. Sardet, M. Sieracki, D. Velayoudon, Structure and function of the global ocean microbiome. *Science*. **348**, 1261359–1261359 (2015).

4. S. Louca, L. W. Parfrey, M. Doebeli, Decoupling function and taxonomy in the global ocean microbiome. *Science*. **353**, 1272–1277 (2016).

5. M. L. Sogin, H. G. Morrison, J. A. Huber, D. M. Welch, S. M. Huse, P. R. Neal, J. M. Arrieta, G. J. Herndl, Microbial diversity in the deep sea and the underexplored "rare biosphere." *Proceedings of the National Academy of Sciences*. **103**, 12115–12120 (2006).

6. M. D. J. Lynch, J. D. Neufeld, Ecology and exploration of the rare biosphere. *Nat Rev Microbiol*. **13**, 217–229 (2015).

7. S. Kleindienst, S. Grim, M. Sogin, A. Bracco, M. Crespo-Medina, S. B. Joye, Diverse, rare microbial taxa responded to the Deepwater Horizon deep-sea hydrocarbon plume. *ISME J*. **10**, 400–415 (2016).

8. H. Dang, M. G. Klotz, C. R. Lovell, S. M. Sievert, Editorial: The Responses of Marine Microorganisms, Communities and Ecofunctions to Environmental Gradients. *Front. Microbiol.* **10**, 115 (2019).

9. S. Joye, J. E. Kostka, "Microbial Genomics of the Global Ocean System: Report on an American Academy of Microbiology (Academy), The American Geophysical Union (AGU), and The Gulf of Mexico Research Initiative (GoMRI) Colloquium held on 9 and 10 April 2019" (American Society for Microbiology, 2020), , doi:10.1128/AAMCol.Apr.2019.

10. S. Kleindienst, M. Seidel, K. Ziervogel, S. Grim, K. Loftis, S. Harrison, S. Y. Malkin, M. J. Perkins, J. Field, M. L. Sogin, T. Dittmar, U. Passow, P. M. Medeiros, S. B. Joye, Chemical dispersants can suppress the activity of natural oil-degrading microorganisms. *Proceedings of the National Academy of Sciences*. **112**, 14900–14905 (2015).

11. T. J. Crone, M. Tolstoy, Magnitude of the 2010 Gulf of Mexico oil leak. *Science*. **330**, 634–634 (2010).

12. National Commission on the BP Deepwater Horizon Oil Spill and Offshore Drilling, *The use of surface and subsea dispersants during the BP Deepwater Horizon oil spill* (National Commission on the BP Deepwater Horizon Oil Spill and Offshore Drilling., Washington, D.C., 2011).

13. S. M. Techtmann, M. Zhuang, P. Campo, E. Holder, M. Elk, T. C. Hazen, R. Conmy, J. W. Santo Domingo, Corexit 9500 enhances oil biodegradation and changes active bacterial community structure of oil-enriched microcosms. *Appl Environ Microbiol*. **83**, e03462-16, e03462-16 (2017).

14. L. Hamdan, P. Fulmer, Effects of COREXIT® EC9500A on bacteria from a beach oiled by the Deepwater Horizon spill. *Aquat. Microb. Ecol.* **63**, 101–109 (2011).

15. O. U. Mason, T. C. Hazen, S. Borglin, P. S. G. Chain, E. A. Dubinsky, J. L. Fortney, J. Han, H.-Y. N. Holman, J. Hultman, R. Lamendella, R. Mackelprang, S. Malfatti, L. M. Tom, S. G. Tringe, T. Woyke, J. Zhou, E. M. Rubin, J. K. Jansson, Metagenome, metatranscriptome and single-cell sequencing reveal microbial response to Deepwater Horizon oil spill. *ISME J*. **6**, 1715–1727 (2012).

16. L. M. Rodriguez-R, W. A. Overholt, C. Hagan, M. Huettel, J. E. Kostka, K. T. Konstantinidis, Microbial community successional patterns in beach sands impacted by the Deepwater Horizon oil spill. *ISME J*. **9**, 1928–1940 (2015).

17. E. A. Dubinsky, M. E. Conrad, R. Chakraborty, M. Bill, S. E. Borglin, J. T. Hollibaugh, O. U. Mason, Y. M. Piceno, F. C. Reid, W. T. Stringfellow, L. M. Tom, T. C. Hazen, G. L. Andersen, Succession of hydrocarbon-degrading bacteria in the aftermath of the Deepwater Horizon oil spill in the Gulf of Mexico. *Environ. Sci. Technol.* **47**, 10860–10867 (2013).

18. T. C. Hazen, E. A. Dubinsky, T. Z. DeSantis, G. L. Andersen, Y. M. Piceno, N. Singh, J. K. Jansson, A. Probst, S. E. Borglin, J. L. Fortney, W. T. Stringfellow, M. Bill, M. E. Conrad, L. M. Tom, K. L. Chavarria, T. R. Alusi, R. Lamendella, D. C. Joyner, C. Spier, J. Baelum, M. Auer, M. L. Zemla, R. Chakraborty, E. L. Sonnenthal, P. D'haeseleer, H.-Y. N. Holman, S. Osman, Z. Lu, J. D. Van Nostrand, Y. Deng, J. Zhou, O. U. Mason, Deep-sea oil plume enriches indigenous oil-degrading Bacteria. *Science*. **330**, 204–208 (2010).

19. D. L. Valentine, J. D. Kessler, M. C. Redmond, S. D. Mendes, M. B. Heintz, C. Farwell, L. Hu, F. S. Kinnaman, S. Yvon-Lewis, M. Du, E. W. Chan, F. G. Tigreros, C. J. Villanueva, Propane respiration jump-starts microbial response to a deep oil spill. *Science*. **330**, 208–211 (2010).

20. M. C. Redmond, D. L. Valentine, Natural gas and temperature structured a microbial community response to the Deepwater Horizon oil spill. *Proceedings of the National Academy of Sciences*. **109**, 20292–20297 (2012).

21. J. W. Deming, L. K. Somers, W. L. Straube, D. G. Swartz, M. T. Macdonell, Isolation of an Obligately Barophilic Bacterium and Description of a New Genus, *Colwellia* gen. nov. *Systematic and Applied Microbiology*. **10**, 152–160 (1988).

22. M. E. Campeão, L. Reis, L. Leomil, L. de Oliveira, K. Otsuki, P. Gardinali, O. Pelz, R. Valle, F. L. Thompson, C. C. Thompson, The Deep-sea microbial community from the Amazonian Basin associated with oil degradation. *Front. Microbiol.* **8**, 1019 (2017).

23. J. Baelum, S. Borglin, R. Chakraborty, J. L. Fortney, R. Lamendella, O. U. Mason, M. Auer, M. Zemla, M. Bill, M. E. Conrad, S. A. Malfatti, S. G. Tringe, H.-Y. Holman, T. C. Hazen, J. K. Jansson, Deep-sea bacteria enriched by oil and dispersant from the Deepwater Horizon spill: Enrichment of oil degraders from Gulf of Mexico. *Environmental Microbiology*. **14**, 2405–2416 (2012).

24. M. J. Gauthier, B. Lafay, R. Christen, L. Fernandez, M. Acquaviva, P. Bonin, J.-C. Bertrand, *Marinobacter hydrocarbonoclasticus* gen. nov., sp. nov., a new, extremely halotolerant, hydrocarbon-degrading marine bacterium. *International Journal of Systematic Bacteriology*. **42**, 568–576 (1992).

25. E. P. Ivanova, H. J. Ng, H. K. Webb, G. Feng, K. Oshima, M. Hattori, M. Ohkuma, A. F. Sergeev, V. V. Mikhailov, R. J. Crawford, T. Sawabe, Draft genome sequences of *Marinobacter similis* A3d10T and *Marinobacter salarius* R9SW1T. *Genome Announcements*. **2**, e00442-14, 2/3/e00442-14 (2014).

26. E. Singer, E. A. Webb, W. C. Nelson, J. F. Heidelberg, N. Ivanova, A. Pati, K. J. Edwards, Genomic Potential of Marinobacter aquaeolei, a Biogeochemical "Opportunitroph." *Appl. Environ. Microbiol.* **77**, 2763–2771 (2011).

27. N. Dombrowski, J. A. Donaho, T. Gutierrez, K. W. Seitz, A. P. Teske, B. J. Baker, Reconstructing metabolic pathways of hydrocarbon-degrading bacteria from the Deepwater Horizon oil spill. *Nature Microbiology*, 16057 (2016).

28. J. Yuan, The diversity of PAH-degrading bacteria in a deep-sea water column above the Southwest Indian Ridge. *Front. Microbiol.* **6** (2015), doi:10.3389/fmicb.2015.00853.

29. J. Tremblay, E. Yergeau, N. Fortin, S. Cobanli, M. Elias, T. L. King, K. Lee, C. W. Greer, Chemical dispersants enhance the activity of oil- and gas condensate-degrading marine bacteria. *ISME J*. **11**, 2793–2808 (2017).

30. S. Rughöft, A. L. Vogel, S. B. Joye, T. Gutierrez, S. Kleindienst, Starvation-Dependent Inhibition of the Hydrocarbon Degrader *Marinobacter* sp. TT1 by a Chemical Dispersant. *JMSE*. **8**, 925 (2020).

31. S. D. Allison, J. B. H. Martiny, Resistance, resilience, and redundancy in microbial communities. *Proceedings of the National Academy of Sciences*. **105**, 11512–11519 (2008).

32. M. Seidel, S. Kleindienst, T. Dittmar, S. B. Joye, P. M. Medeiros, Biodegradation of crude oil and dispersants in deep seawater from the Gulf of Mexico: Insights from ultra-high

resolution mass spectrometry. *Deep Sea Research Part II: Topical Studies in Oceanography*. **129**, 108–118 (2016).

33. A. M. Eren, Ö. C. Esen, C. Quince, J. H. Vineis, H. G. Morrison, M. L. Sogin, T. O. Delmont, Anvi'o: an advanced analysis and visualization platform for 'omics data. *PeerJ*. **3**, e1319 (2015).

34. T. O. Delmont, A. M. Eren, Linking pangenomes and metagenomes: the *Prochlorococcus* metapangenome. *PeerJ*. **6**, e4320 (2018).

35. L. My, B. Rekoske, J. J. Lemke, J. P. Viala, R. L. Gourse, E. Bouveret, Transcription of the *Escherichia coli* fatty acid synthesis operon *fabHDG* Is directly activated by FadR and Inhibited by ppGpp. *Journal of Bacteriology*. **195**, 3784–3795 (2013).

36. A. D. Kappell, Y. Wei, R. J. Newton, J. D. Van Nostrand, J. Zhou, S. L. McLellan, K. R. Hristova, The polycyclic aromatic hydrocarbon degradation potential of Gulf of Mexico native coastal microbial communities after the Deepwater Horizon oil spill. *Front. Microbiol.* **5** (2014), doi:10.3389/fmicb.2014.00205.

37. P. C. Dos Santos, D. C. Johnson, B. E. Ragle, M.-C. Unciuleac, D. R. Dean, Controlled Expression of *nif* and *isc* iron-sulfur protein maturation components reveals target specificity and limited functional replacement between the two systems. *JB.* **189**, 2854–2862 (2007).

38. Y. Darzi, I. Letunic, P. Bork, T. Yamada, iPath3.0: interactive pathways explorer v3. *Nucleic Acids Res*. **46**, W510–W513 (2018).

39. A. Krivoruchko, Y. Zhang, V. Siewers, Y. Chen, J. Nielsen, Microbial acetyl-CoA metabolism and metabolic engineering. *Metabolic Engineering*. **28**, 28–42 (2015).

40. J. Mounier, A. Camus, I. Mitteau, P.-J. Vaysse, P. Goulas, R. Grimaud, P. Sivadon, The marine bacterium *Marinobacter hydrocarbonoclasticus* SP17 degrades a wide range of lipids and hydrocarbons through the formation of oleolytic biofilms with distinct gene expression profiles. *FEMS Microbiol Ecol*. **90**, 816–831 (2014).

41. H. Ennouri, P. d'Abzac, F. Hakil, P. Branchu, M. Naïtali, A. Lomenech, R. Oueslati, J. Desbrières, P. Sivadon, R. Grimaud, The extracellular matrix of the oleolytic biofilms of *Marinobacter hydrocarbonoclasticus* comprises cytoplasmic proteins and T2SS effectors that promote growth on hydrocarbons and lipids. *Environ Microbiol*. **19**, 159–173 (2017).

42. M. Espinosa-Urgel, S. Marqués, New insights in the early extracellular events in hydrocarbon and lipid biodegradation. *Environ Microbiol.* **19**, 15–18 (2017).

43. A. Goyal, Metabolic adaptations underlying genome flexibility in prokaryotes. *PLoS Genet.* **14**, e1007763 (2018).

44. J. McCarren, J. W. Becker, D. J. Repeta, Y. Shi, C. R. Young, R. R. Malmstrom, S. W. Chisholm, E. F. DeLong, Microbial community transcriptomes reveal microbes and

metabolic pathways associated with dissolved organic matter turnover in the sea. *Proceedings of the National Academy of Sciences*. **107**, 16420–16427 (2010).

CHAPTER 3

METATRANSCRIPTOMIC RESPONSE OF DEEP OCEAN MICROBIAL POPULATIONS TO INFUSIONS OF OIL AND/OR SYNTHETIC CHEMICAL DISPERSANT [2]

[2] Peña-Montenegro TD, Kleindienst S, Allen AE, Eren AM, McCrow JP, Sánchez-Calderón JD, Arnold J, Joye SB. To be submitted to *mBio*

3.1. Abstract

Oil spills are a frequent perturbation to the marine environment, one that has rapid and significant impacts on the local microbiome. A previous study reported that exposure to different combinations of dissolved oil versus dissolved synthetic dispersant drove diverging patterns of microbial community composition and activity. Synthetic dispersant alone did not enhance heterotrophic microbial activity or oxidation rates of specific hydrocarbon components, but dispersant exposure increased the abundance of some taxa (*e.g.*, *Colwellia*). Exposure to oil, but not dispersants, increased the abundance of other taxa (*e.g., Marinobacter*) and stimulated oxidation rates of hydrocarbons. Here, we advance these findings by interpreting metatranscriptomic data from this experiment to explore how and why specific components of the microbial community responded to distinct exposure regimes. Dispersants alone selected for a unique community and for dominant organisms that reflected treatment- and time-dependent responses. Dispersant amendment also led to diverging functional profiles amongst the different treatments. Similarly, oil alone selected for a community that was distinct from treatments amended with dispersants. The presence of oil and dispersants with added nutrients led to substantial differences in microbial responses, likely reflecting increased fitness driven by additional inorganic nutrients. The oil-only additions led to a marked increase in expression of phages, prophages, transposable elements, and plasmids, suggesting that aspects of microbial community response to oil are driven by the 'mobilome', potentially through viral-mediated regulation of ciliates and flagellates that would otherwise top-down regulation on the microbial community via grazing.

3.1 Introduction

Oil spills frequently occur in the marine environment, sometimes with calamitous consequences (1). Most marine oil spills have involved accidents in the coastal ocean, including pipeline discharges and accidents, vessel accidents (*e.g.*, Exxon Valdez), and platform accidents (*e.g.,* MC20 Taylor Energy accident) (2, 3), but offshore spillage of oil occurs as well, via operational discharges and drilling accidents, *e.g.*, the Ixtoc oil well blowout in the Southern Gulf of Mexico in 1979 (3) and the Deepwater Horizon (DWH) oil well blowout in the Northern Gulf of Mexico in 2010 (1). Such discharges provide acute, chronic, or pulsed inputs of oil into the marine environment that modify the structure and function of marine microbial communities (1).

The Deepwater Horizon disaster began on April 20th, 2010, when a catastrophic loss of well control resulted in a massive explosion on the drilling platform that caused it to sink two days later, rupturing the riser pipe at the seabed and initiating an uncontrolled deep-sea oil well blowout. The ensuing discharge of hydrocarbons continued for 84 days and released approximately 4.9 million barrels of oil and some 250,000 metric tons of natural gas into the Gulf of Mexico at a depth of 1,500m. The Gulf of Mexico's microbial communities responded rapidly to the oil spill in the pelagic ocean (4), along beaches (5), and at the seafloor, and these microbes played a key role in hydrocarbon bioremediation across these habitats (1).

Given the magnitude of the Deepwater Horizon oil spill, synthetic chemical dispersants were used (6), both at the discharging wellhead and along with surface oil slicks, as a response measure to move of oil from the organic phase (slick, discharge plume) to the aqueous phase to minimize environmental damage (*e.g.,* oiled beaches and marshes) and to accelerate microbial oil biodegradation via the creation of small droplets with enhanced bioavailability (6). Synthetic

chemical dispersants are comprised of petroleum distillates and nonionic and anionic surfactants (7); these organic substrates are extremely labile, offering microbial populations an additional organic carbon source to fuel their metabolism (8, 9). Some 7 million liters of synthetic dispersant were applied in response to the Deepwater Horizon oil spill – with 2.9 million liters were applied at the discharging wellhead at the seabed. While it is clear that synthetic dispersants altered microbial communities and potentially slowed oil degradation (4), exactly how dispersant-derived organic carbon modulated the microbial response is unclear.

We used metatranscriptomic data collected during a laboratory experiment (10) to compare and contrast the response of key taxa to exposure to synthetic dispersant and/or oil to reveal how communities responded to distinct organic carbon exposure regimes. This effort builds on the foundational study of Kleindienst et al. (10), which simulated the environmental conditions in the hydrocarbon-rich 1,100 m deep water plume that formed during the DWH spill. In the Kleindienst et al. (2010) experiment, deepwater (~200 L) from about 1,400m water depth in a vertical oil plume at a natural oil seep (Green Canyon 600 in the Northern Gulf of Mexico) was collected onboard a research vessel and returned to the laboratory for manipulation in a laboratory experiment.

The Kleindienst et al. experiment involved exposing replicate (n=3) microcosms to a matrix of controlled conditions to isolate the community response to oil-only versus dispersant exposure. Oil-only treatments were amended with a water-accommodated fraction ("WAF") of oil. A water accommodated fraction of synthetic dispersant, Corexit 9500, was used to identify the microbial impact of dispersant along ("dispersant-only"). Finally, water accommodated fractions of oil and Corexit mixtures (=chemically enhanced water-accommodated fraction, CEWAF) or CEWAF plus nutrients (CEWAF+nutrient) were used to examine the impact of oil

plus dispersant on microbial communities. All water accommodated fractions contained dissolved components and microscopic droplets. No additional controls were included for comparison. The response of Gulf deepwater microbial populations to these additions was tracked over several weeks, during which time replicate samples were sacrificed to assess microbial community composition, microbial activity, chemistry, and metatranscriptomics. This experiment revealed the impact of distinct chemical exposure – oil versus dispersant versus oil and dispersant – regimes on microbial community evolution and activity over time (denoted by t_x where x refers to the time point, see Ref. (10)) and **Supplementary Information**).

In the original paper, Kleindienst et al. (2015) reported that exposure to different organic carbon regimes drove diverging patterns of microbial community composition and activity (11). Exposure to synthetic dispersant alone did not enhance heterotrophic microbial activity or hydrocarbon oxidation rates (10) but did increase the abundance of particular taxa (*e.g.*, *Colwellia*). In contrast, exposure to oil, but not dispersants, increased abundance of other taxa (*e.g., Marinobacter*) and oil also stimulated oxidation rates of hydrocarbons. Here, we advance the findings of Kleindienst et al. (10) by interpreting metatranscriptomic data from their experiment to explore how and why specific components of the microbial community responded to distinct exposure regimes.

3.2 Results

Transcriptomic libraries (n=27) ranged in size from 4.6 to 18.75 million reads, with a mean of 10.58 million reads per sample and an average read length of 97 bp. About 44.38% of reads remained after quality control and removal of sequencing artifacts and duplicates (Supplementary Figure S3.1 A). Predicted features were assigned to 68% of these reads, and

2.74% of reads were associated with rRNA transcripts (Supplementary Figure S3.1 B). In total, 11.3 million reads mapped taxonomic features with an average of 1,638 reads assigned to archaea, 403,781 reads assigned to bacteria, 5,357 reads assigned to eukaryotes, and 10,542 reads assigned to viruses. Roughly 3.1 million reads per library were annotated at the functional level (Supplementary Figure S3.1 B). Further analysis on a functional or taxonomic level used normalized mRNA read counts assigned to known functions or taxa, respectively (Supplementary Data 1). The distribution of unique annotation features across the database sources was: NR-Blast, 18,869; UNIPROT, 16,547; KO, 2,963; GO, 5,387; COG, 6,468; and eggNOG 3,822 (Supplementary Data 1). On average, metabolism was the functional category with the largest fraction of mapped reads from the COG (41.8%) and KEGG (48.1%) annotations; while the information, storage, and processes category was the top hit mapping category with the eggNOG database (78.6%) (Supplementary Figure S3.2).

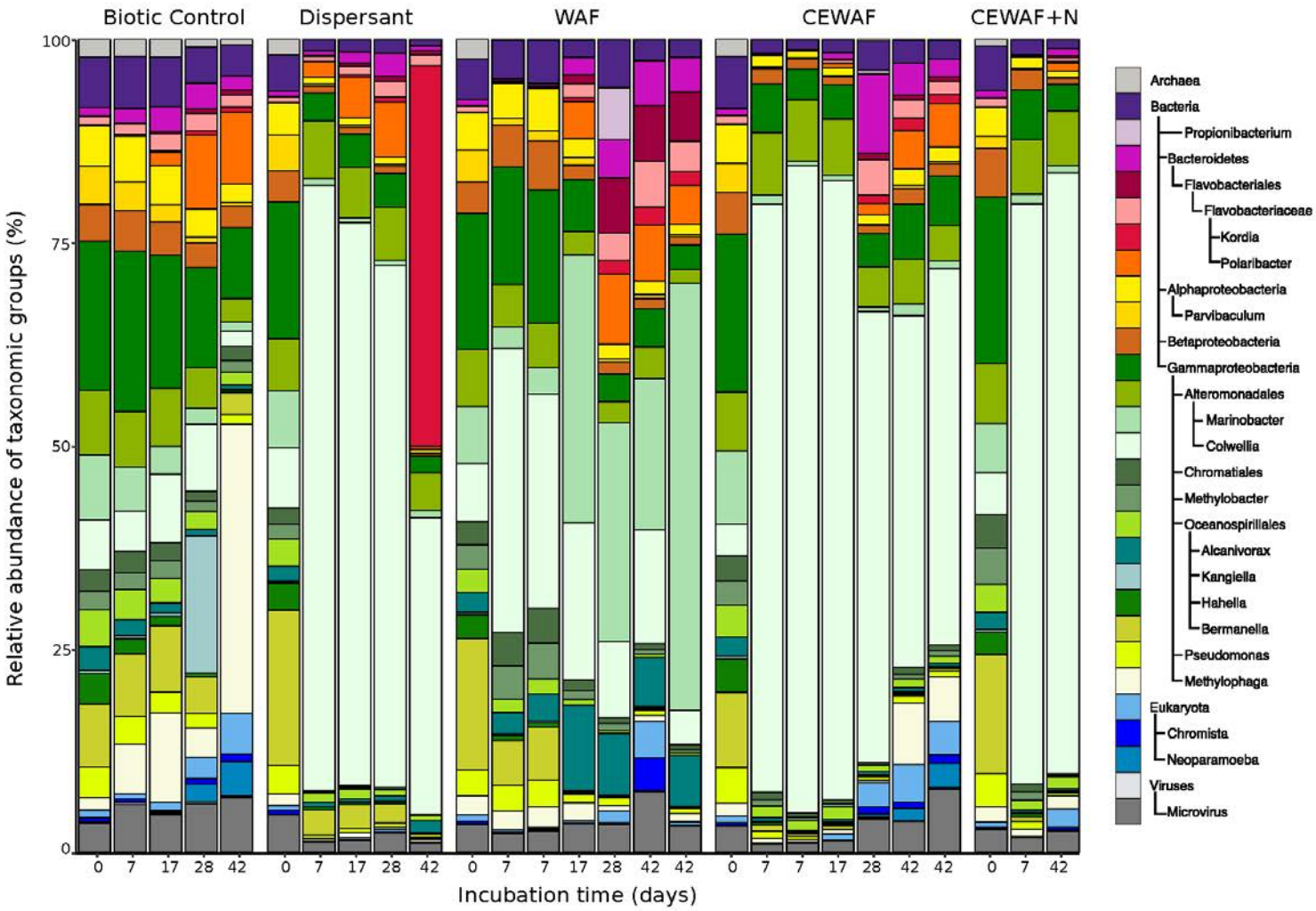

Figure 3.1. Relative abundance of merged taxonomic ranks in the K2015 metatranscriptomic libraries at a minimum allowed resolution of 4% based on taxonomy assignment performed in MG-RAST.

Rarefaction analysis provided insight on the influence of chemical exposure on the richness saturation index in each treatment. Except for the biotic control and dispersant treatments, the samples showed differences of more than 1,000 species between the early stages of the experiment (t_0, t_1) and the end of the experiment (t_4), possibly driven to some degree by limitations in sequencing depth or inherent variability on diversity richness at a given sample (Supplementary Figure S3.3). Most of the trends in the biotic control followed a similar rarefaction trend, although the α-diversity index decreased from 250 to 200 during the experiment (Supplementary Figure S3.3, F). For instance, using a sampling depth of 13.9 million reads as the cutoff, after 42 days of dispersant exposure, only ~4,095 species were recovered (*i.e.,* α-diversity = 27); this was the lowest number compared to the WAF (~5,000 species), CEWAF (~6,000 species) and CEWAF+nutrients (~5,000 species) treatments (Supplementary Figure S3.3). Interestingly, the α-diversity index for the CEWAF(±nutrients) treatments increased over time, while the rest of the treatments declined over time (Supplementary Figure S3.3, F).

Exposure to synthetic dispersants generated taxa-specific responses in expression that modulated the community response to different chemical combinations of oil and/or dispersant. The taxonomic profile of the active population identified by the annotated transcripts resembled the community structure shown through 16S rRNA gene sequencing (10). The rarefaction analysis showed decreased diversity in the dispersants-only and oil-only treatments (Supplementary Figure S3.3). All dispersant amended samples showed transcriptional enrichment for *Colwellia,* an organism known for its role in hydrocarbon and dispersant degradation (12). After one week, the relative abundance of *Colwellia* transcripts increased from 3.9–7.4% to 71.4–79.6% in dispersant-only and CEWAF ±nutrients treatments (Figure 3.1) and

from 7.2% to 26.3–34.9% in WAF treatments. *Colwellia* showed a more substantial increase in gene expression (by 30.6%) than in abundance (16S rRNA gene counts increased by 2.5%) in the WAF treatment. *Marinobacter* accounted for most of the increase in transcriptional signals in WAF treatments, with a relative increase from 7.0% to 18.7–52.5% after four weeks (Figure 3.1). In dispersant-only and CEWAF ± nutrients treatments, *Marinobacter* transcripts decreased from 6.0–9.0% to 0.5–0.8%. After the first week, the *Colwellia* transcriptomic response declined in WAF treatments while that of *Marinobacter* increased. After six weeks of dispersant-only exposure, increased expression (up by 46.8%) by *Kordia* was observed; this relative increase was far more pronounced than the relative 16S rRNA gene counts of *Kordia* (up by 11.8%) (10).

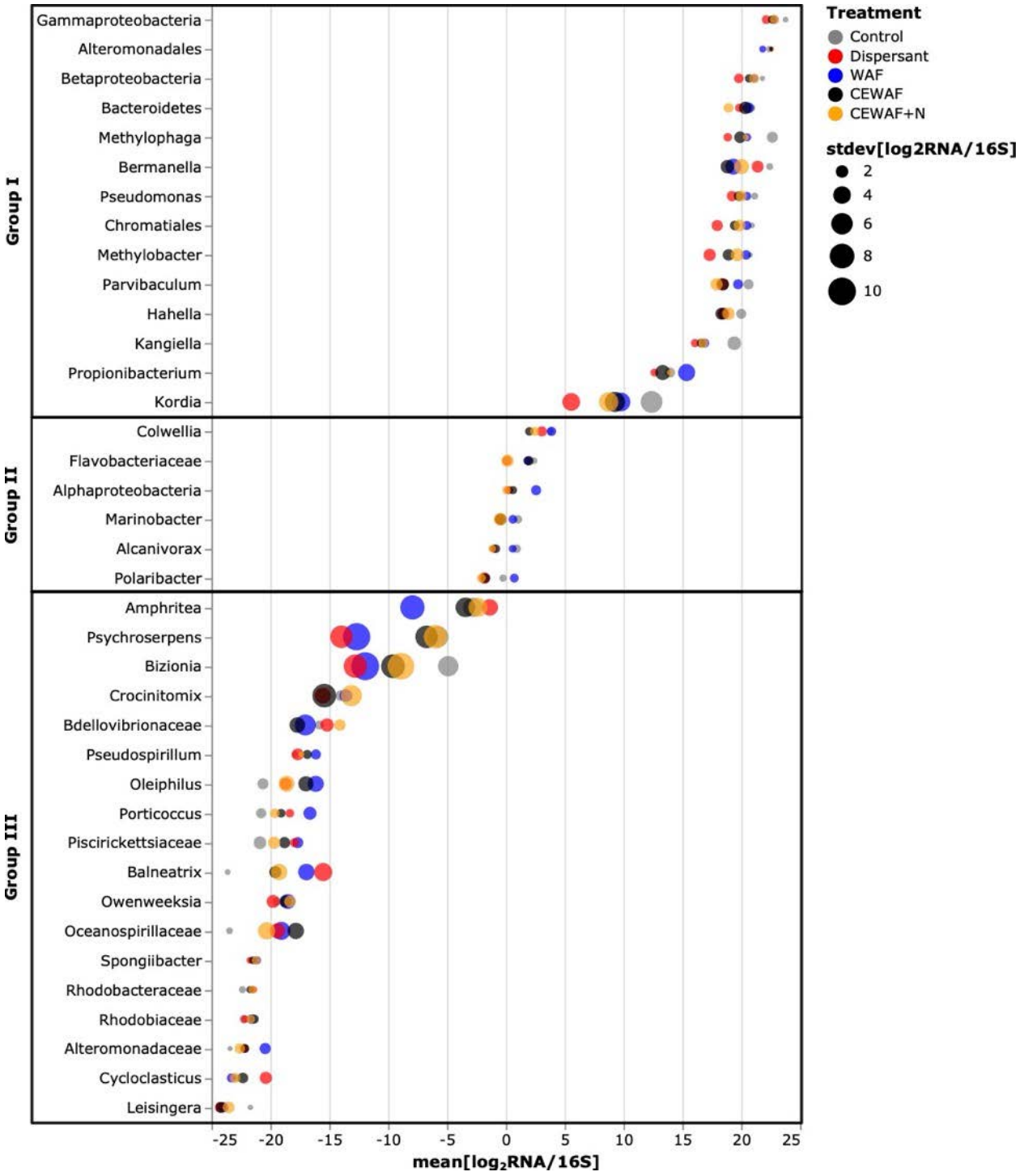

Figure 3.2. Indigenous hydrocarbon degraders are consistently found in 16S rRNA gene sequences as well as in transcriptomic libraries. Log-transformed RNA:DNA ratio (LRD ratio) distribution across K2015 metatranscriptomic libraries. Taxonomic groups are sorted from top to bottom by descending mean of LRD scores. Biosynthetic capacity estimation is expected to be Group I > Group II > Group III.

To estimate the level of correspondence between transcriptomic and 16S rRNA gene signals (10), the mean log-transformed RNA:DNA ratio (LRD ratio) across treatments was calculated. The largest fraction of relative counts at the transcriptomic and 16S rRNA gene level were distributed proportionately across treatments (Figure 3.2 Group II: $|LRD| < 5$), including many indigenous hydrocarbon degraders as well as *Marinobacter* and *Colwellia*. The group of organisms had a larger relative synthetic capacity (Figure 3.2 Group I: $LRD > 5$) was comprised of members associated typically with methylotrophic metabolism (*Methylophaga*, *Methylobacter*), oil influence (*Bermanella),* hydrocarbon degradation (*Pseudomonas),* and alkylbenzenesulfonate degradation (*Parvibaculum*) (13). Organisms with a low LRD index (Figure 3.2 Group III: $LRD < 5$) included members of the family *Oceanospirillaceae,* such as *Amphritea, Pseudospirillum,* and *Balneatrix*, hydrocarbon degraders, including *Oleiphilus, Porticoccus, Cycloclasticus, Rhodobacteraceae, Rhodobiaceae,* and *Alteromonadaceae*, and members of *Flavobacteria, Bacteroidetes, Bdellovibrionaceae,* and *Spongibacter.*

Beta-diversity was assessed via Bray-Curtis dissimilarity-based principal component analysis (PCA) of metatranscriptomic reads (Figure 3.3 A). Consistent with the taxonomic profile (Figure 3.1**)**, all treatments amended with dispersants clustered with *Colwellia*. Oil-only samples occupied a separate cluster transitioning over time from a broad positive association with *Gammaproteobacteria* towards a positive association with *Marinobacter* specifically. A third cluster comprising the biotic control spanned a positive association with *Gammaproteobacteria* with small positive contributions from *Marinobacter, Bacteroidetes*, *Polaribacter, Flavobacteriales,* and *Alcanivorax.*

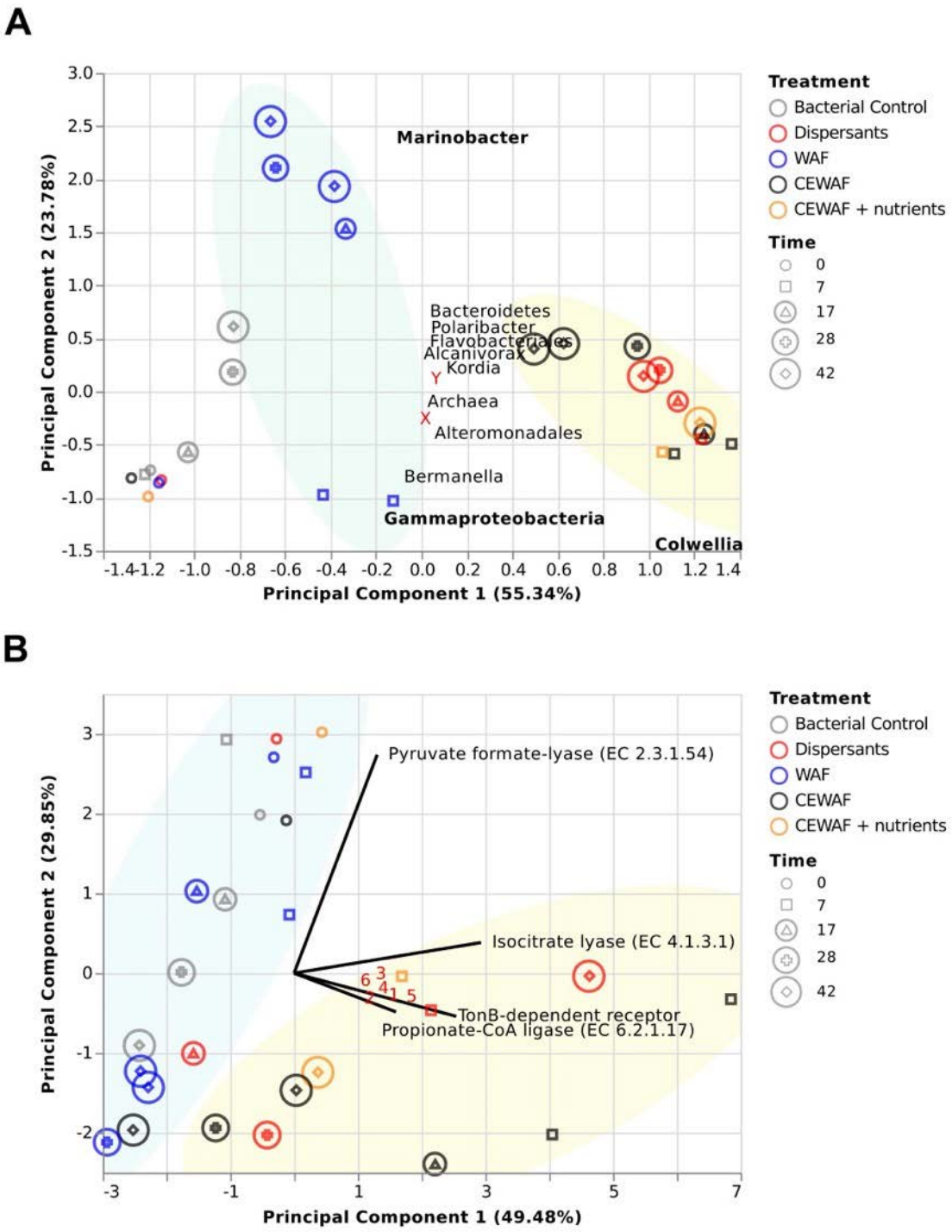
A
Marinobacter
Bacteroidetes
Polaribacter
Flavobacteriales
Alcanivorax
Kordia
Archaea
Alteromonadales
Bermanella
Gammaproteobacteria
Colwellia
Principal Component 2 (23.78%)
Principal Component 1 (55.34%)
Treatment
Bacterial Control
Dispersants
WAF
CEWAF
CEWAF + nutrients
Time
0
7
17
28
42
B
Pyruvate formate-lyase (EC 2.3.1.54)
Isocitrate lyase (EC 4.1.3.1)
TonB-dependent receptor
Propionate-CoA ligase (EC 6.2.1.17)
Principal Component 2 (29.85%)
Principal Component 1 (49.48%)
Treatment
Bacterial Control
Dispersants
WAF
CEWAF
CEWAF + nutrients
Time
0
7
17
28
42

Figure 3.3. Diversity and functional dimensional analysis of the K2015 metatranscriptomic dataset. A) Principal coordinates analysis of relative abundance of taxonomic groups. Nearby the X label, we found the following microbial groups: *Alphaproteobacteria, Betaproteobacteria, Oceanospirillales, Methylobacter, Parvibaculum*, Chromatiales, *Hahella*. Nearby the Y label, we found the following microbial groups: *Neoparamoeba, Kangiella, Methylophaga, Chromista, Propionibacterium*, and *Microvirus* B) Functional expression of gene abundances assigned to the SEED subsystems: motility and chemotaxis, carbohydrates, membrane transport, and respiration. Solid lines represent the top ten loading vectors explaining the variation of expressed genes in the analysis. Numbers in red are as follows, 1: 2-methylcitrate dehydratase FeS (EC 4.2.1.79), 2: Acetoacetyl-CoA reductase (EC 1.1.1.36), 3: Aconitate hydratase 2 (EC 4.2.1.3), 4: Acetolactase synthase large subunit (EC 2.2.1.6), 5: Acetyl-coenzyme A synthetase (EC 6.2.1.1), and 6: Malate synthase G (EC 2.3.3.9).

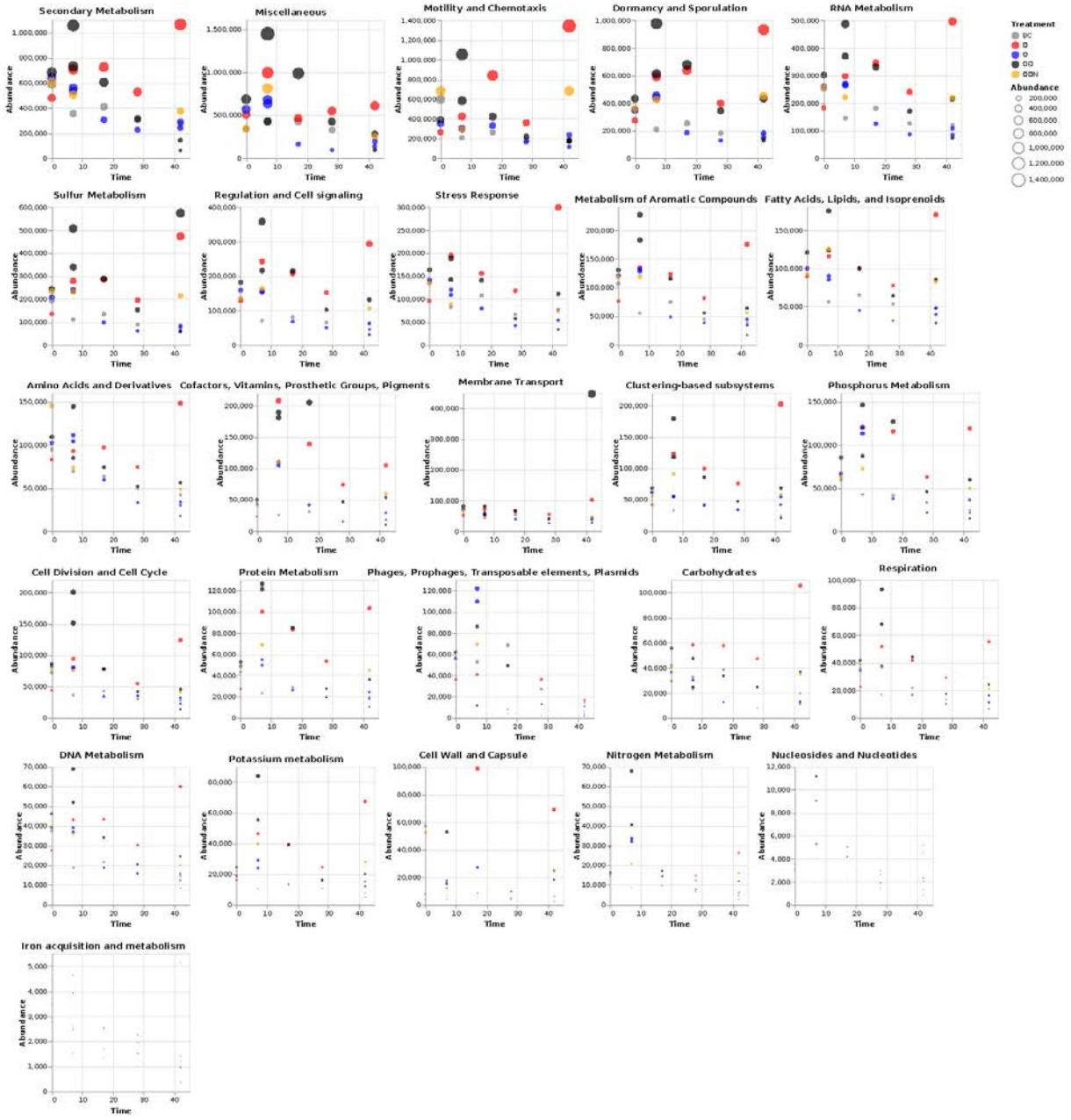

Figure 3.4. Abundance of gene expression based on automated SEED subsystems in MG-RAST for the K2015 metatranscriptomic data set. Observations are color-coded by treatment: Biotic control (BC), Dispersants (D), Oil (O), CEWAF (OD), CEWAF+N (ODN). Dot sizes are proportional to the absolute abundance in a library.

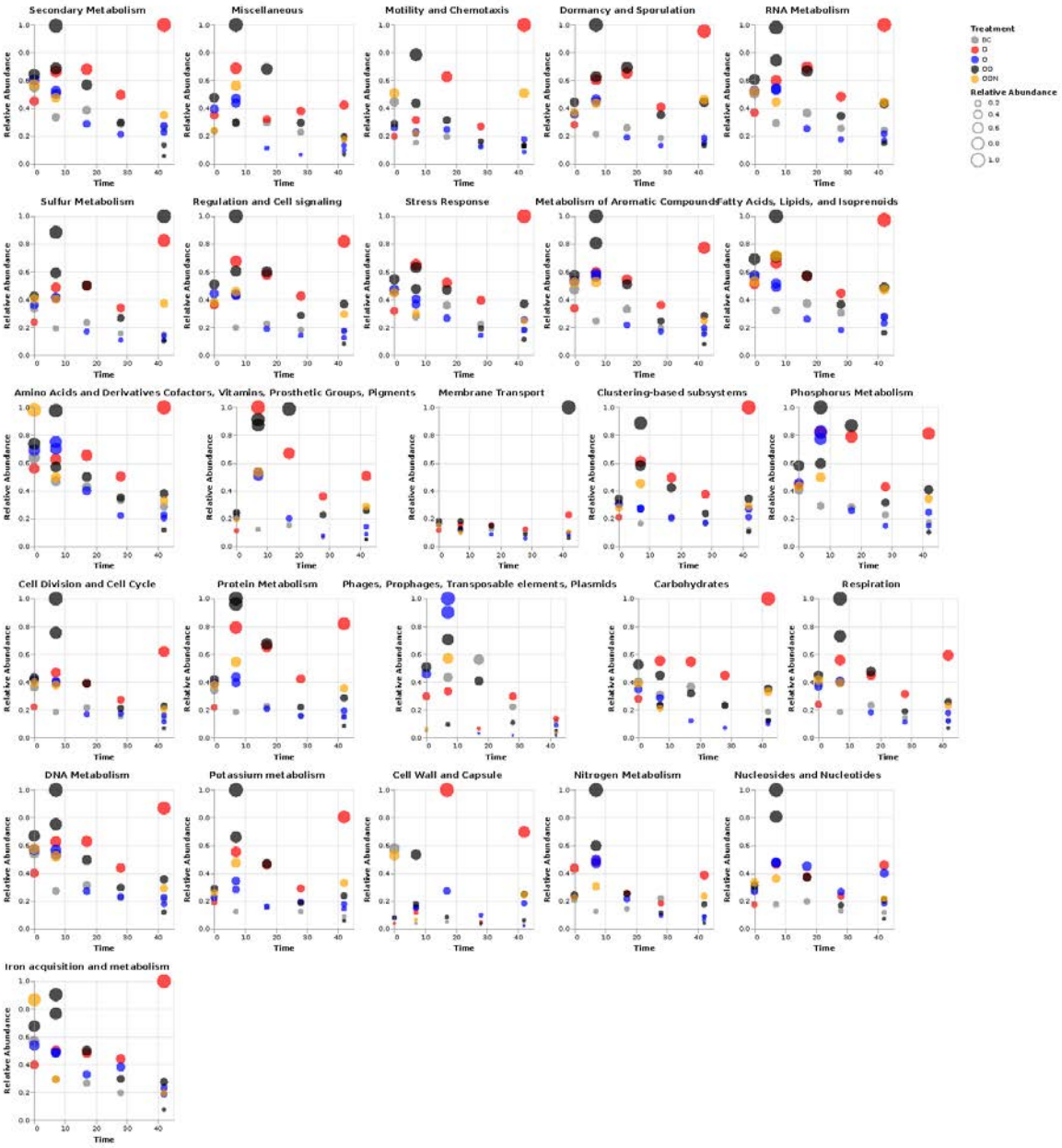

Figure 3.5. Relative gene expression based on automated SEED subsystems in MG-RAST for the K2015 metatranscriptomic data set. Profiles are normalized with respect to the largest expression peak at a given functional category across all treatments. Observations are color-coded by treatment: Biotic control (BC), Dispersants (D), Oil (O), CEWAF (OD), CEWAF+N (ODN). Dot sizes are proportional to the relative abundance score.

To assess effects of chemical exposure and time, we performed a permutational multivariate analysis of variance (PERMANOVA) on I) taxonomic dissimilarity (*i.e.*, Bray-Curtis) distances, and II) phylogenetic dissimilarity via weighted mean pairwise distances (MPD) and weighted mean nearest taxon distances (MNTD). Dispersant ($p = 0.001$) and time ($p = 0.001$) terms significantly explained the variability of the Bray-Curtis distances profile. Similarly, dispersant ($p = 0.001$), time ($p = 0.015$), and dispersant × time ($p = 0.037$) explained the MPD phylogenetic distance profile. In contrast, oil × time ($p = 0.010$) and dispersant × oil × time ($p = 0.005$) explained the MNTD phylogenetic distance profile, indicating that higher levels of dissimilar transcriptional responses were observed in dispersant treatments and over time. By weighting transcriptional abundances and phylogenetic proximity among taxa, we observed that the interaction terms oil × time and dispersant × oil × time became significant for explaining MNTD dissimilarity distances in the dataset. The interaction of oil ± dispersants and time was correlated significantly with changes in the phylogenetic distances associated with the evolution of the microbial community.

The metatranscriptomic libraries showed major functional enrichment in the areas of secondary metabolism, motility, and chemotaxis, dormancy and sporulation, sulfur metabolism, and stress response categories; ranging around ~300k to over 1 million mapping reads at peak expression across treatments (Figure 3.4). Functional category profiles were also apparent after normalization with respect to the largest expression peak at a given functional category across all treatments (Figure 3.5). In the first two weeks after chemical exposure, the CEWAF treatment exhibited a relative expression increase in 20 functional categories (Figures 3.4 and 3.5), including secondary metabolism, motility, and chemotaxis, dormancy, sporulation, sulfur metabolism, and stress response categories. In contrast, the dispersant treatment showed a

delayed transcriptional response in the same categories. In 17 out of 20 categories, two behaviors occurred: (1) a fast, strong response near t_1 and then a decay for the CEWAF treatment, and (2) a slow incremental response with a maximum peak at t_4 for the dispersant treatment. Phages, prophages, transposable elements, and plasmids were the only functional category where the oil-only treatment showed the largest relative expression peak across treatments. The relative expression of cofactors, vitamins, and prosthetic groups increased in the first weeks followed by a decrease towards the end of the experiment for all treatments, except the biotic control. Here we also observed a signature expression of tryptophan halogenase, precursor of the antibiotic pyrrolnitrin, in *Colwellia* in all the dispersant amended treatments, suggesting an effort by *Colwellia* to inhibit competition by other microorganisms. The expression of the tryptophan halogenase coding genes is associated with the accessory component of the *Colwellia* pangenome (Peña-Montenegro et al., parallel submission to *Science*).

To further assess the influence of the chemical exposure on the metabolic variation among the metatranscriptomes, a PCA of the functional features abundance across the SEED annotation levels was conducted (Figures 3.3 B, 3.4, Supplementary Results). Dispersant amended samples showed a transcriptional divergence away from samples lacking dispersants (*i.e.*, WAF and biotic controls) at the level of functions of major non-housekeeping modules (Figure 3.3 B). Biotic control and WAF libraries showed similar clustering trends along the Pyruvate Formate Lyase (PFL) (E.C. 2.3.1.54) loading vector. Higher expression of PFL was strongly associated with the t_0 libraries. On the other hand, CEWAF (t_1, t_2) and dispersants (t_4) samples showed a strong positive association with PC1, supported by the contribution of isocitrate lyase (EC 4.1.3.1), TonB-dependent receptor (TBDR), propionate-CoA ligase (E.C. 6.2.1.17), and other features involved in the biosynthesis of amino acids; biosynthesis of storage

compounds (*i.e.*, polyhydroxybutanoate biosynthesis via acetoacetyl-CoA reductase E.C. 1.1.1.36); generation of metabolite and energy precursors; and degradation of carboxylates, carbohydrates, and alcohols.

Transcription profiles in dispersant treatments followed a different trend in the clustering space compared to the CEWAF treatments (Supplementary Figure 3.4B) early in the experiment (*i.e.*, t_1) when stronger transcriptomic responses were apparent in CEWAF amended samples. The dispersants-only samples showed stronger transcriptomic signals towards the end of the experiment (*i.e.*, t_4). Over time, transcriptional profiles shifted toward a negative association with PC1 and PC2 for all except the dispersant-only treatments, potentially indicating systematic transcriptional changes associated with the transition from an open-water system to a microcosm setting.

Forty-seven differentially expressed genes associated to viruses or prophages were identified in the transcriptomic dataset, ranging from 8 (WAF treatment) to 17 (CEWAF+N) genes per treatment (Figure 3.6, Supplementary Data 1). The two most common DE genes were Hsp70 (n=6) and PQQ (n=6), although several genes were frequently perturbed across treatments (e.g., GDCP n=4, SDR n=3, TPP n=3, RpB1 n=3). In terms of taxonomy, 55.3% of the DE viral genes were assigned to Megaviruses or Jumbophages. The rest of the DE viral diversity was covered by Cyanobacteria-host viruses (12.8%), Myoviridae, Enterobacterales-host viruses, and other viral groups including *Chrysochromulina ericina* virus (17%). The majority of the DE genes were upregulated (78.7%), and similarly, the majority of viral DE genes for the WAF, Dispersants, and CEWAF treatments were upregulated.

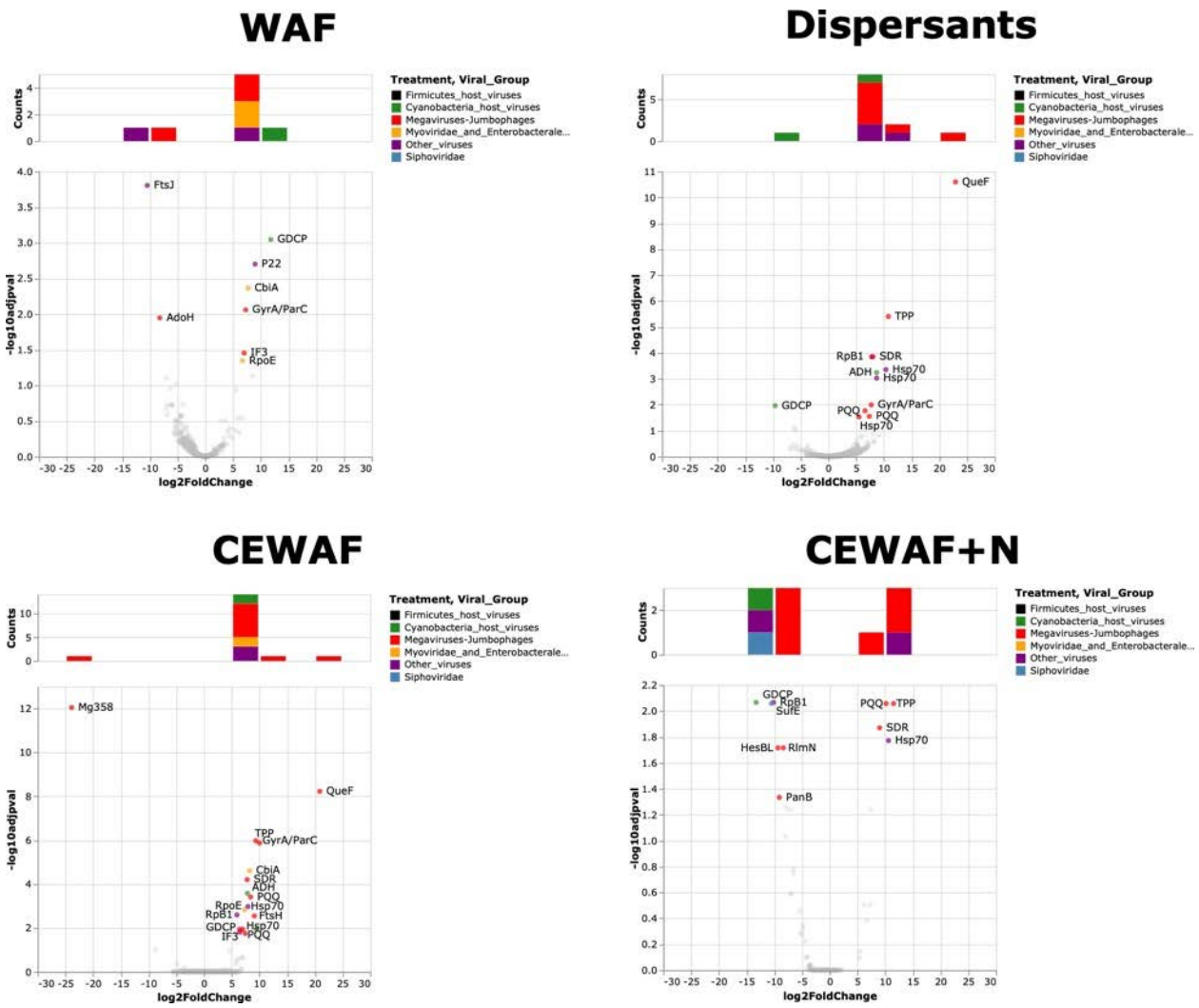

Figure 3.6. Volcano plots of genes assigned to viruses or prophages. Genes with an adj-p-value<0.5 were considered differentially expressed and are highlighted with their assigned functional and viral group. Histograms on top of each volcano plot represent the distribution of DE genes by viral group and log2FoldChange.

The stress response chaperon protein Hsp70 was consistently upregulated in all the treatments, and it was associated to a *Chrysochromulina ericina* virus or a *Bathycoccus* sp. RCC1105 virus BpV1 (Supplementary Data 1). Similarly, the quinoprotein ethanol dehydrogenase PQQ was upregulated in all the treatments, and it was associated to *Pandoravirus inopinatum* or *Pithovirus sibericum*, both classified as Megaviruses (14). As expected, genes

involved in translation, transcription, and replication such as GyrA, RpB1, RpoE, Mg358, and IF3 dominated the upregulation of viral genes for the WAF, dispersant, and CEWAF treatments.

A few viral signatures were exclusively significant for certain species and treatments. An AdoH-AhcY ortholog, with strong similarities to SAH hydrolases of potent antiviral activity (15), were exclusively downregulated only in the WAF treatment. This result could suggest that dispersants inhibit natural antiviral genes acting in place. Similarly, the major capsid gene P22 associated to the *Alteromonas* phage vB_AmaP_AD45-P1 was only upregulated in the WAF treatment.

3.3 Discussion

Detailed analyses of metatranscriptomic data from the Kleindienst et al. (10) microcosm experiment revealed interesting dynamics that were not obvious in the initial assessment of the microbial response to different cocktails of organic matter. This new information elucidates the underlying modes of response of the microbial population to differential exposure of oil, dispersant, and nutrients. Dispersants alone selected for a unique community and for dominant organisms that reflected unique treatment- and time-dependent responses. Similarly, oil alone selected for a community that was distinct from treatments amended with dispersants. In particular, dispersant- versus oil- amended treatments selected for different dominant taxa, with *Colwellia* dominating dispersant treatments and Marinobacter dominating oil-only treatments, mirroring the results of Kleindienst et al. (10). The species-specific responses of these two dominant microorganisms are presented separately (Peña-Montenegro et al. under review), but general aspects of their response are presented here. Dispersant amendment also led to diverging functional profiles amongst the different treatments. The presence of oil and dispersants with

added nutrients led to substantial differences in microbial responses, likely reflecting increased fitness driven by additional inorganic nutrients. Finally, the oil-only additions led to fascinating increases in the expression of phages, prophages, transposable elements, and plasmids, suggesting that aspects of microbial community response to oil are driven by the 'mobilome' (16), mobile genetic elements in the microbiome.

Dispersants altered the expression of key microorganisms – Colwellia and Marinobacter

Comparison of results from 16S rRNA gene sequencing and metatranscriptomic libraries from the Kleindienst et al. (11) experiment provided insight into the response of microbial communities to an environmental perturbation, in this case, exposure to differential cocktails of organic carbon that were derived from oil and/or dispersant. Based on 16S rDNA gene sequence data, two microorganisms – *Colwellia* and *Marinobacter* - dominated in different treatments: *Colwellia* was more abundant in dispersant amended treatments while *Marinobacter* was more abundant in oil amended treatments. Metatranscriptomics data help explain the differential success of these organisms (Peña-Montenegro et al. under review) to the experimental treatment regime.

The presence of dispersant increased transcriptomic activity of *Colwellia* spp. (Figure 3.1, Figure 3.3), confirming the results from the original microcosm paper (10) that documented increases in *Colwellia* using 16S rDNA gene sequence data. Similar increases in abundance of *Colwellia* in samples from the Deepwater Horizon ~1,000 m deep hydrocarbon plume that was enriched with oil (17), low molecular weight dissolved alkanes (18), and a key component of the synthetic dispersant Corexit, dioctyl sodium sulfosuccinate, DOSS (19). *Colwellia* is able to

thrive under conditions of low temperature and high loading of hydrocarbon and dispersant (20, 21).

Colwellia is a psychrophile that possesses substantial metabolic flexibility (22, 23). Genomic data illustrates a broad metabolic potential for *Colwellia* since its genome encodes the capacity for fermentation (propionate catabolism), beta-oxidation of fatty acids, glycolysis, the tricarboxylic acid cycle, and the pentose phosphate cycle (22). Previous studies have shown that *Colwellia* easily metabolizes glucose, acetate, and lactate (23); furthermore, *Colwellia* may play a role in ethane and propane cycling (20). *Colwellia* produces polyhydroxyalkanoates as carbon and energy reserves, potentially accounting for the documented upregulation of these compounds in dispersant amended treatments (Figure 3.3 B). *Colwellia* is particularly well-suited for polyhydroxyalkanoate production. The *C. psychrerythraea* genome (22) contains a diverse suite of genes involved in polyhydroxyalkanoate metabolism, including several that lack homologs in other lineages. Though *Colwellia* spp. have not been shown to oxidize oil- or dispersant- derived organic compounds, genomic data suggests that these microbes could play important roles either in primary or secondary oxidation of oil- and dispersant- derived organic matter (22).

Marinobacter is one of the most common genera found in the global ocean and, as such, plays an important role in pelagic biogeochemical cycles (24). Dubbed a biogeochemical 'opportunitroph', *Marinobacter* exploits a number of environmental niches and survives, even thrives, under a diverse array of conditions (24). *Marinobacter* is known to oxidize saturated hydrocarbons (alkanes), cycloalkanes, aromatics (toluene, polycyclic aromatic hydrocarbons) through coupling to aerobic or anaerobic (nitrate reduction) respiration. Unlike *Colwellia*, *Marinobacter* is not a psychrophile. It is quite the opposite; *Marinobacter* can thrive in surface and deep waters, in deep-sea sediments, as well as in beach sands.

The addition of dissolved oil as a WAF without dispersants stimulated *Marinobacter*'s transcriptomic signals (Figure 3.1, Figure 3.3). In contrast to *Colwellia*, dispersants limited the growth and replication of *Marinobacter* (10) and muted their transcriptional activity. The stimulation of *Marinobacter's* growth in oil-exposed microcosms, in the absence of dispersants, is consistent with reports of *Marinobacter* thriving in oil-rich marine snow flocs generated in the laboratory (25) and in pyrosequencing surveys of *in situ* seawater samples impacted by the Deepwater Horizon oil spill (26, 27). The transcriptomic data suggests that the reduction in *Marinobacter* abundance and activity (10) was not due to competition with *Colwellia* but rather a function of reduced activity, as evidenced by the decrease of transcriptional signal in dispersant treatments. This pattern suggests that dispersants inhibited the metabolic activity of the cosmopolitan oil degrader, *Marinobacter*, reducing its role in oil degradation in treatments amended with dispersants.

Chemical exposure led to rapidly diverging functional profiles

Analyzing the metatranscriptomic data from the Kleindienst et al. (10) experiment also revealed the ecophysiological responses of all microbial groups. The log-transformed RNA:DNA ratio (LRD ratio) assesses ecophysiological activity where a higher relative cell synthetic capacity, *e.g.*, higher transcription read counts (RNA) relative to DNA, correlates with growth and nutritional status (28, 29). The underlying assumption of the LRD is that the amount of DNA in a system is stable under changing environmental conditions, while that the amount of RNA is altered in response to changing conditions. Relatively speaking, organisms thriving under a certain set of conditions will have a higher LRD ratio, while organisms poorly adapted to a given set of conditions will have a lower LRD ratio.

The LRD Group-I, with LRD>5, likely contained highly active microorganisms given the extreme enrichment of transcription read counts over 16S rRNA gene read counts (Figure 3.2). Methylotrophs (*i.e*., *Methylophaga*, *Methylobacter*) and native hydrocarbon degraders (*i.e*., *Bermanella* and *Parvibaculum*) were affiliated with this group (13, 30), consistent with previous reports of active indigenous oil degraders including members of these genera (31). *Methylophaga* was also stimulated by the by-products of high molecular weight dissolved organic matter metabolism in seawater, suggesting that they are important components of aerobic microbial associations that play key roles in organic carbon turnover (11).

To the best of our knowledge, this is the first report of transcriptional enrichment of *Kordia* in response to dispersants (Figure 3.1). Previous studies reported ecological succession of bacterial clades with Flavobacteriaceae and Rhodobacteraceae in late August and September 2010 (32, 33). *Kordia*, a member of the Flavobacteriaceae family, was recently described at the pangenomic level (34), revealing that its core pangenome comprised a large fraction of cell wall and membrane biogenesis genes, peptidase, and TBDR encoding genes. At t_4 in the dispersants-only treatment, *Kordia* increased transcriptional activity of TBDR, glyoxylate shunt, membrane biogenesis, and peptidase biosynthesis (Figures 3.3 B, 3.4, and 3.5), matching previous descriptions of *Kordia* as an active player in niche colonization (34). Interestingly, the role of *Kordia* in the dispersants treatment was not apparent from the 16S rDNA gene sequence data. Clearly, the role of *Kordia* in dispersant degradation warrants further exploration.

LRD Group-II contained taxa with the largest contribution to the microbial transcriptomic profile, underscoring its effective and rapid response to the different chemical cocktails. This group included indigenous hydrocarbon degraders *Oceanospirillales*, *Marinobacter*, *Alcanivorax,* and *Polaribacter,* as well as *Colwellia* and *Marinobacter* (Figure

3.2), as did several other known oil degraders, *Alcanivorax*, a slow-growing n-alkane degrading member of the Gammaproteobacteria (35), and *Polaribacter*, a member of the Flavobacteria known to degrade polysaccharides (36) as well as hydrocarbons (9). The LRD Group-II also included various members of the Flavobacteriaceae, the largest family in the phylum Bacteroidetes with members capable of aerobic and microaerophilic degradation of polysaccharides and members of the Alphaproteobacteria, a class of metabolically diverse microorganisms.

Members of LRD Group-III were poorly adapted for the experimental conditions, relative to members of LRD Group-I and LRD Group-II. LRD Group-III included members of the family *Oceanospirillaceae,* such as *Amphritea, Pseudospirillum,* and *Balneatrix*, hydrocarbon degraders, including *Oleiphilus, Porticoccus, Cycloclasticus, Rhodobacteraceae, Rhodobiaceae,* and *Alteromonadaceae*, and members of *Flavobacteria, Bacteroidetes, Bdellovibrionaceae* and *Spongibacter* (Figure 3.2). Many hydrocarbon degraders are slow-growing in nature, and membership in LRD Group-III could reflect time-sensitive, adaptive responses that occur in different groups of hydrocarbon-degrading bacteria over longer time scales. This pattern may also reflect specific niche adaptation strategies in hydrocarbon-degrading microbial communities.

From metabolic variations across treatments to viral-phage DE genes

The strongest transcriptomic signals were observed in the Secondary Metabolism, Miscellaneous, Motility and Chemotaxis, Dormancy and Sporulation and RNA Metabolism categories (Figure 3.4). Over time, the trends usually showed an expression peak either near t_1 for the CEWAF treatment or towards t_4 for the Dispersants treatment. The unique trajectories observed in the expression profiles across treatments suggest that different cocktails of complex

organic carbon led to distinct time-dependent responses of the microbial populations. These results are consistent with significant shifts observed in the DEM-pangenome of *Colwellia* and *Marinobacter* (Peña-Montenegro et al., under review), as well as the clustering transitions of taxonomic and functional profiles in the microbial community (Figure 3.3)

By the inspection of relative counts of transcriptional signals, we observed common trends across functional groups, such as secondary metabolism, dormancy and sporulation, RNA metabolism, regulation, and cell signaling, metabolism of aromatic compounds, among others (Figure 3.5). These results would suggest a regulation network acting simultaneously upon several metabolic functions of the community. In contrast, other functional categories showed different transcriptional profiles. For instance, phages, prophages, transposable elements, and plasmids, was the only functional group where the WAF treatment reached the largest relative abundance after one week of incubation. Cell wall and capsule category showed the largest relative abundance for the dispersant-only treatment at t_3 and t_4.

Pyrrolnitrin is a secondary metabolite derived from tryptophan and was first isolated from *Pseudomonas pyrrocinia*. It is described as a broad-spectrum antifungal and antibacterial agent with application to control soilborne pathogens and postharvest diseases, including *Rhizoctonia solani* and *Botrytis cinerea* (37). It has been used to treat human infections by opportunistic fungi due to its very low toxicity to animals and humans. Pyrrolnitrin has a relatively short half-life in the environment, and it is currently used as precursor of the widely used fungicide fludioxonil (38). Finding the association of the expression of genes involved in the biosynthesis of pyrrolnitrin with the accessory DEM-pangenome of *Colwellia* (Peña-Montenegro, parallel submission to *Science*) suggests that this antibiotic could serve as a competitive agent to improve the ecological fitness of *Colwellia* in polluted environments.

We selected the gene counts associated to phages or viruses after performing DE analysis on the complete dataset to inspect their expression. The megaviruses and jumbophages were the only functional group that showed the highest relative peak in the oil-only treatment (Figures 3.5). Further inspection of DE genes assigned to viral groups revealed that viral DE genes were upregulated in all of the amended treatments, while downregulation was observed only in the CEWAF+N treatment (Figure 3.6).

Megaviruses are important, yet poorly understood, components of ocean ecosystems (14, 16, 39, 40). Megaviruses can infect the ciliate and flagellate grazers that impart top-down control on microbial populations (41, 42). As such, an intriguing possibility is that the stimulation of megaviruses in response to oil exposure could relax predation and allow populations of oil degraders to bloom in the absence of predation. Megaviruses could serve as key components of the system, serving to promote the success of oil-degrading microbial communities in a direct fashion (43). Genomic comparisons of megaviruses isolated in coastal waters revealed the paradox of megaviruses showing convergent evolution while the number of unique protein-coding genes overwhelmingly outnumbers their core genes (44). This data set offers a first look at the role of megaviruses through the lens of a metatranscriptomic dataset. Further megavirus DEM-pangenome analysis is under development by Peña-Montenegro et al. (parallel submission to *Science*).

The viral repertoire was different in the CEWAF versus the CEWAF+nutrient treatment. The inherent stress imposed on the microbial community through nutrient limitation appears to have led to a more substantial viral-induced stress response in the CEWAF treatment, as revealed by a direct comparison to results from the CEWAF+nutrient treatment (Figure 3.6). Previous studies showed the influence of environmental conditions on the relationship between viruses

and bacteria using multivariate models demonstrating that environmental factors, such as inorganic nutrient concentrations, are important predictors of host and viral abundance across a broad range of temporal and spatial scales. (45). Similarly, trophic interactions in the microbial food web, such as predation and the availability of limiting nutrients, affected the structure and function of viral and prokaryote communities (46). We suspect that nutrient limitation in the face of labile organic carbon loading triggered stress-responses in the microbial communities, with a collateral effect on the activation of viral communities.

3.4. Conclusions

Comparison of results from 16S rRNA gene sequencing and metatranscriptomic libraries from the Kleindienst et al. (11) experiment provided insight into the response of microbial communities to an environmental perturbation, in this case, exposure to differential cocktails of organic carbon that were derived from oil and/or dispersant. The presence of dispersant increased transcriptomic activity of *Colwellia* spp., and *Colwellia* may have been involved in the degradation of oil or dispersant components in the microcosms, as well as in field samples (20, 21). In contrast, dispersants limited the growth and replication of *Marinobacter* (10) and also muted their transcriptional activity, reducing its role in oil degradation in treatments amended with dispersants. The LRD ratio proved to be a valid tool to assess the relative ecophysiological activity level of microbial groups across treatments and in response to nutritional status and showed that some oil-degrading microorganisms are more adept at responding to oil or oil plus dispersant exposure than others. Transcriptional data revealed a potentially important role for *Kordia* in metabolism of dispersant-derived organic matter; the importance of these organisms was not clear from 16S rRNA gene composition data. The upregulation of genes from

megaviruses, especially oin oil only treatments, suggest and important role for this organisms in shaping the oil-spill-perturbed microbiome. Accelerated activity of megaviruses could relieve grazing pressure on oil-degrading microorganisms, hence promoting their rapid growth in response to oil infusions. The presence of dispersants may inhibit this, which could explain why different microbial populations thrive under conditions of oil versus dispersant exposure.

3.5 Methods

Filters were frozen in liquid nitrogen, kept on dry ice for shipping and stored in the laboratory at -80°C. RNA was purified from filters using the Trizol reagent (Life Technologies; Carlsbad, CA, USA) and treated with DNase (Qiagen, Valencia, CA, USA). RNA quality was analyzed using a 2100 Bioanalyzer with Agilent RNA 6000 Nano Kits (Agilent Technologies, Santa Clara, CA, USA) and quantified using the Qubit Fluorometric Quantification system (ThermoFisher, Waltham, MA, USA). 10-100 ng of total RNA was subjected to amplification and cDNA synthesis using the Ovation RNA-Seq System V2 (NuGEN). One microgram of the resulting high-quality cDNA pool was fragmented to a mean length of 200 bp, and Truseq (Illumina) libraries were prepared and subjected to paired-end sequencing via Illumina HiSeq.

Paired-end libraries were imported into FASTQC (http://www.bioinformatics.bbsrc.ac.uk/projects/fastqc) to scan for sequencing quality. Adapter removal, read and quality trimming were completed in Trimmomatic (version: 0.36)(47), where a 4 bp sliding window was applied to retain bases with quality scores greater than 20. Trimmed paired-end reads were assembled with Trinity (version: r20140717) (48) to generate *de novo* reference transcriptomes (mean contig length: 460 bp, mean N50: 487 bp, mean total: 34 million bp) for each of the samples. We used Prodigal v2.6.3 (49) with default settings to identify open

reading frames. Reference assembly annotations were determined by BLASTX (version: 2.2.31) query searches against the NCBI non-redundant protein database, SwissProt and TrEMBL (50, 51). Gene ontology annotations were determined by mapping SwissProt/TrEMBL IDs to the UniProt-GOA database (52). To compensate for potential data processing biases of our selected annotation procedure, we included an automatic annotation strategy as follows. Paired-end reads for each library were merged and imported into MG-RAST (version:4.0.3) (53). Taxonomic and functional hits were queried against the MG-RAST Subsystems database (≤1e−4, ≥33% identity, min alignment length 15 aa). MG-RAST annotation output is publicly available at https://www.mg-rast.org/mgmain.html?mgpage=token&token=X6fIwsOSjEr6SwdDHjfs_ZD_p4xiGjRafO6HTpx54ogNTz7eXq. Annotation calls from BLASTX and MG-RAST were integrated by using the totalannotation.py script found in the De Wit et al pipeline (54).

Given the complex and variable taxonomic labeling systems across the annotation sources, we developed an R script to I) translate from a variable taxonomic labels into a unified and restricted vocabulary space and II) aggregate a large list of taxonomic labels into a smaller list by combining taxonomic calls of low relative abundance into higher-rank taxonomic groups until reaching a minimum relative abundance threshold. To do that, we generated an SQLite reference table with the following structure: ID, SOURCE, SOURCE_ID, DOMAIN, KINGDOM, PHYLUM, CLASS, ORDER, FAMILY, GENUS, SPECIES and QUERY. Here, the QUERY field included the taxonomic label of any annotation hit in our dataset based on the notation nomenclature of the SOURCE database. The input for the script was an array with observations in tuple format [*sample_id*, *query*, *counts*]. Then, the script generated a matrix representation of the query label in terms of the SQLite reference table. If relative *counts* (*r*) for

a certain *query* representation (q) was below a minimum threshold (T) (for example 4%), the script merged r to the next higher taxonomic rank until $r \geq T$. See the Code availability section for details in the workflow.

To calculate log-transformed RNA:DNA (LRD) ratios, we used operational taxonomic unit (OTU) abundance counts obtained from the Kleindienst et al. dataset (10). Raw 16S rRNA gene amplicon sequences are available under the NCBI Bioproject PRJNA253405. Relative OTU abundance triplicates were averaged ($\underline{d}$) and subjected to a higher-rank taxonomic merging with minimum relative abundance threshold of 4%. LRD index is defined as:

$$LRD_{ij} = \frac{1}{n}\sum_{t=1}^{n} log_2 \frac{r_{ijt}}{d_{ijt}}$$

where the log fold ratio between metatranscriptomic (r) and 16S rDNA gene ($\underline{d}$) relative counts are averaged across time (t), for each taxonomic group (i) and treatment (j).

Rarefaction and alpha diversity analyses of metatranscriptomic datasets were performed through MG-RAST. To evaluate beta-dispersion at the expression level of the microbial communities between all treatments, beta-phylogenetic differences weighted by abundance were tested using comdist (the average MPD for each species in a sample to all species in another sample) and comdistnt (the average MNTD for all species in a sample to the nearest neighbors in another sample) using the package Picante (55). A sequence-based reference phylogenetic tree was used as input parameter for the MPD and MNTD distance matrix calculations. To build the reference phylogenetic tree we followed procedures described previously (56). In brief, taxonomic representatives shown in Figure 1 were selected for searches of archaeal, bacterial and eukaryotic ribosomal small subunit sequences as well as viral capside and coat protein coding sequences. A full description of taxonomic representative sequences is available in

Supplementary Data 4. Sequences were aligned in MAFFT. Maximum likelihood phylogenetic trees of aligned sequences were inferred with RAxML, using the general time-reversible model of substitution and the GAMMA model of rate heterogeneity; tree topologies were checked by 100 bootstrapping replicates.

Bray–Curtis dissimilarity among all treatments was calculated as an abundance-weighted measure of beta-diversity. The output distance matrix was visualized via PCA ordinations using the pcoa function from the ape package. The function adonis from the vegan package was used to examine the significant relationship between distance matrices (U) (*i.e.*, Bray-Curtis, MPD or MNTD) and experimental factors: dispersant (D), WAF (O), nutrients (N), time (t). Each test comprised 999 permutations. The testing model was defined as follows:

$$U = D + O + D * O + D * O * N + t + D * t + O * t + D * O * t + D * O * N * t$$

All scripts are found on Github (https://github.com/biotemon/K2015). Raw sequencing reads generated for this study can be found in the Sequence Read Archive under the BioProject PRJNA640753. Taxonomy rank database and all other data are available in the Open Science Framework repository at https://osf.io/fu9bw/.

Acknowledgements

This study was funded by the Gulf of Mexico Research Initiative grant: "Ecosystem Impacts of Oil and Gas Inputs to the Gulf". This study was also supported in part by resources and technical expertise from the Georgia Advances Computing Resource Center, a partnership between the University of Georgia's Office of the Vice President for Research and the Office of the Vice President for Information Technology and by funding provided by the University of Georgia's Office of the Provost and Office of the Vice President for Research. T.D.P.M. was

supported by a Fulbright Colombia fellowship. We thank Kimberley S. Hunter for assistance with laboratory measurements.

3.6 Supplementary Materials

Supplementary Figures

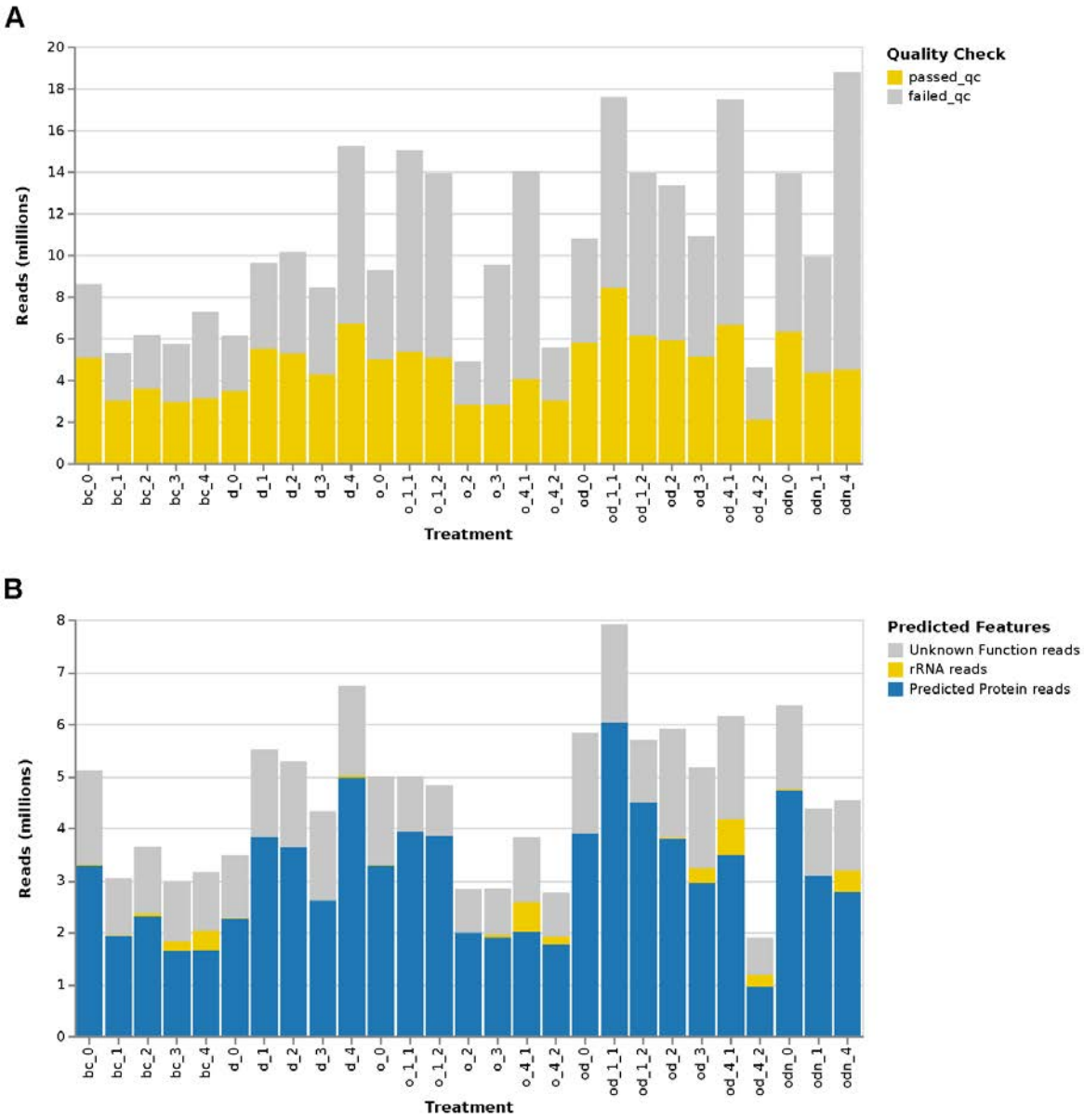

Supplementary Figure S3.1: Total reads per sequencing library after quality filter (A) and after annotation (B).

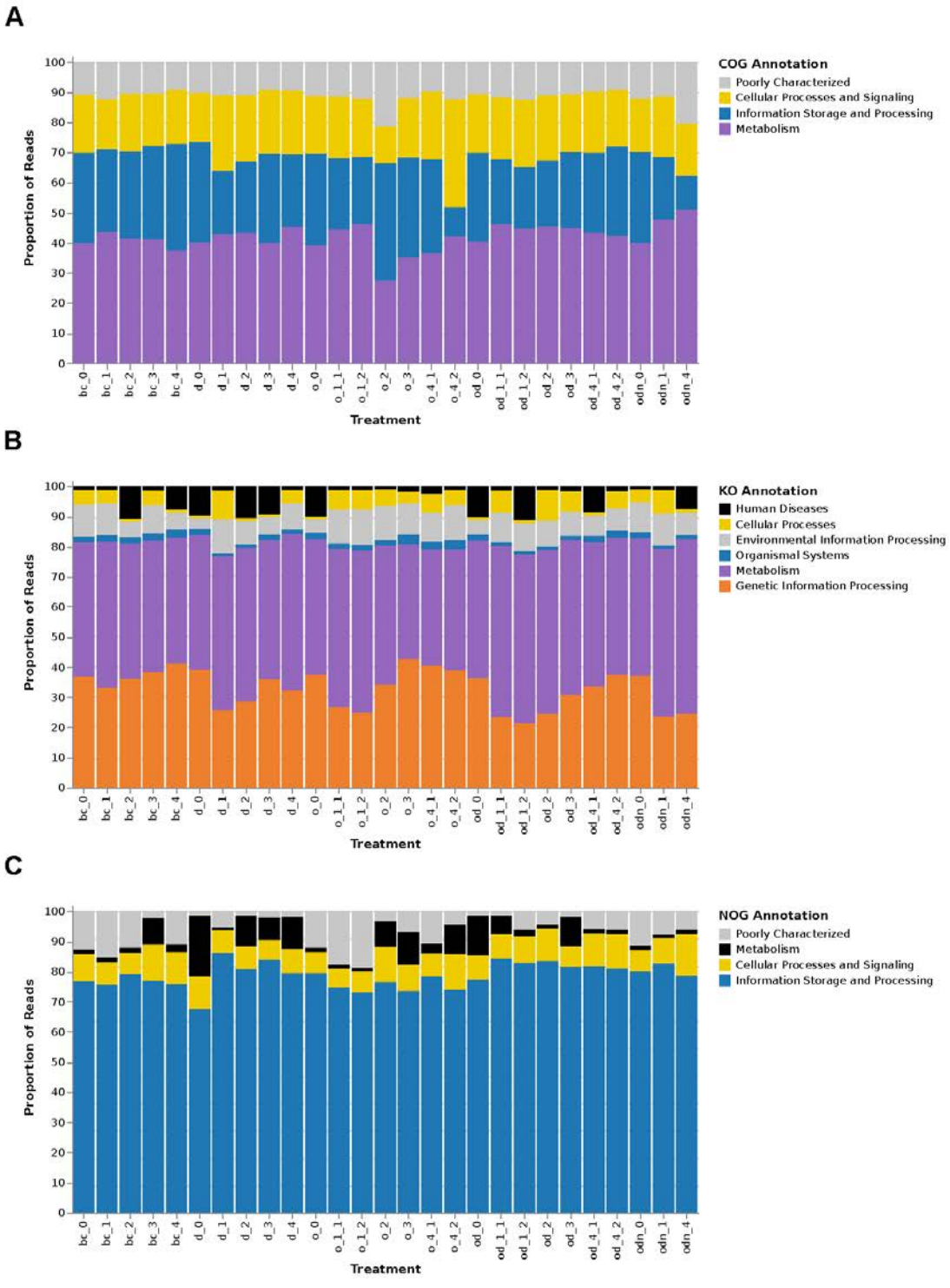

Supplementary Figure S3.2: Relative sequence abundance assigned to functional categories using (A) COG, (B) KEGG Orthology, (C) and eggNOG database as references.

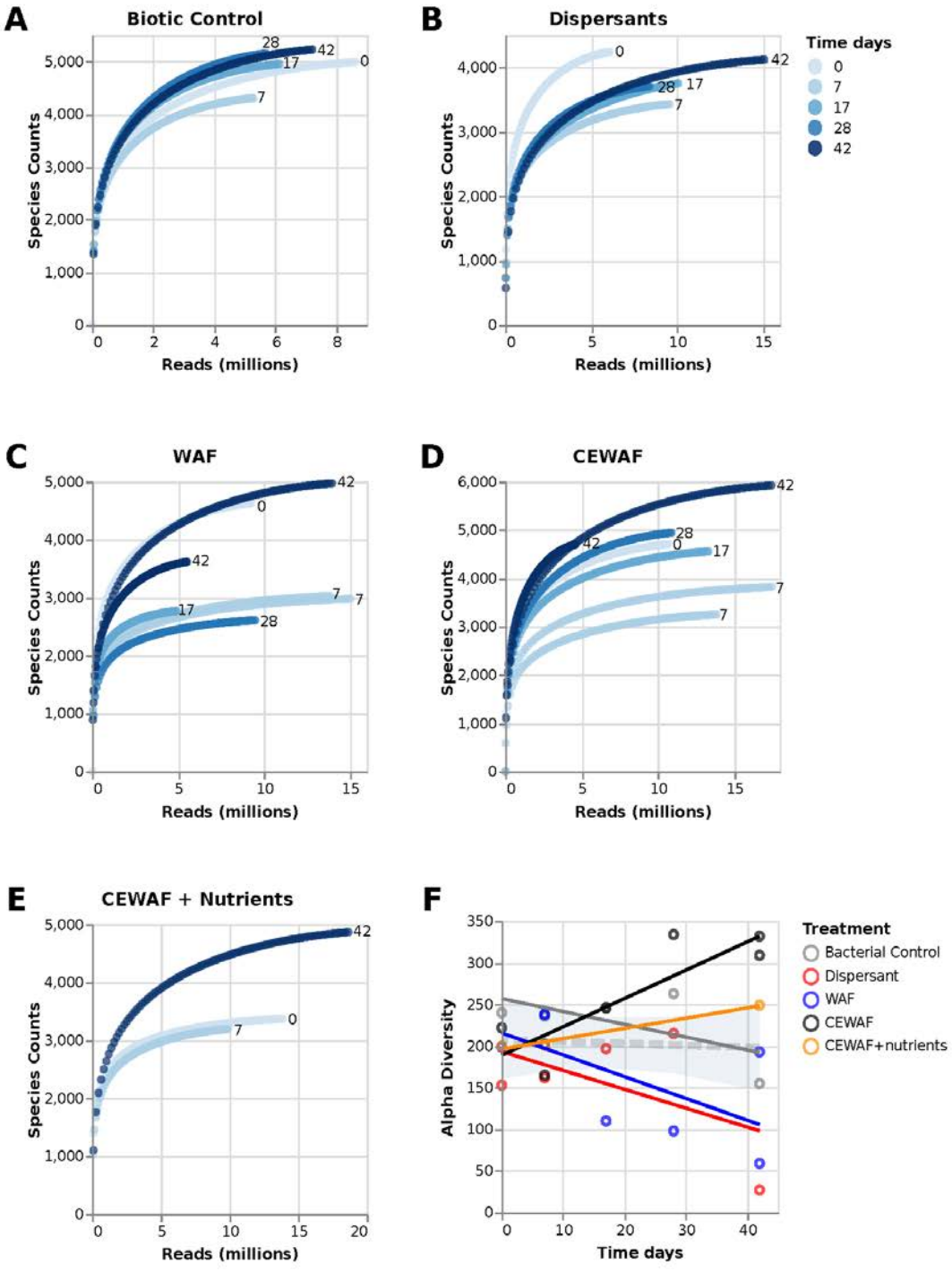

Supplementary Figure S3.3: (A-E) Rarefaction analysis showing the distribution of the total distinct species annotations as a function of the number of sequences sampled for each of the libraries in the metatransciptomic K2015 data set. (F). Alpha diversity trends across time and treatments of K2015 data set.

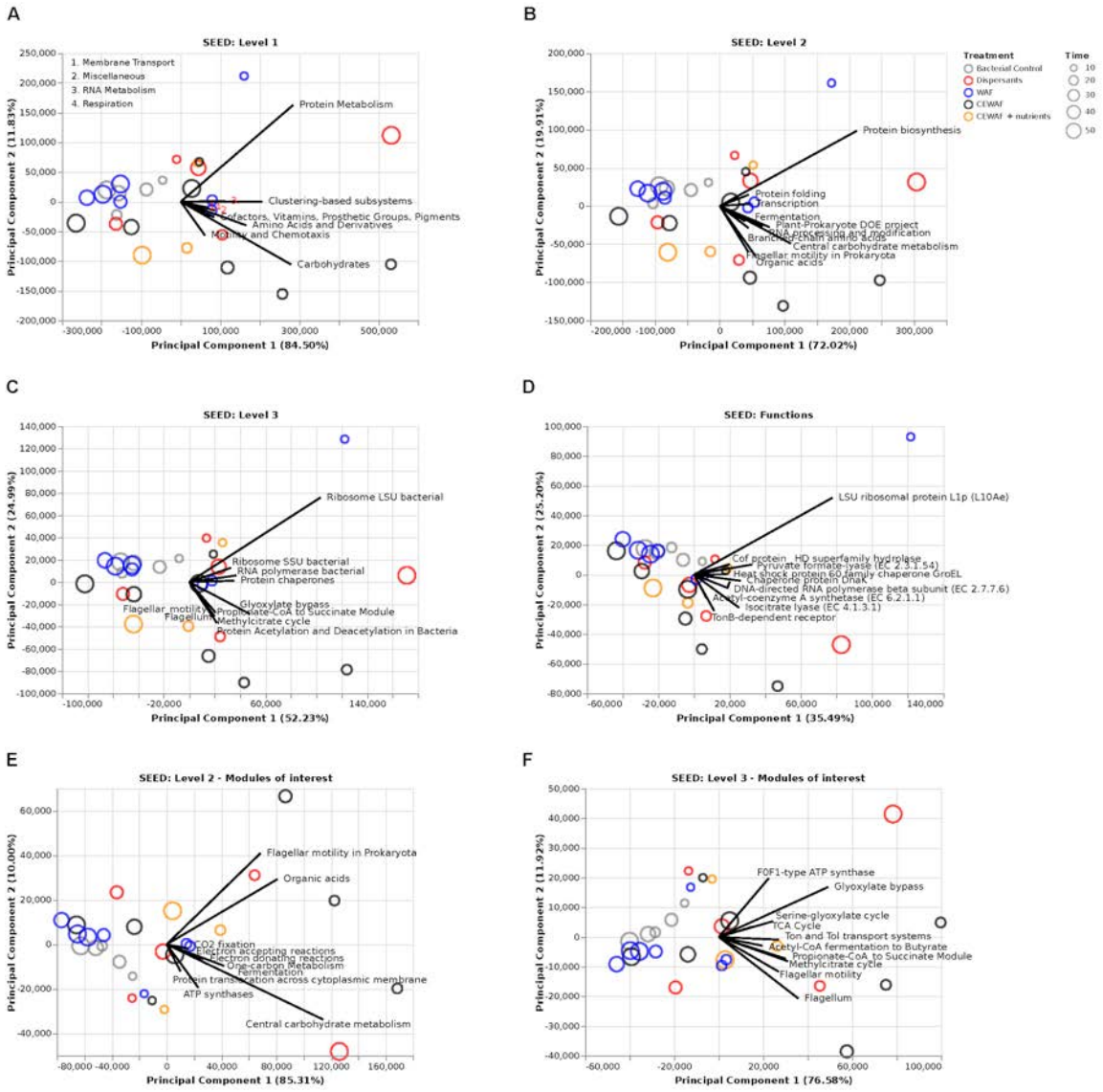

Supplementary Figure S3.4: Principal component analysis (PCA) of functional features abundance for the K2015 data set across SEED annotation levels 1 (A), 2 (B), 3 (C), and SEED functions (D). PCA focused on the functional categories Motility and Chemotaxis, Carbohydrates, Membrane Transport and Respiration are shown for levels 2 (E), and 3 (F). Solid lines represent the top ten loading vectors explaining the variation of expressed genes in the analysis

3.7 References

1. Joye S, Kostka JE. 2020. Microbial Genomics of the Global Ocean System: Report on an American Academy of Microbiology (Academy), The American Geophysical Union (AGU), and The Gulf of Mexico Research Initiative (GoMRI) Colloquium held on 9 and 10 April 2019. American Society for Microbiology.

2. Harrison S. 2017. Lessons from the Taylor Energy oil spill: history, seasonality, and nutrient limitation. University of Georgia, Athens, GA, USA.

3. Committee on Oil in the Sea: Inputs, Fates, and Effects, Ocean Studies Board, Marine Board, Transportation Research Board, Division on Earth and Life Studies, National Research Council. 2003. Oil in the Sea III: Inputs, Fates, and Effects. National Academies Press, Washington, D.C.

4. Kleindienst S, Grim S, Sogin M, Bracco A, Crespo-Medina M, Joye SB. 2016. Diverse, rare microbial taxa responded to the Deepwater Horizon deep-sea hydrocarbon plume. ISME J 10:400–415.

5. Kostka JE, Prakash O, Overholt WA, Green SJ, Freyer G, Canion A, Delgardio J, Norton N, Hazen TC, Huettel M. 2011. Hydrocarbon-Degrading Bacteria and the Bacterial Community Response in Gulf of Mexico Beach Sands Impacted by the Deepwater Horizon Oil Spill. Appl Environ Microbiol 77:7962–7974.

6. Committee on the Evaluation of the Use of Chemical Dispersants in Oil Spill Response, Ocean Studies Board, Board on Environmental Studies and Toxicology, Division on Earth and Life Studies, National Academies of Sciences, Engineering, and Medicine. 2020. The

Use of Dispersants in Marine Oil Spill Response. National Academies Press, Washington, D.C.

7. Place BJ, Perkins MJ, Sinclair E, Barsamian AL, Blakemore PR, Field JA. 2016. Trace analysis of surfactants in Corexit oil dispersant formulations and seawater. Deep Sea Research Part II: Topical Studies in Oceanography 129:273–281.

8. Baelum J, Borglin S, Chakraborty R, Fortney JL, Lamendella R, Mason OU, Auer M, Zemla M, Bill M, Conrad ME, Malfatti SA, Tringe SG, Holman H-Y, Hazen TC, Jansson JK. 2012. Deep-sea bacteria enriched by oil and dispersant from the Deepwater Horizon spill: Enrichment of oil degraders from Gulf of Mexico. Environmental Microbiology 14:2405–2416.

9. Brakstad OG, Throne-Holst M, Netzer R, Stoeckel DM, Atlas RM. 2015. Microbial communities related to biodegradation of dispersed Macondo oil at low seawater temperature with Norwegian coastal seawater: Microbial communities during oil biodegradation. Microbial Biotechnology 8:989–998.

10. Kleindienst S, Seidel M, Ziervogel K, Grim S, Loftis K, Harrison S, Malkin SY, Perkins MJ, Field J, Sogin ML, Dittmar T, Passow U, Medeiros PM, Joye SB. 2015. Chemical dispersants can suppress the activity of natural oil-degrading microorganisms. Proceedings of the National Academy of Sciences 112:14900–14905.

11. McCarren J, Becker JW, Repeta DJ, Shi Y, Young CR, Malmstrom RR, Chisholm SW, DeLong EF. 2010. Microbial community transcriptomes reveal microbes and metabolic

pathways associated with dissolved organic matter turnover in the sea. Proceedings of the National Academy of Sciences 107:16420–16427.

12. Chakraborty R, Borglin SE, Dubinsky EA, Andersen GL, Hazen TC. 2012. Microbial Response to the MC-252 Oil and Corexit 9500 in the Gulf of Mexico. Front Microbiol 3.

13. Schleheck D, Weiss M, Pitluck S, Bruce D, Land ML, Han S, Saunders E, Tapia R, Detter C, Brettin T, Han J, Woyke T, Goodwin L, Pennacchio L, Nolan M, Cook AM, Kjelleberg S, Thomas T. 2011. Complete genome sequence of *Parvibaculum lavamentivorans* type strain DS-1T. Stand Genomic Sci 5:298–310.

14. Legendre M, Fabre E, Poirot O, Jeudy S, Lartigue A, Alempic J-M, Beucher L, Philippe N, Bertaux L, Christo-Foroux E, Labadie K, Couté Y, Abergel C, Claverie J-M. 2018. Diversity and evolution of the emerging Pandoraviridae family. Nat Commun 9:2285.

15. De Clercq E. 2005. John Montgomery's Legacy: Carbocyclic Adenosine Analogues as Sah Hydrolase Inhibitors with Broad-Spectrum Antiviral Activity. Nucleosides, Nucleotides & Nucleic Acids 24:1395–1415.

16. Carr VR, Shkoporov A, Hill C, Mullany P, Moyes DL. 2021. Probing the Mobilome: Discoveries in the Dynamic Microbiome. Trends in Microbiology 29:158–170.

17. Wade TL, Sweet ST, Sericano JL, Guinasso NL, Diercks A-R, Highsmith RC, Asper VL, Joung D, Shiller AM, Lohrenz SE, Joye SB. 2011. Analyses of Water Samples From the Deepwater Horizon Oil Spill: Documentation of the Subsurface Plume, p. 77–82. *In* Liu, Y, MacFadyen, A, Ji, Z-G, Weisberg, RH (eds.), Geophysical Monograph Series. American Geophysical Union, Washington, D. C.

18. Joye SB, MacDonald IR, Leifer I, Asper V. 2011. Magnitude and oxidation potential of hydrocarbon gases released from the BP oil well blowout. Nature Geosci 4:160–164.

19. Kujawinski EB, Kido Soule MC, Valentine DL, Boysen AK, Longnecker K, Redmond MC. 2011. Fate of Dispersants Associated with the Deepwater Horizon Oil Spill. Environ Sci Technol 45:1298–1306.

20. Redmond MC, Valentine DL. 2012. Natural gas and temperature structured a microbial community response to the Deepwater Horizon oil spill. Proceedings of the National Academy of Sciences 109:20292–20297.

21. Mason OU, Han J, Woyke T, Jansson JK. 2014. Single-cell genomics reveals features of a *Colwellia* species that was dominant during the Deepwater Horizon oil spill. Frontiers in Microbiology 5.

22. Methe BA, Nelson KE, Deming JW, Momen B, Melamud E, Zhang X, Moult J, Madupu R, Nelson WC, Dodson RJ, Brinkac LM, Daugherty SC, Durkin AS, DeBoy RT, Kolonay JF, Sullivan SA, Zhou L, Davidsen TM, Wu M, Huston AL, Lewis M, Weaver B, Weidman JF, Khouri H, Utterback TR, Feldblyum TV, Fraser CM. 2005. The psychrophilic lifestyle as revealed by the genome sequence of Colwellia psychrerythraea 34H through genomic and proteomic analyses. Proceedings of the National Academy of Sciences 102:10913–10918.

23. Czajka JJ, Abernathy MH, Benites VT, Baidoo EEK, Deming JW, Tang YJ. 2018. Model metabolic strategy for heterotrophic bacteria in the cold ocean based on *Colwellia psychrerythraea* 34H. Proc Natl Acad Sci USA 115:12507–12512.

24. Singer E, Webb EA, Nelson WC, Heidelberg JF, Ivanova N, Pati A, Edwards KJ. 2011. Genomic Potential of Marinobacter aquaeolei, a Biogeochemical "Opportunitroph." Appl Environ Microbiol 77:2763–2771.

25. McKay LJ, Gutierrez T, Teske AP. 2016. Development of a group-specific 16S rRNA-targeted probe set for the identification of *Marinobacter* by fluorescence in situ hybridization. Deep Sea Research Part II: Topical Studies in Oceanography 129:360–367.

26. Gutierrez T, Singleton DR, Berry D, Yang T, Aitken MD, Teske A. 2013. Hydrocarbon-degrading bacteria enriched by the Deepwater Horizon oil spill identified by cultivation and DNA-SIP. ISME J 7:2091–2104.

27. Yang T, Nigro LM, Gutierrez T, D′Ambrosio L, Joye SB, Highsmith R, Teske A. 2016. Pulsed blooms and persistent oil-degrading bacterial populations in the water column during and after the Deepwater Horizon blowout. Deep Sea Research Part II: Topical Studies in Oceanography 129:282–291.

28. Dlott G, Maul JE, Buyer J, Yarwood S. 2015. Microbial rRNA:rDNA gene ratios may be unexpectedly low due to extracellular DNA preservation in soils. Journal of Microbiological Methods 115:112–120.

29. Chícharo M, Chícharo L. 2008. RNA:DNA ratio and other nucleic acid derived indices in marine ecology. IJMS 9:1453–1471.

30. King GM, Kostka JE, Hazen TC, Sobecky PA. 2015. Microbial Responses to the *Deepwater Horizon* Oil Spill: From Coastal Wetlands to the Deep Sea. Annual Review of Marine Science 7:377–401.

31. Chen Q, Bao B, Li Y, Liu M, Zhu B, Mu J, Chen Z. 2020. Effects of marine oil pollution on microbial diversity in coastal waters and stimulating indigenous microorganism bioremediation with nutrients. Regional Studies in Marine Science 39:101395.

32. Dubinsky EA, Conrad ME, Chakraborty R, Bill M, Borglin SE, Hollibaugh JT, Mason OU, M. Piceno Y, Reid FC, Stringfellow WT, Tom LM, Hazen TC, Andersen GL. 2013. Succession of hydrocarbon-degrading bacteria in the aftermath of the Deepwater Horizon oil spill in the Gulf of Mexico. Environ Sci Technol 47:10860–10867.

33. Hazen TC, Dubinsky EA, DeSantis TZ, Andersen GL, Piceno YM, Singh N, Jansson JK, Probst A, Borglin SE, Fortney JL, Stringfellow WT, Bill M, Conrad ME, Tom LM, Chavarria KL, Alusi TR, Lamendella R, Joyner DC, Spier C, Baelum J, Auer M, Zemla ML, Chakraborty R, Sonnenthal EL, D'haeseleer P, Holman H-YN, Osman S, Lu Z, Van Nostrand JD, Deng Y, Zhou J, Mason OU. 2010. Deep-sea oil plume enriches indigenous oil-degrading Bacteria. Science 330:204–208.

34. Royo-Llonch M, Sánchez P, González JM, Pedrós-Alió C, Acinas SG. 2020. Ecological and functional capabilities of an uncultured *Kordia* sp. Systematic and Applied Microbiology 43:126045.

35. Schneiker S, dos Santos VAM, Bartels D, Bekel T, Brecht M, Buhrmester J, Chernikova TN, Denaro R, Ferrer M, Gertler C, Goesmann A, Golyshina OV, Kaminski F, Khachane AN, Lang S, Linke B, McHardy AC, Meyer F, Nechitaylo T, Pühler A, Regenhardt D, Rupp O, Sabirova JS, Selbitschka W, Yakimov MM, Timmis KN, Vorhölter F-J, Weidner S, Kaiser O, Golyshin PN. 2006. Genome sequence of the ubiquitous hydrocarbon-degrading marine bacterium Alcanivorax borkumensis. Nat Biotechnol 24:997–1004.

36. Xing P, Hahnke RL, Unfried F, Markert S, Huang S, Barbeyron T, Harder J, Becher D, Schweder T, Glöckner FO, Amann RI, Teeling H. 2015. Niches of two polysaccharide-degrading Polaribacter isolates from the North Sea during a spring diatom bloom. ISME J 9:1410–1422.

37. Zhang J, Mavrodi DV, Yang M, Thomashow LS, Mavrodi OV, Kelton J, Weller DM. 2020. *Pseudomonas synxantha* 2-79 Transformed with Pyrrolnitrin Biosynthesis Genes Has Improved Biocontrol Activity Against Soilborne Pathogens of Wheat and Canola. Phytopathology® 110:1010–1017.

38. Brandhorst TT, Kean IRL, Lawry SM, Wiesner DL, Klein BS. 2019. Phenylpyrrole fungicides act on triosephosphate isomerase to induce methylglyoxal stress and alter hybrid histidine kinase activity. Sci Rep 9:5047.

39. Arslan D, Legendre M, Seltzer V, Abergel C, Claverie J-M. 2011. Distant Mimivirus relative with a larger genome highlights the fundamental features of Megaviridae. Proceedings of the National Academy of Sciences 108:17486–17491.

40. Tokarz-Deptuła B, Niedźwiedzka-Rystwej P, Czupryńska P, Deptuła W. 2019. Protozoal giant viruses: agents potentially infectious to humans and animals. Virus Genes 55:574–591.

41. Talmy D, Beckett SJ, Zhang AB, Taniguchi DAA, Weitz JS, Follows MJ. 2019. Contrasting Controls on Microzooplankton Grazing and Viral Infection of Microbial Prey. Front Mar Sci 6:182.

42. Chow C-ET, Kim DY, Sachdeva R, Caron DA, Fuhrman JA. 2014. Top-down controls on bacterial community structure: microbial network analysis of bacteria, T4-like viruses and protists. ISME J 8:816–829.

43. Breitbart M, Bonnain C, Malki K, Sawaya NA. 2018. Phage puppet masters of the marine microbial realm. Nat Microbiol 3:754–766.

44. Gallot-Lavallée L, Blanc G, Claverie J-M. 2017. Comparative Genomics of Chrysochromulina Ericina Virus and Other Microalga-Infecting Large DNA Viruses Highlights Their Intricate Evolutionary Relationship with the Established Mimiviridae Family. Journal of Virology 91.

45. Finke J, Hunt B, Winter C, Carmack E, Suttle C. 2017. Nutrients and Other Environmental Factors Influence Virus Abundances across Oxic and Hypoxic Marine Environments. Viruses 9:152.

46. Sandaa R-A, Pree B, Larsen A, Våge S, Töpper B, Töpper J, Thyrhaug R, Thingstad T. 2017. The Response of Heterotrophic Prokaryote and Viral Communities to Labile Organic Carbon Inputs Is Controlled by the Predator Food Chain Structure. Viruses 9:238.

47. Bolger AM, Lohse M, Usadel B. 2014. Trimmomatic: a flexible trimmer for Illumina sequence data. Bioinformatics 30:2114–2120.

48. Haas BJ, Papanicolaou A, Yassour M, Grabherr M, Blood PD, Bowden J, Couger MB, Eccles D, Li B, Lieber M, MacManes MD, Ott M, Orvis J, Pochet N, Strozzi F, Weeks N, Westerman R, William T, Dewey CN, Henschel R, LeDuc RD, Friedman N, Regev A. 2013.

De novo transcript sequence reconstruction from RNA-seq using the Trinity platform for reference generation and analysis. Nature Protocols 8:1494–1512.

49. Hyatt D, Chen G-L, LoCascio PF, Land ML, Larimer FW, Hauser LJ. 2010. Prodigal: prokaryotic gene recognition and translation initiation site identification. BMC Bioinformatics 11:1–11.

50. Boeckmann B. 2003. The SWISS-PROT protein knowledgebase and its supplement TrEMBL in 2003. Nucleic Acids Research 31:365–370.

51. Altschul SF, Gish W, Miller W, Myers EW, Lipman DJ. 1990. Basic local alignment search tool. Journal of Molecular Biology 215:403–410.

52. Dimmer EC, Huntley RP, Alam-Faruque Y, Sawford T, O'Donovan C, Martin MJ, Bely B, Browne P, Mun Chan W, Eberhardt R, Gardner M, Laiho K, Legge D, Magrane M, Pichler K, Poggioli D, Sehra H, Auchincloss A, Axelsen K, Blatter M-C, Boutet E, Braconi-Quintaje S, Breuza L, Bridge A, Coudert E, Estreicher A, Famiglietti L, Ferro-Rojas S, Feuermann M, Gos A, Gruaz-Gumowski N, Hinz U, Hulo C, James J, Jimenez S, Jungo F, Keller G, Lemercier P, Lieberherr D, Masson P, Moinat M, Pedruzzi I, Poux S, Rivoire C, Roechert B, Schneider M, Stutz A, Sundaram S, Tognolli M, Bougueleret L, Argoud-Puy G, Cusin I, Duek- Roggli P, Xenarios I, Apweiler R. 2012. The UniProt-GO Annotation database in 2011. Nucleic Acids Research 40:D565–D570.

53. Meyer F, Paarmann D, D'Souza M, Olson R, Glass E, Kubal M, Paczian T, Rodriguez A, Stevens R, Wilke A, Wilkening J, Edwards R. 2008. The metagenomics RAST server – a

public resource for the automatic phylogenetic and functional analysis of metagenomes. BMC Bioinformatics 9.

54. De Wit P, Pespeni MH, Ladner JT, Barshis DJ, Seneca F, Jaris H, Therkildsen NO, Morikawa M, Palumbi SR. 2012. The simple fool's guide to population genomics via RNA-Seq: an introduction to high-throughput sequencing data analysis. Molecular Ecology Resources 12:1058–1067.

55. Kembel SW, Cowan PD, Helmus MR, Cornwell WK, Morlon H, Ackerly DD, Blomberg SP, Webb CO. 2010. Picante: R tools for integrating phylogenies and ecology. Bioinformatics 26:1463–1464.

56. Gregoire Taillefer A, Wheeler TA. 2018. Tracking wetland community evolution using Diptera taxonomic, functional and phylogenetic structure. Insect Conservation and Diversity 11:276–293.

CHAPTER 4

THE ROLE OF NUTRIENTS VERSUS DISPERSANTS AS MODULATORS OF OIL BIODEGRADATION CAPACITY IN GULF OF MEXICO SURFACE WATERS [3]

[3] Peña-Montenegro TD, Shepard CG, Hunter KS, Sánchez-Calderón JD, Joye SB. To be submitted to *Marine Pollution Bulletin*

Note to Committee: The experiments described here were carried out collaboratively by Catherine Shepard and Tito Peña-Montenegro. Shepard's M.Sc. thesis (Shephard, C.G., 2019, 'Nutrient availability modulate the effects of Corexit 9500A on oil biodegradation') described results from chemical and microbial activity assessments. Peña-Montenegro carried out the metagenomics work and is leading development of the manuscript which we will submit for publication. Some of the material presented in this chapter (chemistry and rate assays) were published in Shepard's thesis and are credited as such. These materials are included here because they represent a key part of the paper we plan to publish.

3.1 Abstract

Perturbations like oil spills alter the structure and function of oceanic microbial communities. Understanding how microbial fitness and stress affect the microbiome's ability to respond to perturbations is important. Generally speaking, the open ocean is profoundly nutrient limited, exerting a stress on microbial populations that may impact their ability to respond to other stressors. We examined the interacting stressors of nutrient limitation and organic carbon loading in oligotrophic pelagic microbial communities from the Gulf of Mexico. The response to organic carbon loading from oil or synthetic chemical dispersants was a function of nutrient availability. Nutrient additions altered microbial community composition and the potential hydrocarbon oxidation rates. These results suggest that conducting dispersant investigations solely under nutrient replete conditions is not be representative the natural environment, and in fact can provide a false impression that dispersants enhance oil biodegradation rates. Nutrient limited microbial communities are, in fact, very ineffective at degrading oil and dispersants.
Keywords: oil spill, synthetic dispersants, multiple stressors, nutrient limitation,

3.2 Introduction

Oil is introduced into the marine environment through natural and accidental discharges. Accidental discharges include production, well control, pipeline, and tanker related spillages and discharges and are often of sufficient size to warrant response measures. The Deepwater Horizon oil spill is the largest marine oil spill in history, to date: some 4.9 million barrels of oil along with 250,000 metric tonnes of methane gas were discharged into the Gulf of Mexico, with substantial environmental negative impacts to the Gulf's pelagic and coastal habitats. The Deepwater Horizon disaster in the Gulf of Mexico began April 20, 2010, when a catastrophic loss of well control and subsequent blowout sparked a fire that consumed and ultimately sank the drilling platform on April 22, 2010. Hydrocarbon discharge at the seafloor (1,500 m) began that day (April 22) and stopped on July 15, 2010, when the well was capped. The well was permanently sealed on Sept. 19, 2010 by cementing drill pipe shut, deep below the seafloor.

Given the magnitude of the Deepwater Horizon oil spill, a number of response measures were implemented by the National Incident Command Team, including booming and skimming oil from the surface, controlled burns of surface oil, tapping the discharging well and sequestering some of discharging oil to a surface vessel, and the application of synthetic chemical dispersants (hereafter, 'dispersants'). Dispersants act to solubilize oil by reducing the surface tension and driving oil into the aqueous phase (Figure 1, next page) through the formation of small, high surface area droplets; these dispersant-created droplets are presumed to be bioavailable and highly reactive in terms of potential for biodegradation (Committee on the Evaluation of the Use of Chemical Dispersants in Oil Spill Response et al., 2020). During the Deepwater Horizon disaster, two dispersants were used, COREXIT 9500A (Nalco, Sugar Land, TX) and COREXIT 9527 (Nalco, Sugar Land, TX); the main difference between

Figure 4.1. Cartoon showing how dispersants act to solubilize oil (Source: Kleindienst et al., 2015a).

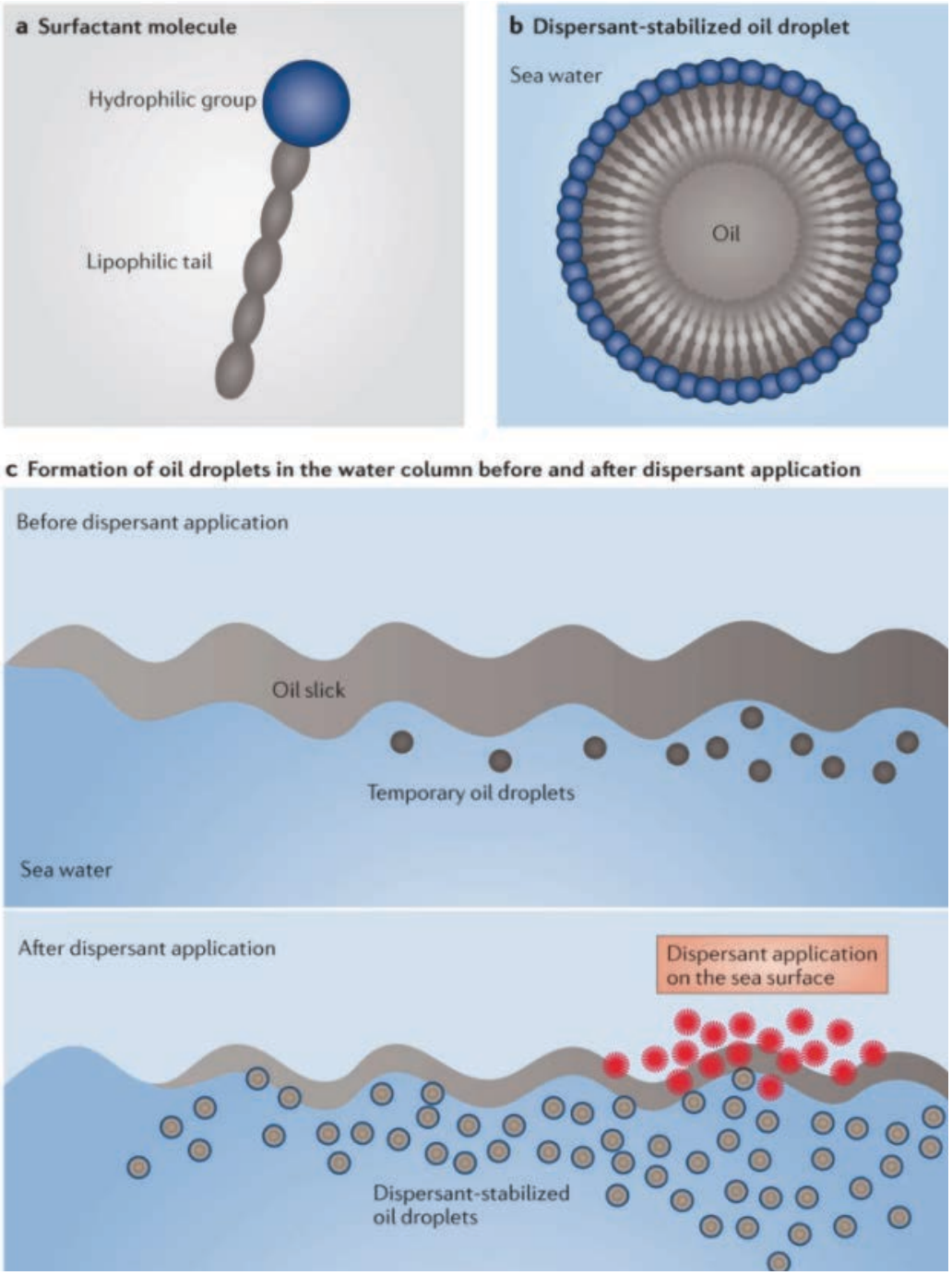

these two dispersant formulations is that COREXIT 9527 contains 2-butoxyethanol, a known carcinogen. Both formulations of COREXIT contains propylene glycol and petroleum distillates, common solvents, and ionic (dioctyl sodium sulfosuccinate, 18 w/w) and anionic (Span 80, Tween 80, and Tween 85; 25% w/w) surfactants (Place et al., 2016). During the Deepwater Horizon disaster, dispersants were applied to surface oil slicks and at the discharging wellhead to increase the amount of oil dissolved in the deepwater.

The natural cycle of petroleum involves production of petroleum in deep reservoirs through high temperature catalytic processes (Joye, 2020). Subsequently, each year, some fraction of this petroleum moves through the sediment column and is released to the environment where biotic and abiotic processes recycle oil components to their original inorganic building blocks. This natural cycle of petroleum – formation in sediments, release to the environment, and recycling to inorganic constituents occurs over time scales of tens of millions of years (Joye 2020). A key part of this cycle is mediated by specialized microorganisms whose metabolism acts to convert complex hydrocarbons to inorganic building blocks (Joye et al., 2014). Prior to the Deepwater Horizon oil spill, very little was known about the regulation and dynamics of microbial oil biodegradation in the open ocean (Joye and Kostka, 2020).

Hydrocarbon degrading microorganisms exist in soils, sediments, and waters from tropical environments to polar habitats (Joye et al., 2018). Hydrocarbon degraders are members of the “rare biosphere”, microbes present in low abundance and a cosmopolitan distribution (Kleindienst et al., 2016). The factors that regulate the activity of hydrocarbon degrading microorganisms include availability of hydrocarbons, electron acceptors, and the nutrients and co-factors that are required for cell growth (Joye et al., 2018). Hydrocarbons are inherently

inaccessible because of their low solubility in water. This infers that actions taken to increase hydrocarbon concentrations in water – such as the application of synthetic chemical dispersants - will increase hydrocarbon degradation rates. When hydrocarbon availability increases, the activity and abundance of microbial hydrocarbon degraders increases, often rapidly, with days to weeks (Joye et al., 2018, 2014) until another factor limits their activity. Since hydrocarbons represent a source of structural carbon and energy for these organisms, nutrient limitation of their activity is possible and even likely (Joye et al., 2018, 2014).

The unprecedented application of synthetic dispersants during the Deepwater Horizon response raised a number of important questions regarding the impact of dispersant components on hydrocarbon degrading microorganisms (Kleindienst et al., 2015a). Most hydrocarbon degrading microorganisms are facultative, meaning that they also oxidize non-hydrocarbon compounds to obtain energy and, possibly, structural carbon. Dispersants include of a number of labile components, including petroleum distillates and sulfosuccinates (Place et al., 2016), that can serve as microbial growth and energy substrates. Many dispersants are more soluble than hydrocarbons, so it is possible that dispersant components are present in higher concentrations in the dissolved phase and that they may be preferred by some hydrocarbon degrading microorganisms. In this way, oxidation of dispersant components could reduce the oxidation of oil components. Alternatively, dispersant components may inhibit the activity of some hydrocarbon degraders by reducing their fitness (Peña-Montenegro et al. 2021, mBio).

The open ocean is a nutrient limited environment, and the Gulf of Mexico is no exception. Despite intense nutrient loading from the Mississippi River along the Texas-Louisiana shelf, in offshore surface waters, concentrations of dissolved inorganic nitrogen and phosphorus are often below detection and concentrations of organic nitrogen and phosphorus are extremely

low (nM range) (Cardona et al., 2016), presenting a fundamental metabolic challenge for the autotrophic and heterotrophic microbes that compete for the limited pool of bioavailable nitrogen and phosphorus. In fact, Warr et al. (2013) suggested adding nutrients as fertilized clay mineral flakes to stimulate oil degradation during the event of an oil spill. Such actions are not currently permitted but underscore the recognized role of nutrients in limiting the potential for oil bioremediation by naturally occurring populations of microorganisms.

Nutrient availability influences the fitness of microbial populations in numerous ways (Carrero-Colón et al., 2006; Ghoul and Mitri, 2016; Ni et al., 2020) and the intrinsic stress of nutrient limitation can lead to increased sensitivity to other stressors (Sexton and Schuster, 2017), such as exposure to dispersant components or even oil components in situations like the Deepwater Horizon. The present work aimed to assess the interactive role of dispersants and nutrient availability on oil biodegradation potential of microbial populations in Gulf of Mexico (hereafter 'Gulf') surface waters. Microorganisms in offshore waters, especially in the Gulf, have been shown to be phosphorus limited (Edwards et al., 2011; Pomeroy et al., 1995). Nitrogen limitation is also likely (Ryther and Dunstan, 1971).

We conducted experiments in which we exposed microbial communities to water accommodated fractions (WAFs) of dispersant (dispersant equilibrated with seawater to produce a dispersant water accommodated fraction, 'D-WAF'), dissolved oil (oil equilibrated with seawater the aqueous phase to an oil water accommodated fraction, 'O-WAF'), chemically dispersed oil (oil and dispersant equilibrated to produce a chemically enhanced water accommodated fraction, 'CE-WAF'). The experiments were designed to assess how exposure to cocktails of additional organic matter affect the potential for microbial populations to effectively degrade oil. The experimental results show that the presence of dispersants alone can reduce oil

degradation rates while the presence of nutrients, with or without, dispersants accelerates oil biodegradation substantially. Nutrients replete conditions influenced microbial community composition, selecting for unique ecotypes that were not able to thrive under nutrient limited conditions. Thus, nutrient availability seems to be the factor limiting oil biodegradation potential.

3.2 Methods

Study Sites

Samples were collected from two sites in the Gulf of Mexico, one site is a natural hydrocarbon seep and the other was impacted by the Deepwater Horizon oil spill. The Green Canyon lease block 600 (GC600; 27° 21.5387’ N, 90° 33.682’ W) site is a vigorous natural oil seep located at 1,200m to 1,400m water depth about 120 nautical miles offshore in deep, oligotrophic water (Johansen et al., 2020). At GC600, oil and gas are discharged from numerous at the seabed creating visible sea surface oil slicks and the surface water microbial community is exposed to oil almost daily. The Oceanus 26 (OC26; 28° 42.234’ N, 88° 21.629’ W) site was chosen because of its proximity to the DWH oil spill site. Like GC600, OC26 is a deepwater (1,500m water depth), oligotrophic offshore site, but the area lacks widespread natural seepage, so the pelagic microbial community is not regularly exposed to hydrocarbons. These two sites provide a valuable contrast in hydrocarbon exposure history and allowed us to assess how the microbial communities from different locales respond to hydrocarbon infusions.

Surface water was collected using 5L bucket casts (3× sample rinsed prior to sample collection) during three research expeditions to the Gulf of Mexico (Shepard, 2019): Research Vessel (R/V) Endeavor expedition 600 (EN600; June 2017), R/V Pelican expedition PE-18-06 (August 2017), and R/V Pelican expedition PE-18-08 (September 2017). On the R/V Endeavor,

samples were processed, amended, and treated within 24 hours of collection. For the R/V Pelican expeditions, water for rate assays was stored at 4ºC, processed, amended, and injected back in the UGA lab within three days of collection. During the PE-18-06 cruise, water was collected from GC600 for experiments. On all expeditions, DNA samples were collected into 5 L PETG bottles and water was filtered immediately through 0.2 μm Sterivex® filters using a peristaltic pump. Filters were kept frozen until DNA was extracted back at the UGA lab. Water samples for microbial activity measurements and nutrient concentration determination were collected into 1 L glass amber bottles and stored at 4 ºC until processing. On the EN600 cruise, water was collected from GC600. Oceanus 26 was sampled again on the R/V Pelican cruises.

Preparation of water accommodated fractions

The goal of this work was to assess the response of surface water microbial communities to different cocktails of organic carbon that the communities could be exposed to in the event of an oil spill and associated response effort (Shepard, 2019). The additive impact of inherent nutrient stress was assessed directly by exposing samples to different cocktails of organic carbon with or without additional nutrients. The treatments with organic carbon plus nutrients served to assess whether organic carbon degradation was limited by nutrients under field conditions. We prepared water accommodated fractions of dispersants (**D-WAF**), oil (**O-WAF**), and chemically dispersed oil (**CE-WAF**; CEWAF stands for Chemically Enhanced Water Accommodated Fraction) using the methods outlined in Kleindienst et al., (2015b) and Shepard (2019). Briefly, seawater was sterile-filtered with Millipore Express PLUS® 0.22 μm filters and then pasteurized at 65 ºC for 2 hours. Once water cooled to room temperature, a volume of oil, Corexit®9500, or oil+Corexit®9500 were added to create water accommodated fractions of each organic fraction.

For the oil water accommodated fraction (O-WAF), 0.15 L Marlin platform Macondo surrogate oil was added to 0.85L of sterile seawater. For the dispersant water accommodated fraction (D-WAF), 0.015 L of Corexit®9500 (Corexit) was added to 0.85L of sterile seawater. For the chemically enhanced water accommodated fraction (CE-WAF), 0.015 L of Corexit®9500 and 0.15 L of Macondo surrogate oil were added to 0.85 L of sterile seawater. All treatments were amended with a sterile stir bar, sealed, wrapped in aluminum foil, and stirred gently for 48 hours in the dark at room temperature to equilibrate the organic and aqueous phases.

After 48 hours, each solution was transferred to a combusted separatory funnel and settled for one hour as described by Shepard (2019). During the equilibration period, organic constituents moved into the aqueous phase and the resulting water-soluble fraction was separated from the organic phase using the separatory funnel and dispensed into two combusted glass bottles which were stored at room temperature until they were used in laboratory experiments. The next day, total organic carbon (TOC) in the aqueous phase was determined using a high temperature catalytic combustion system (Shimadzu®TOC-V; see below) to determine the concentration of total organic carbon. The WAF concentration data were used to calculate the amount of each WAF to add to the experimental bottles to achieve a target TOC concentration of around 350 μM DOC above the background DOC concentration (Kleindienst et al., 2015b). The water accommodated fractions were not filtered before addition to experimental bottles, so all treatment additions included dissolved organics plus microscopic droplets of oil and/or dispersant.

Microcosm Preparation and Sampling

Sterile (autoclaved and combusted) 2 L glass Schott bottles with Teflon lined caps were used as microcosms. Six replicates of each treatment – unamended controls and three different organic carbon additions – were prepared. The same amount of organic carbon – whether it was derived from dispersant, oil, or oil plus dispersant – was added to each treatment suite; controls received no carbon addition. The sample volume of sample in each bottle was 1.8 L and three replicates of each treatment were amended to achieve instantaneous concentration increases of ammonium (10 μM added as ammonium chloride) and phosphorus (1 μM added as potassium phosphate).

During the incubations, bottles were maintained at 24ºC on a roller table in the dark. The roller table was used to mimic mixing regimes in the surface ocean. The OC26 incubations were sampled immediately (time-zero) and the one week (time-one) after additions. After sampling at time-one, two mL of bulk crude oil was added to each bottle to assess how a microbial community grown up on one organic carbon cocktail responded to oil addition. Bottles were returned to roller table and maintained at 24 ºC in the dark for 32 hours at which point a second (time-two) set of samples were collected. For GC600, a fourth sampling point (time-three, one week after the crude oil addition) was added to evaluate long-term community effects.

Sampling Scheme

At time-zero samples for determining dissolved organic carbon (DOC) and dissolved nutrient concentrations were collected from each sample (Figure S3.1). A single representative time-zero sample was sacrificed for subsequent nucleic acid sequencing. Sampling at later time points was similar to time-zero except that one DNA filter and AODC sample was collected for

each treatment condition by pooling sub-samples from treatment replicates. After bulk crude oil addition (time-two and time-three) were collected by inverting the stoppered bottle and removing the desired volume through a special sampling apparatus (Shepard, 2019), avoiding sampling the added bulk crude oil.

Samples for DOC and nutrients were filtered through a pre-rinsed and dried 0.2 μm Target® filter, frozen upright and stored at -20 ºC until analysis. Prior to freezing, a 2.5 mL sub-sample was transferred to a 15 mL falcon tube containing 100 μL phenol for subsequent determination of ammonium concentration using colorimetry (Solórzano, 1969). To determine dissolved organic carbon (DOC), total dissolved nitrogen (TDN), ammonium (NH_4^+), nitrite plus nitrate (NO_2^-+ NO_3^-), nitrite (NO_2^-), and phosphate (HPO_4^{3-}), samples were thawed and mixed well and then split between analyses as follows (Shepard, 2019). For DOC, a 5 mL sample was analyzed on a total organic carbon analyzer (Shimadzu® TOC-Vcph). Samples were run in tandem with potassium hydrogen phthalate standards to determine concentrations. TDN was also measured using the Shimadzu analyzer utilizing a TNM-1 module. TDN samples were run in tandem with glycine standards. Nitrite plus nitrate concentrations were determined using a vanadium reduction assembly, an Antek 745 chemiluminescent nitric acid detector, and an Antek 7050, as described previously (Braman and Hendrix, 1989). Concentrations were determined by comparing sample peak area to peak areas of KNO_3 standards. Nitrite concentration was determined using colorimetry (Bendschneider and Robinson 1952). Finally, dissolved phosphate concentrations were determined using a molybdate blue colorimetric method (Solórzano and Sharp, 1980).

We tracked the organic carbon added to the microcosms as dissolved organic carbon (DOC). We initially determined total dissolved organic carbon, TOC, which accounts for

dissolved components plus droplets. During the incubations, some droplets were observed (visual observation) to stick to the wall of the glass incubation vessel and organic carbon moves from droplets into the dissolved phase during the incubations (unpublished observation). Most of the trends in DOC over time reflected this dynamic.

Rates of Microbial Activity

Bacterial production rates were determined using the ^{3}H-leucine incorporation method (Shepard, 2019; Smith and Farooq, 1992). Briefly, 1.5 mL of sample was transferred to a 2 mL microcentrifuge tube. Three replicates were included for each sample/treatment along with a killed control, which were generated by adding 100 μL of 100% trichloroacetic acid (TCA) to the sample prior to radiotracer addition. Each sample was amended with 16.67 kBq ^{3}H-leucine and incubated in the dark at room temperature for three hours. Incubations were terminated by addition of 100 μL of TCA, as per the controls. Fixed samples were stored in the laboratory at room temperature before processing.

To quantify leucine incorporation, samples were centrifuged (10,300 RPM × 15 minutes) to isolate the cell pellet and the liquid phase was aspirated. Next, an additional 1.5 mL of 5% TCA was added and the centrifugation/aspiration process was repeated. Then, 1.5 mL of ethanol (80%) was added to each sample before centrifuging a final time at 10,300 RPM for 5 minutes and aspirating the ethanol and avoiding the pellet. The tube with the remaining sample (pellet) was left uncapped to dry in the fume hood overnight. Once dry, scintillation fluid (1.75 mL of BioSafe II Scintillation Cocktail; Fisher) was added to each sample, and after vortexing, the sample was counted on a Beckman 6500 liquid scintillation counter. Bacterial production rates were calculated using the equation of Kirchman et al. (Kirchman, 2001).

Two radioactive hydrocarbon substrates – ^{14}C-hexadecane and ^{14}C-naphthalene – were used to estimate potential rates of biological hydrocarbon oxidation using previously described methods (Kleindienst et al., 2015b; Sibert et al., 2016). We selected these substrates because they are excellent proxies for their representative crude oil fractions – hexadecane for the saturates fraction and naphthalene for the polycyclic aromatic hydrocarbons (PAH) fraction. Hexadecane is paraffin hydrocarbon ($C_{16}H_{34}$) that is immiscible with water. Hexadecane metabolism is representative of this class of hydrocarbons. Naphthalene ($C_{10}H_8$) is the simplest condensed ring aromatic hydrocarbon, essentially two benzene rings that share two adjacent carbons. Naphthalene is also insoluble in water and is highly volatile. It is good representative for PAH cycling, in general, and offers a window into the cycling of the compound class.

For hydrocarbon oxidation rate assays, triplicate samples were transferred to a 7 mL glass vial and each vial was closed headspace-free with a PTFE Teflon lined septa and sealed with a screw cap. Glass gas-tight syringes were used to inject 16.67 kBq ^{14}C-hexadecane or ^{14}C-naphthalene (in 20 μL, dissolved in molecular grade ethanol) into triplicate sample alongside a killed control. Killed controls amended with radiotracer and then transferred immediately to a 50 mL plastic Falcon tube containing 2 mL of a 2 M NaOH kill solution. Then the vial was rinsed twice with pH-8.5 tap water and the rinse water added to the centrifuge tube for counting. Live samples were incubated for two days at room temperature in the dark, and after incubation, activity was terminated using the same procedure described for killed controls.

To recover the product of hydrocarbon oxidation, $H^{14}CO_3^-$, each sample was transferred to a 250 mL Erlenmeyer flask that contained one gram of activated charcoal. For hexadecane amended samples, 250 mg of C18 reverse phase silica gel was also added because charcoal alone

was not an effective scrubber for the hexadecane parent tracer. Each falcon tube was rinsed with basified tap water (twice) and rinse solution was added to the matching Erlenmeyer flask.

Flasks were capped with rubber stoppers and clamps and shaken for at least 18 hours to bind parent tracer to the charcoal or charcoal-silica mix. Afterwards, samples were removed from the shaker table and a carbon dioxide trap (Shepard, 2019) amended with 1.5 mL of a CarboSorb® (Perkin Elmer) CO_2 trap was secured within each flask. The liquid sample was acidified by addition of concentrated phosphoric acid (Shepard, 2019). Acidified samples were shaken overnight (approximately 12 hours) at 50 RPM after which time the traps were removed and amended with 4.5 mL of scintillation fluid. Samples were allowed to sit for 24 hours to reduce quenching (chemiluminescence) and then counted for five minutes on a Beckmann 9500 Liquid Scintillation Counter. Hydrocarbon oxidation rates were calculated according to Kleindienst et al. (2015b) and Sibert et al. (2016); concentrations of hexadecane and naphthalene were calculated from tracer additions and known solubility coefficients to estimate hydrocarbon concentrations in the experimental bottles. As such, these rates should be considered to reflect potential activity.

DNA Filtering, Extraction, and Sequencing

At each time point, a pooled sample reflecting three equal parts of each replicate, was filtered through a 0.2 μm Sterivex® filter. Filters were flash frozen in liquid nitrogen and stored in the laboratory at -80 °C until DNA extraction. To recover DNA for sequencing, samples were thawed on ice and extracted according to the DNAeasy kit instructions and DNA was stored at –20 °C. Library preparation was performed according to the standard instructions of the 16S Sequencing Library Preparation protocol (Illumina™, Inc., San Diego, CA, United States). The

V4–V5 region was amplified using the 515F-Y (5′-GTGYCAGCMGCCGCGGTAA-3′) and the 926R (5′-CCGYCAATTYMTTTRAGTTT-3′) primers (Parada et al., 2016). Sequences were obtained on the Illumina MiSeq™ platform in a 2 × 300 bp paired-end run, following the standard instructions of the 16S Metagenomic Sequencing Library Preparation protocol. Extracted samples were sequenced at University of Illinois at Chicago's Sequencing Core. DNA extracted from select times points from OC26 incubations, *time-zero*, control+nutrients *time-two*, dispersants+nutrients *time-two*, dispersants+nutrients *time-two*, WAF+nutrients *time-two*, and CEWAF+nutrients *time-two*, were sent to CosmosID (Rockville, MD, USA) for metagenomic sequencing using the HiSeq platform, as described previously (Hasan et al., 2014).

Bioinformatic and Statistical Analysis

FastQC analysis (Andrews, 2010) was performed to assess the quality of the obtained raw reads and to establish the quality threshold for further filtering steps. Afterwards, adapters removal and quality filtering of reads was performed using Trimmomatic (Bolger et al., 2014) with the following parameters: quality trimming with a sliding window of 4 pb and quality threshold of 20, and final length cutoff 100 pb. QIIME v1.9.1(Caporaso et al., 2010) was used for OTU clustering at 97% similarity using the UCLUST algorithm, taxonomic assignment against the Greengenes Database version 13_5, estimates of α diversity (Phylogenetic Diversity, Observed OTUs, Chao1, Shannon, Simpson) and β diversity (Bray–Curtis, weighted and unweighted UniFrac). The OTUs with no assignable taxonomy in the Greengenes Database, were further taxonomically annotated using BLAST algorithm against the nucleotide database of NCBI. Sequences with no match with e-values below 1e-10 and identity above 90%, and no clear alignment to other 16S rDNA sequences, were removed as they likely reflect either high

sequencing error rate or low-level contamination. Afterward, assigned OTUs were filtered out for sequences present in only one sample and below the 0.01% relative abundance. The resulting taxonomy, of the sequences not assigned by QIIME was visualized using hierarchical taxonomy merging scripts described elsewhere (Peña-Montenegro et al., 2020, 2021 under review) .

To gain insight into the metabolic potential of the community, we used the Piphillin server (Narayan et al., 2020) with the KEGG and BioCyc databases as references. Piphillin provides functional profiles of microbial communities using the 16S rDNA profile as input by applying an extended ancestral-state algorithm that predicts the gene content from a marker gene survey. The algorithm uses an existing database of reference microbial genome and generates an annotated table of predicted KEGG orthologs (KOs) counts. OTU abundance was normalized previously in QIIME.

Metagenomic data was processed as described previously (Zhuang et al., 2018). Briefly, raw shotgun sequencing reads were de-replicated and trimmed using Sickle (https://github.com/najoshi/sickle). Processed reads of each sampling site were assembled separately using MEGAHIT (Li et al., 2015) with a k-mer range of 21-101 and a step size of 10 bp. Coding DNA Sequence (CDS) genes were identified using Prodigal v2.6.3 (Hyatt et al., 2010) (parameter: -p meta) and MetaGeneMark v3.25 (Zhu et al., 2010).

Predicted CDSs were translated and subjected to blastp (Altschul et al., 1997) searches (e-value < 1e-5, bitscore > 40) against GenBank's nonredundant protein database (NR) and Uniprot's Swiss-Prot and TrEMBL protein databases. To assess the abundance of genes, reads of each sample were aligned to the collection of assemblies with Bowtie2 v2.3.3.1 (default parameters). The estimation of high-quality reads per CDS and data integration of annotation

terms were performed using the SFG RNA-Seq pipeline for population genomics (De Wit et al., 2012).

To investigate the community structure in our samples, we performed taxonomy annotation using the following approaches: First, small subunit (SSU) rRNA gene sequences were reconstructed using a reference-guided method (Tully, 2015). From the high-quality sequencing reads, 16S rRNA associated reads were identified using Meta-RNA (Huang et al., 2009). Putative 16S rRNA reads were processed through EMIRGE (Miller et al., 2011) to generate full-length 16S sequences. Reconstructed 16S rRNA genes were assigned taxonomy using Mothur v1.39.5 by aligning the sequences to the SILVA SSURef128 database, removing sequences that failed to align, if necessary, and classifying the sequences (Quast et al., 2012). Third, sequencing libraries were subjected to the metagenomic platform MG-RAST.

3.3 Results and Discussion

Chemistry Trends Across Incubations

Trends in ammonium concentrations in the unamended treatments for OC26 showed little variability over time, while ammonium concentrations in unamended treatments at GC600 were below detection (Figure 4.1). In contrast, in nutrient amended treatments, ammonium drawdown was most significant in the O-WAF amended treatments for both OC26 and GC600; concentrations were drawn down to zero (GC600) or <1 μM (OC26). Though no significant drawdown was apparent in controls at either site after a week, treatments amended with dispersants – both D-WAF and CE-WAF – and nutrients showed about 50% drawdown of ammonium in a week (Figure 4.1). Ammonium was almost completely depleted in OC26 samples following crude oil addition.

In situ concentrations of nitrate+nitrite were very low, 0.3 ± 0.1 and 0.6 ± 0.2 μM nitrate+nitrite, for OC26 and GC600, respectively. No nitrite was observed in field samples or at any time point during the experiment, so the observed nitrate+nitrite value reflects nitrate concentration. Concentration of nitrate+nitrite showed relative uptake in the D-WAF treatments (Figure 4.1) but not in other treatments. Concentrations of nitrate+nitrite increased in all treatments after crude oil addition, reflecting nitrate accumulation since nitrite was below detection limit. Following crude oil addition, the rapid accumulation of nitrate was followed by similarly rapid consumption across all treatments at GC600 (no data available for OC26; Figure 4.1).

Concentrations of total dissolved nitrogen (TDN) showed little variation at OC26 during the initial incubation and the decreases observed after oil addition were due to biological assimilation of inorganic nitrogen. Addition of the oil-derived carbon specifically drove significant ammonium depletion, likely reflecting N assimilation by the oil-degrading microbial community. Corexit-derived carbon drove less of a nitrogen demand than did oil-derived carbon. A similar trend of nitrogen depletion in O-WAF amended samples was observed by Seidel et al. (2016), and the relative abundance of N-containing hydrocarbons decreased during O-WAF incubations. Rapid assimilation of inorganic nitrogen following oil addition across the treatment regime shows that the community is inherently nitrogen limited and that oil addition exacerbates nitrogen limitation substantially. As such, in the case of an oil spill, it is extremely likely that the microbial community and its activity will be limited by nitrogen availability.

Figure 4.1: *Average concentration of dissolved nitrogen compounds across the sampling points. Time 0 indicates samples collected directly after experimental set up. Time 1 reflects sampling after seven days of roller table incubations. Two mL of crude oil was added after Time 1 and then Time 2 samples were collected 32 hours after oil addition. Time 3 (GC600 only) reflects samples collected one week after oil additions. Bars represent standard deviation of the sample mean. Data from Shephard, 2019.*

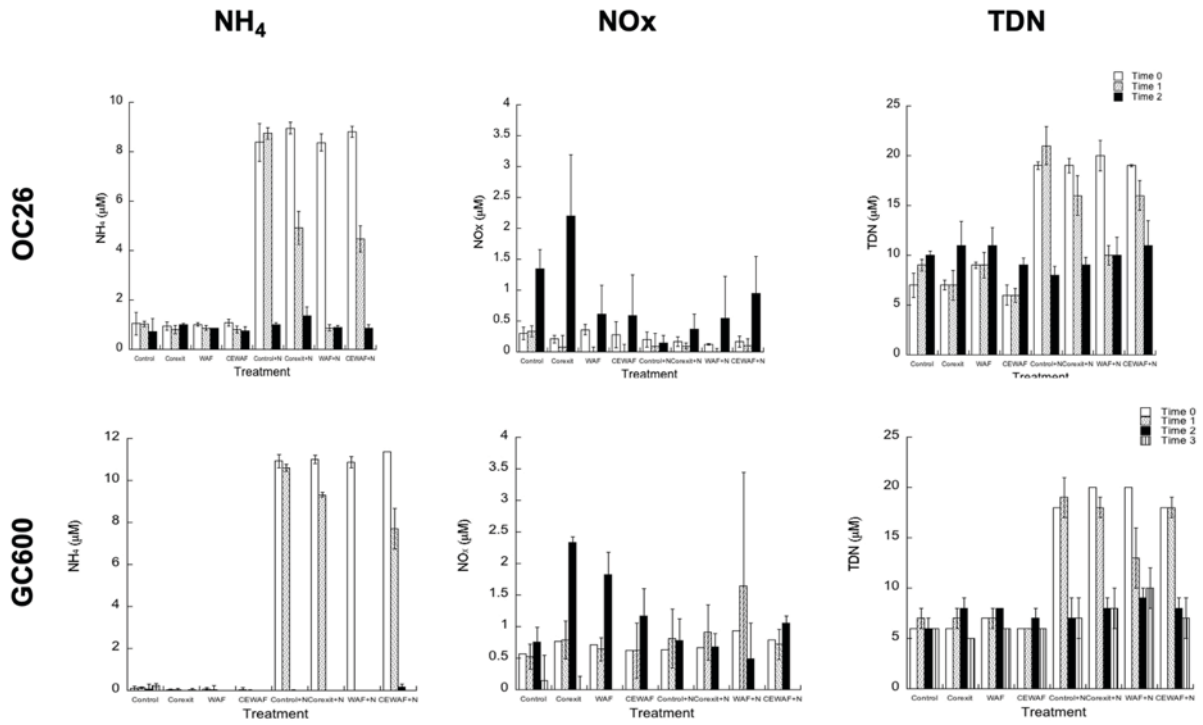

Samples amended with WAF showed a consistent increase in DOC concentration of roughly 350 μM relative to the control treatment (Figure 4.2). Background DOC concentrations were about 100 μM in surface water from OC26 and GC600. In general, at GC600, DOC concentration increased over time, reflecting movement of organic carbon from suspended droplets into the aqueous phase (Figure 4.2). At the OC26 site, substantial consumption of DOC was apparent between time-zero and time-two in all treatments. A week after bulk oil addition at GC600, DOC increased further, reflecting movement of the added oil into the aqueous phase, as expected.

Figure 4.2: *Average concentration of dissolved organic carbon and dissolved inorganic phosphorus across the sampling points. Times the same as described for Figure 1. Data from Shepard, 2019.*

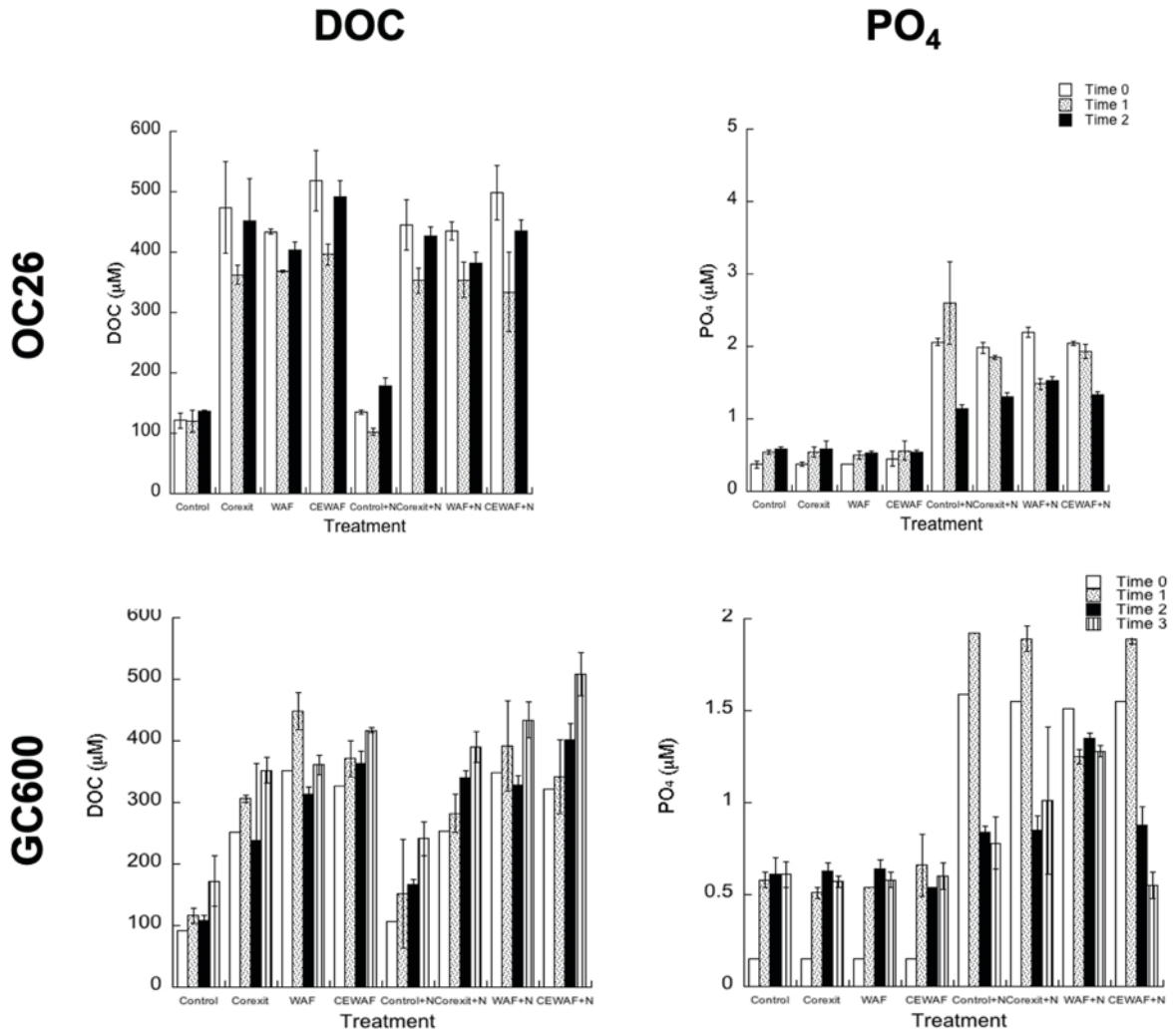

Phosphate was rapidly cycled at both sites. Concentrations of inorganic phosphate increased in unamended treatments, reflecting mineralization of organic phosphorus (Figure 4.2). This was especially true at GC600. In nutrient amended samples, phosphate was rapidly taken up, especially in organic carbon amended samples relative to the control (Figure 4.2). Phosphate

assimilation increased further after crude oil addition. Phosphate and nitrogen seem to limit microbial activity at these sites, which is not surprising given the low nutrient levels these offshore sites experience. It does appear, however, that the system is more nitrogen limited, than it is phosphorus limited since ammonium concentrations were often drawn down to detection limits of our methods, while phosphorus was not.

Bacterial Production

The presence of organic carbon and nutrients led to substantial differences in bacterial production rates (Figure 4.3, Shepard 2019). Bacterial production at OC26 was lower than that at GC600 at baseline, and the addition of nutrients led to an effective doubling of bacterial production at both sites. Immediate increases in bacterial production were observed in the D-WAF amended treatments, even without nutrients in OC26 samples. All WAF amended samples at OC26 showed significant increases in bacterial production, relative to the control, over the first week. Bacterial production in nutrient amended samples at OC26 were higher than in non-amended treatment parallels, but activity did not increase further after crude oil addition (Figure 4.3**)**.

For GC600, bacterial production rates were also higher in nutrient amended treatments. However, organic carbon addition had little impact on bacterial production in the absence of added nutrients, in contrast to the pattern observed at OC26 in the D-WAF treatment. This suggests that the ability of these microbial communities to respond to an oil spill is severely limited due to inherent, chronic nutrient limitation. However, despite the observation that GC600 microbial communities were chronically nutrient limited, these microbial communities exhibited the highest initial rates of bacterial production. A higher baseline level of activity could be

related to the increased frequency of organic carbon (oil) exposure at this site due to the high frequency of oil slicks. In general, Gulf of Mexico microbial communities have a high capacity for bacterial production, as long as nutrients are available.

Figure 4.3*: Bacterial production rates for OC26 and GC600 sites. Times the same as described for Figure 1. Data from Shepard, 2019.*

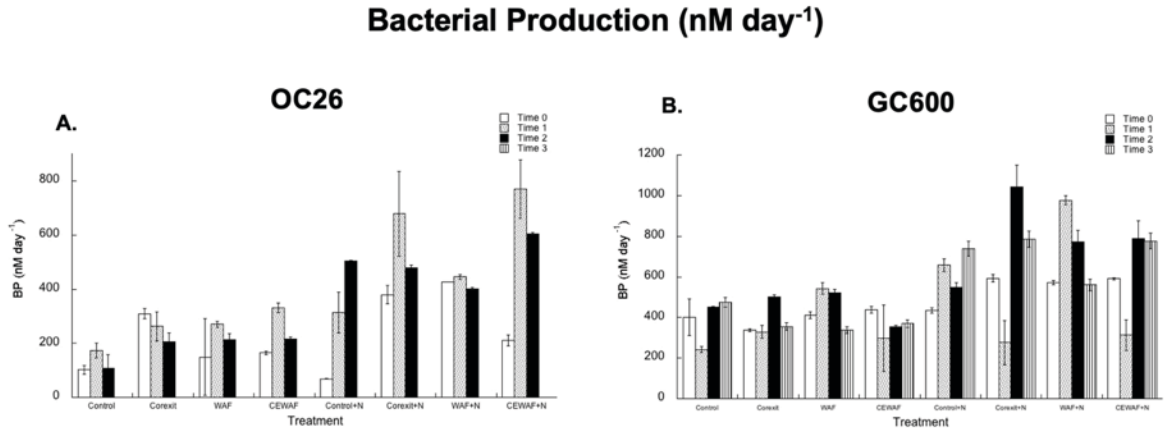

Potential Hydrocarbon Oxidation Rates

Hydrocarbon oxidation rates were inherently variable, but one thing is clear: hydrocarbon oxidation rates in Gulf of Mexico surface waters are profoundly nutrient limited. In the OC26 incubations, low rates of potential naphthalene oxidation rates were noted, and activity was stimulated by oil-derived organic carbon, but only when nutrients were added. Rates of naphthalene oxidation highest in treatments amended with nutrients, at a rate of ~1 nmol C oxidized per liter per day (Figure 4.4). The highest rates of naphthalene oxidation were observed in the O-WAF + nutrient samples, especially after crude oil addition. Unfortunately, the CE-WAF and CE-WAF + nutrient samples for naphthalene oxidation at OC26 were lost during processing and those data are not available.

Figure 4.4*:* *Rates of potential hexadecane and naphthalene oxidation. Times the same as described for Figure 1. Data from Shepard, 2019.*

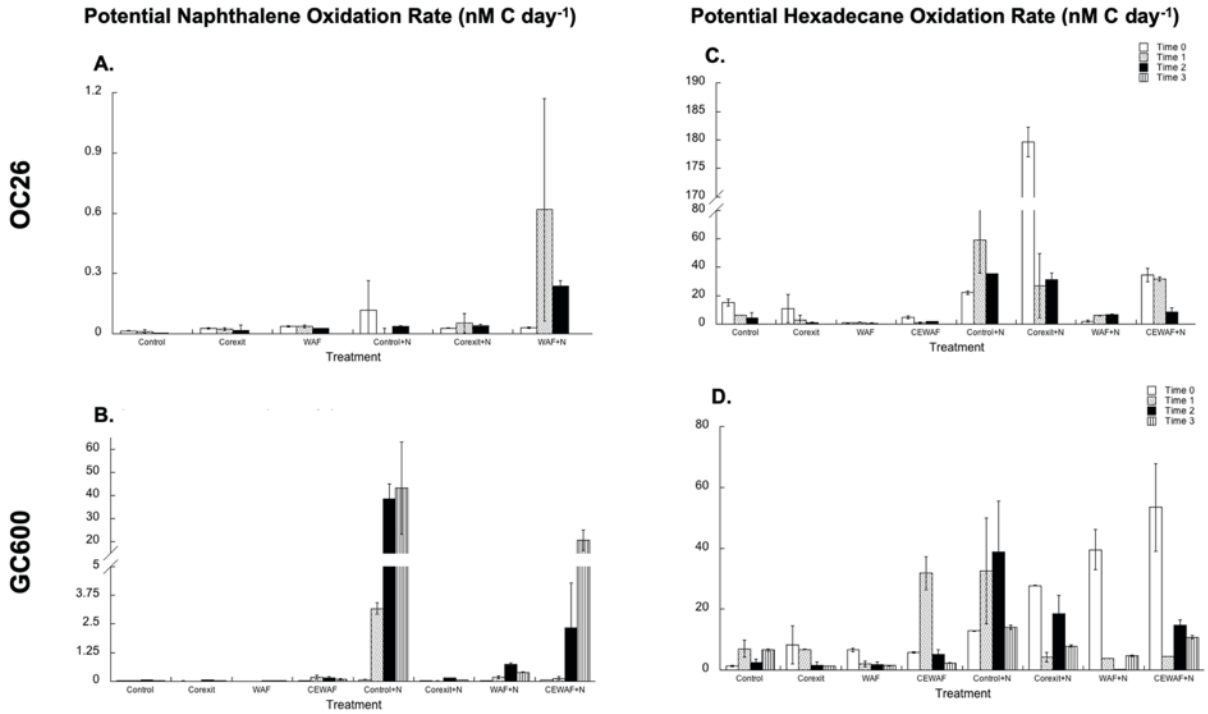

The highest rates of potential naphthalene oxidation rate at GC600, 43.19 ± 20.06 nmol C oxidized per liter per day, were observed in the Control + nutrient amendments (Figure 4.4**)**. The potential for naphthalene oxidation was significantly higher at GC600, compared to OC26, by almost a factor of 50. This suggests a more robust population of PAH degrading microorganisms is present at the GC600 natural seep site. After the initial week of incubation, potential naphthalene oxidation rate remained elevated and different across treatments. The rate of potential naphthalene oxidation rate in the CE-WAF+nutrient treatment increased 32 hours post

crude oil addition (2.36±1.941 nM C/day) and even more one week bulk crude oil addition (20.48±4.32 nM C/day).

Potential naphthalene oxidation rates in the control were much higher than rates in any of the WAF treatments, whether the WAF was from dispersant, oil, or dispersed oil. It is possible that other oil components were oxidized, just not naphthalene. Or, there may have been some component of the organic cocktail in the WAF amended treatments that either inhibited the microbial community's ability to oxidize naphthalene or that organic carbon availability selected for other heterotrophs that were poorly suited for oil oxidation. Clearly, when released from nutrient limitation, the natural background microbial community was the most well suited for naphthalene oxidation.

Similar to the trends observed for potential naphthalene oxidation, potential hexadecane oxidation rates were limited by nutrient availability. Potential hexadecane oxidation rates were stimulated immediately by nutrient addition (Figure 4.4). And, activity was extremely variable, making it difficult to quantify treatment-driven patterns. Unlike the trend observed for naphthalene, potential hexadecane oxidation rates were comparable at OC26 and GC600 in the absence of nutrient addition. (Figure 4.4). Average potential hexadecane oxidation rates in the Corexit+nutrient treatment were 179±2.61 nmol C per liter per day, over five times greater than the next highest potential hexadecane oxidation rate observed in the CE-WAF+nutrient treatment, 34.54±4.72 nmol C per liter per day. Potential hexadecane oxidation activity was not stimulated by crude oil addition, possibly because the community had already drawn down the available nutrient supply and the existing microorganisms were already metabolizing at capacity.

Potential hexadecane oxidation rates for GC600 exhibited significant differences across treatments throughout the experiment (Figure 4.4). At time-zero, the highest rate was observed in

the CE-WAF+nutrient treatment (53.4 ± 14.40 nmol C per liter per day); rates in all +nutrient treatments were higher at *time-zero* than the unamended nutrient-limited treatments. The next highest rate was the O-WAF+nutrient at 40 nmol C per liter per day. Activity generally declined over time in the experiment, probably because nutrient concentrations became more and more depleted, limiting growth. Similar trends of decreasing hydrocarbon oxidation activity over time were observed in deep water incubation experiments (Kleindienst et al., 2015b) and that decline was attributed to decreases in hydrocarbon concentrations over time.

In Gulf of Mexico surface waters, the microbial community's response to Corexit and/or oil exposure was highly dependent upon nutrient availability. Previous work identified a significant correlation to nutrient concentrations and naphthalene oxidation rates (Harrison, 2017). The data presented here calls into question previous results that reported microbial responses to oil-dispersant mixtures only in nutrient amended samples (Campo et al., 2013; McFarlin et al., 2014; Techtmann et al., 2017; Zahed et al., 2011). Clearly, in the absence of nutrients, the capacity for microbial hydrocarbon oxidation is limited, and nutrient stress could lead to inefficient biodegradation of hydrocarbons during a marine oil spill. The interaction between nutrient availability, reduced fitness due to nutrient limitation, and impacts of organic carbon exposure reflect multiple interacting stressors that likely reduce the potential for microbial oil biodegradation during periods of increased oil exposure.

Community Composition

During each individual incubation, community composition changed both with nutrient amendment and hydrocarbon amendment type (Figures 4.5 and 4.6). In the OC26 incubation, *Marinobacter* was most elevated in the $WAF^{+nutrient}$ treatment after the initial exposure period.

The relative abundance of *Marinobacter* increased 32 hours after crude oil addition in all treatments except the unamended WAF treatment, in which *Alteromonas* was elevated both after the initial exposure and after addition of bulk crude oil. *Halomonas,* an organisms that metabolizes the intermediate metabolites who is no a primary oil degrader, was more abundant in the WAF incubations, but not in the WAF+nutrient incubations, or any other treatments, further indicating that biological community composition is determined, in part, by nutrient availability.

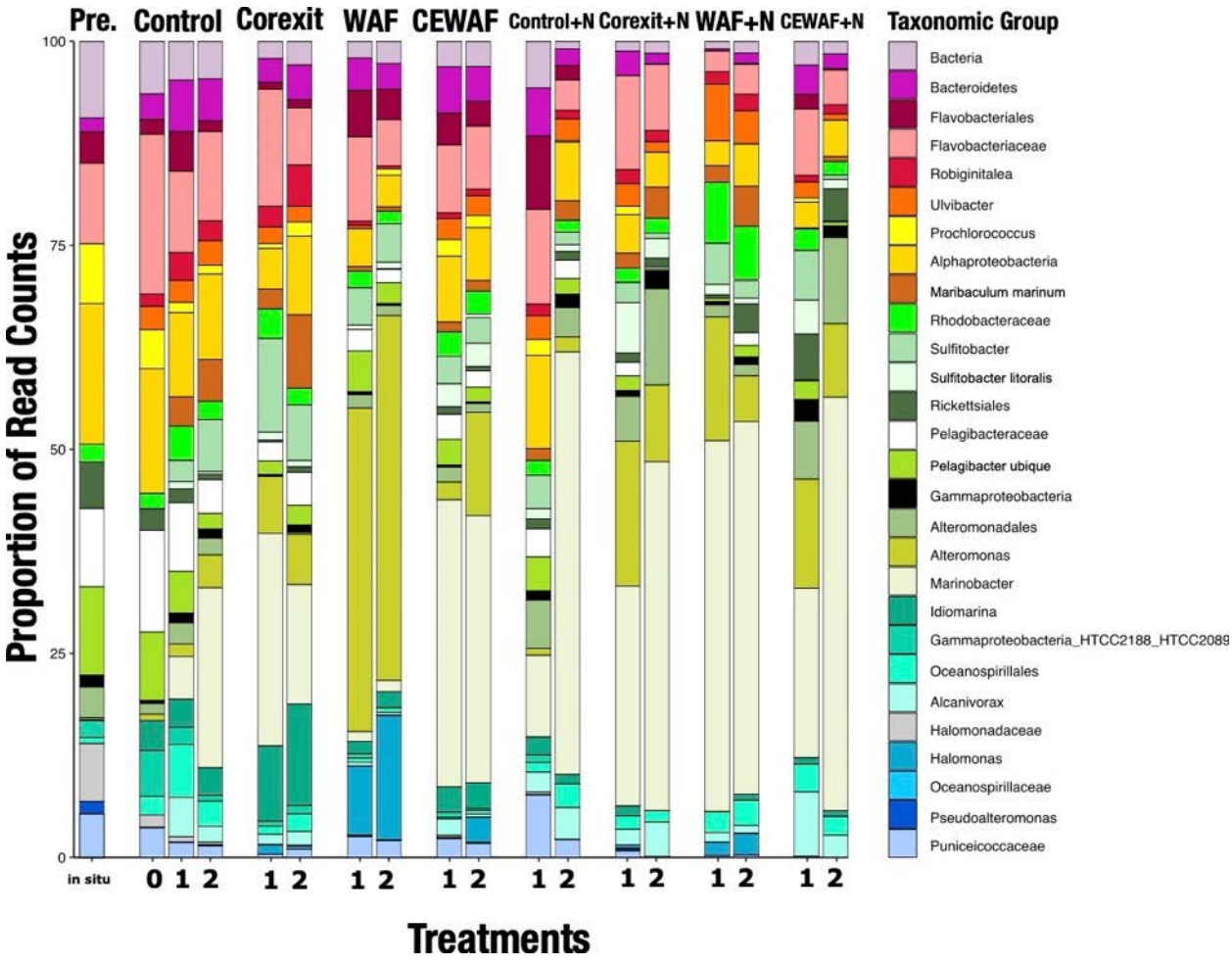

Figure 4.5: Microbial composition based on 16S rRNA amplicon sequences presented in proportion of read counts in OC26 incubations across all time points.

Malkin et al (2021) observed similar trends in which after eight days of incubation surface water amended with $WAF^{+nutrient}$ showed elevated abundance of *Marinobacter*, but other treatments did not show this enrichment. As was observed in the present work, Malkin, et al. did not observe complete inhibition of *Marinobacter* by Corexit or CEWAF conditions in surface waters, as was observed in similarly performed deep water experiments (Kleindienst et al., 2015b). It is possible that the deep water versus surface water ecotypes of Marinobacter exhibit a different response to oil – dispersant exposure regimes.

The major drawdown in ammonium was accompanied with a large increase in the proportion of *Marinobacter* read counts in OC26 incubations, more so than any other treatment at *time-one* (Figures 4.5 and 4.1). In GC600, the major drawdown in ammonium was accompanied by an increased proportion of read counts in *Flavobacteriales* (Figure 4.6). Whether or not these strains were the cause of the ammonium drawdown remains unclear, but there is a correlation between their increased abundance and the drawdown of ammonium.

Dispersant application frequently results in microbial community compositional changes. A decrease in *Marinobacter* relative abundance following addition of Corexit 9500 was observed in Keindienst et al.'s (2015) deepwater incubations. In that work while WAF treatments resulted in *Marinobacter*-dominated communities after two weeks incubations of plume depth water, CEWAF, Dispersant-only, and CEWAF+nutrient treatments led to increases in *Colwellia*. Relative abundance of *Colwellia* increased from 1% to 26-43% in dispersant-only, and CEWAF (± nutrients) treatments while *Colwellia* remained at 1-4% in WAF treatments (Kleindienst et al., 2015). *Colwellia* was not observed to be abundant in these incubations, and that is not surprising given the high temperature (20ºC) of the incubations and the fact that *Colwellia* is a

psychrophile. *Oceanospirillales*, *Alkanivorax*, and/or *Pseudoalteromonas* may have occupied the niche available by *Colwellia's* absence in these experiments.

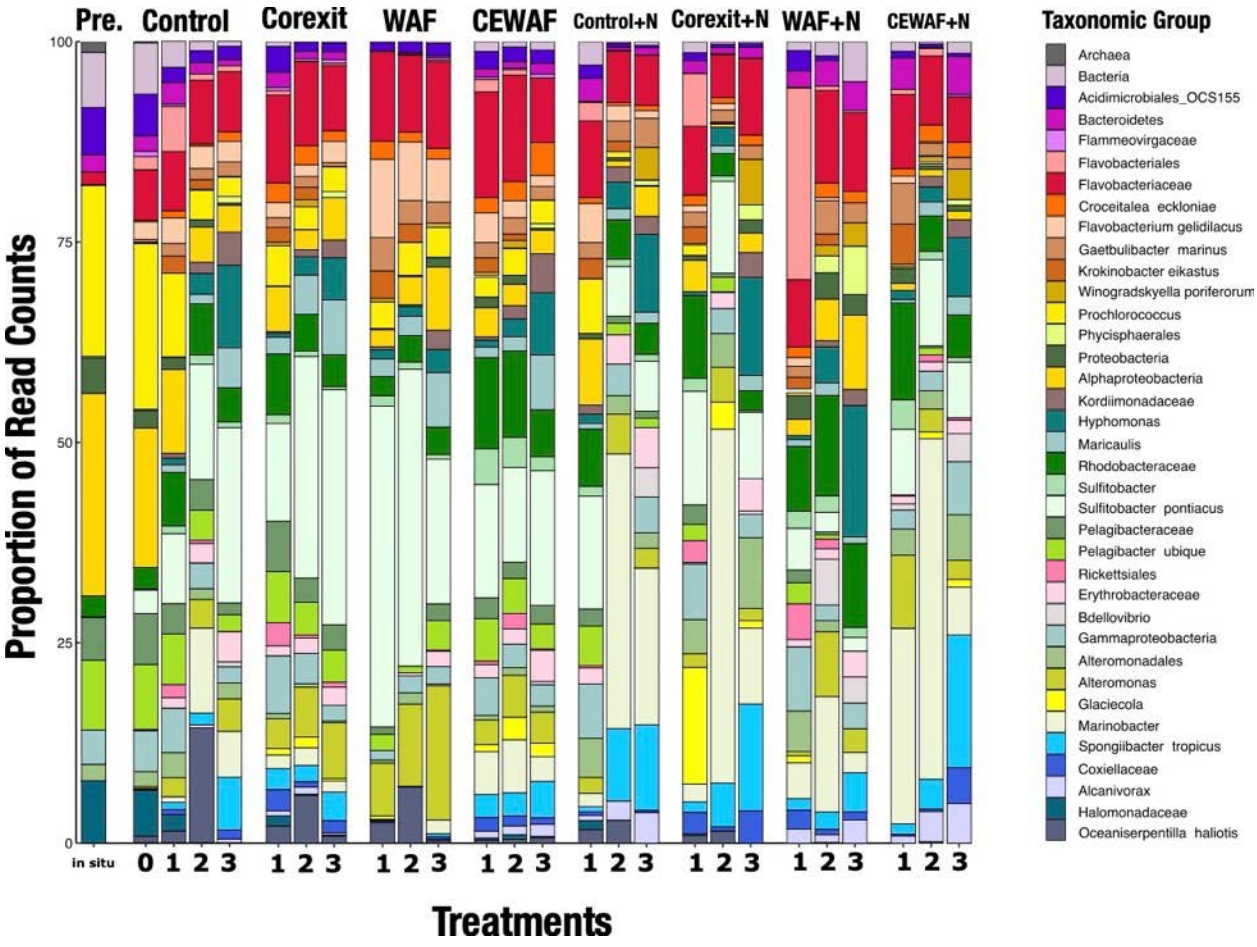

Figure 4.6: Microbial composition based on 16S rRNA amplicon sequences presented in proportion of read counts in GC600 incubations across all time points.

Corexit 9500A additions to culture enrichments of surface water close to the DWH spill resulted in decreased *Marinobacter* relative abundance, though bottom water experiments did not see a significant community structure changes (Techtmann et al., 2017). In contrast, in surface community incubations, Doyle et al. (2018) showed that WAF treatments resulted in about 3-5% relative abundance of *Marinobacter*-related OTUs, while CEWAF treatments resulted in much

higher *Marinobacter*-related OTUs. *Marinobacter* was not dominant in either incubation treatment in these studies. A deeper review of the *Marinobacter* ecotypes present in the current study in comparison to those in Kleindienst et al (2016) work will likely reveal a difference in ecotypes among surface and deepwater habitats and across the treatment regime.

In the GC600 incubation, *Marinobacter* was most elevated in the CEWAF$^{+nutrient}$ treatment, in contrast to their elevation in WAF$^{+nutrient}$ treatments at OC26. Nutrient availability played an important role selecting for *Marinobacter* abundance, independent of carbon source. After the initial exposure period, the WAF$^{+nutrient}$ treatments showed increased relative abundance of *Flavobacteriales*. *Flavobacteriales* degrade hydrocarbons, with a hexadecane degradation rate of 154 ppm h^{-1} in a strain isolated from oil contaminated soils (Salinas-Martínez et al., 2008; Yu et al., 2011). *Flavobacteriales* were abundant in surface oil mousse samples collected near the DWH and in Gulf surface slicks in May 2010, but not in ambient, uncontaminated sea water (Liu and Liu, 2013). All nutrient amended samples showed increases in *Marinobacter* relative abundance 32 hours after bulk crude oil addition, though to differing extents. Control$^{+nutrient}$, Corexit$^{+nutrient}$, and CEWAF$^{+nutrient}$ samples at this time point (32 hours post oil) contained more *Marinobacter* reads than the WAF$^{+nutrient}$ sample. A week after the bulk crude oil addition however, all nutrient amended samples showed decreased *Marinobacter* abundance. This observed decrease in abundance a week after crude oil exposure could indicate that a *Marinobacter* bloom occurred immediately after carbon infusion – meaning that these organisms may have been present in the WAF$^{+nutrient}$ treatments early into the preconditioning period but had diminished by the time of sampling.

Nutrient unamended treatments with hydrocarbon additions (Corexit, WAF, CEWAF) showed elevated levels of *Sulfitobacter pontiacus* after the initial incubation period (*time-one*).

The nutrient unamended control treatment also had *Sulfitobacter pontiacus* present, but to a lesser extent at this (*time-one*) time period. High *Sulfitobacter pontiacus* abundance continued throughout the remainder of the experiment in all nutrient unamended samples. *Sulfitobacter pontiacus* has been elevated in previous oil addition incubation experiments and beached oil (Brakstad and Lødeng, 2005; Gertler et al., 2009; Kostka et al., 2011). Analysis of draft genomes of *Sulfitobacter* sp. revealed genes associated with aromatic hydrocarbon degradation (Mas-Lladó et al., 2014).

Similar to the observations at OC26, *Colwellia* abundance was not elevated in any of the treatments or sampling sites, in contrast to previous incubation deepwater studies (Kleindienst et al., 2015b). *Colwellia* was abundant in deep plume waters during the DWH oil spill and increased in relative abundance in 4 °C incubations (Redmond and Valentine, 2012). Similarly, Redmond and Valentine (2012) did not see increased *Colwellia* in surface incubations underscoring *Colwellia's* preference for cold water. Thus, the absence of *Colwellia* in the present study is not surprising.

Whether or not the observed microbial population shifts are due to taxon specific toxicity or competition remains unclear (Kleindienst et al., 2015b). Hamdan and Fulmer (2011) found that *Marinobacter hydrocarbonoclasticus*, and *Acinetobacter venetianus* strains isolated from beached oil samples were inhibited when exposed to Corexit at 1:10000 and 1:100 dilutions as compared to control conditions (no Corexit, or oil). Interestingly, initial Corexit exposure at both treatment levels resulted in increased bacterial cell production in *Marinobacter* at time zero. After six hours an enhancing effect was still observed for the 1:100 Corexit treatment. By 12 hours however both Corexit treatments resulted in complete inhibition of *Marinobacter hydrocarbonclasticus* heterotrophic secondary production (Hamdan and Fulmer, 2011).

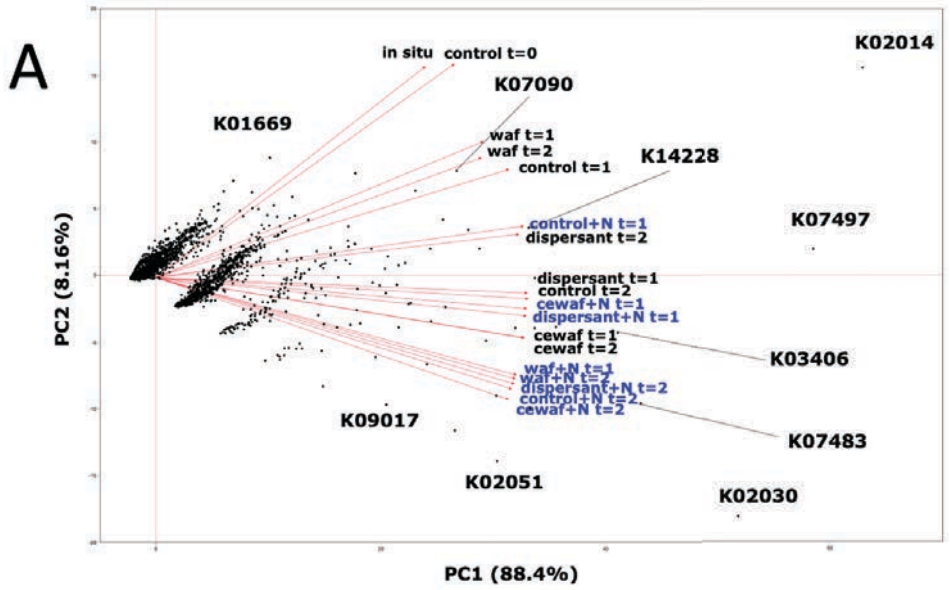
A
in situ
control t=0
K02014
K07090
K01669
waf t=1
waf t=2
control t=1
K14228
K07497
control+N t=1
dispersant t=2
dispersant t=1
control t=2
cewaf+N t=1
dispersant+N t=1
cewaf t=1
cewaf t=2
K03406
waf+N t=1
waf+N t=2
dispersant+N t=2
control+N t=2
cewaf+N t=2
K09017
K07483
K02051
K02030
PC2 (8.16%)
PC1 (88.4%)

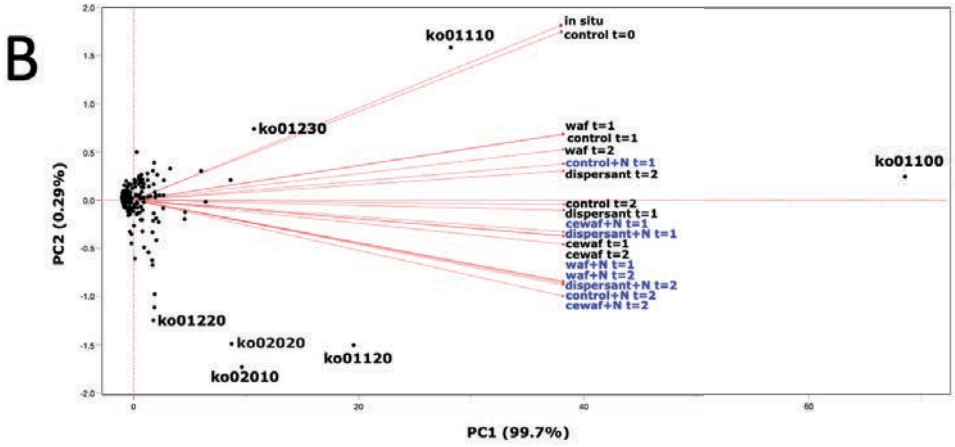
B
ko01110
in situ
control t=0
ko01230
waf t=1
control t=1
waf t=2
control+N t=1
dispersant t=2
ko01100
control t=2
dispersant t=1
cewaf+N t=1
dispersant+N t=1
cewaf t=1
cewaf t=2
waf+N t=1
waf+N t=2
dispersant+N t=2
control+N t=2
cewaf+N t=2
ko01220
ko02020
ko01120
ko02010
PC2 (0.29%)
PC1 (99.7%)

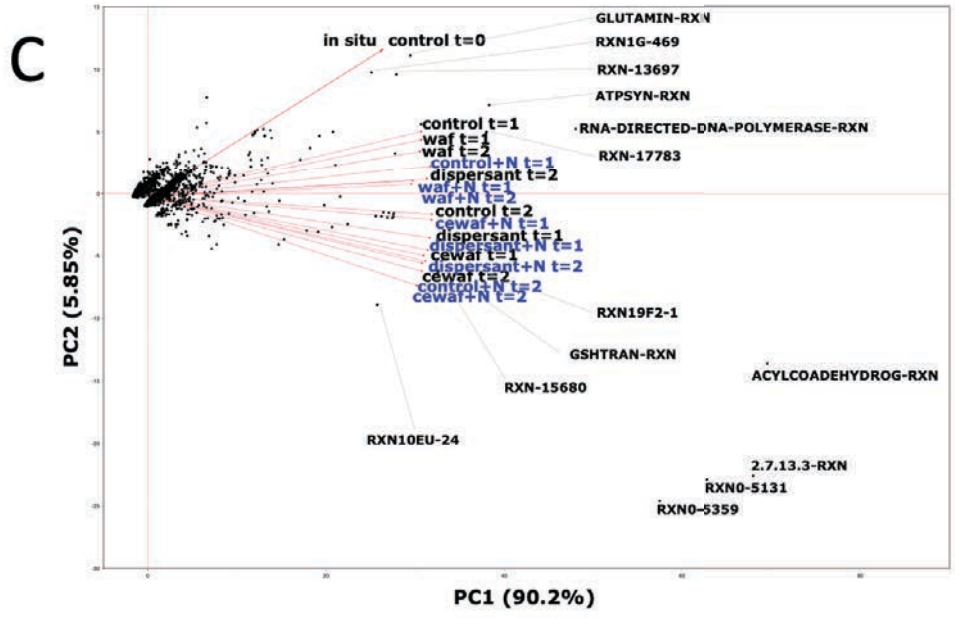
C
GLUTAMIN-RXN
in situ
control t=0
RXN1G-469
RXN-13697
ATPSYN-RXN
control t=1
waf t=1
waf t=2
RNA-DIRECTED-DNA-POLYMERASE-RXN
RXN-17783
control+N t=1
dispersant t=2
waf+N t=1
waf+N t=2
control t=2
cewaf+N t=1
dispersant t=1
dispersant+N t=1
cewaf t=1
dispersant+N t=2
cewaf t=2
control+N t=2
cewaf+N t=2
RXN19F2-1
GSHTRAN-RXN
ACYLCOADEHYDROG-RXN
RXN-15680
RXN10EU-24
2.7.13.3-RXN
RXN0-5131
RXN0-5359
PC2 (5.85%)
PC1 (90.2%)

Figure 4.7: Dimensional analysis of the predicted A) KEGG terms B) KEGG pathways and C) BioCyc reaction profiles predicted from 16S amplicon sequencing data of OC26 incubations across all time points. Loading vectors for each treatment are overlapped on red arrows, and those treatments supplemented with nutrients are highlighted in blue

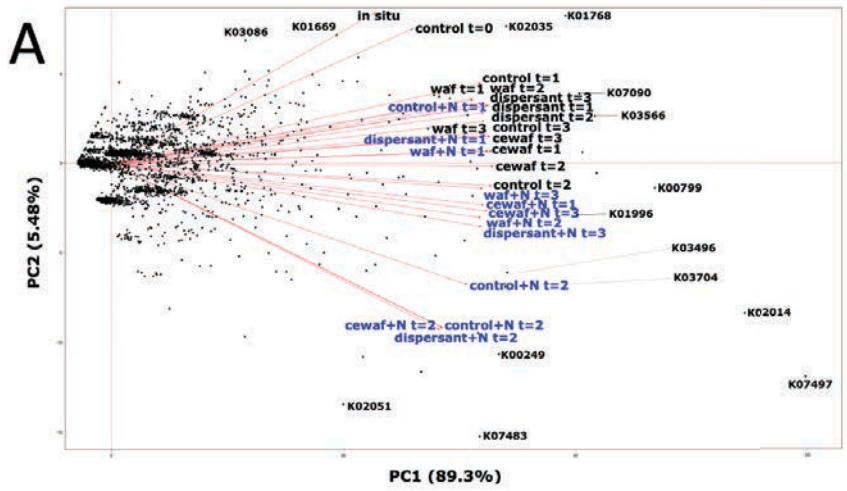
A
in situ
K03086
K01669
control t=0
K02035
K01768
control t=1
waf t=1
waf t=2
dispersant t=3
K07090
control+N t=1
dispersant t=1
dispersant t=2
K03566
waf t=3
control t=3
dispersant+N t=1
cewaf t=3
waf+N t=1
cewaf t=1
cewaf t=2
control t=2
K00799
waf+N t=3
cewaf+N t=1
cewaf+N t=3
K01996
waf+N t=2
dispersant+N t=3
K03496
K03704
control+N t=2
K02014
cewaf+N t=2
control+N t=2
dispersant+N t=2
K00249
K07497
K02051
K07483
PC2 (5.48%)
PC1 (89.3%)

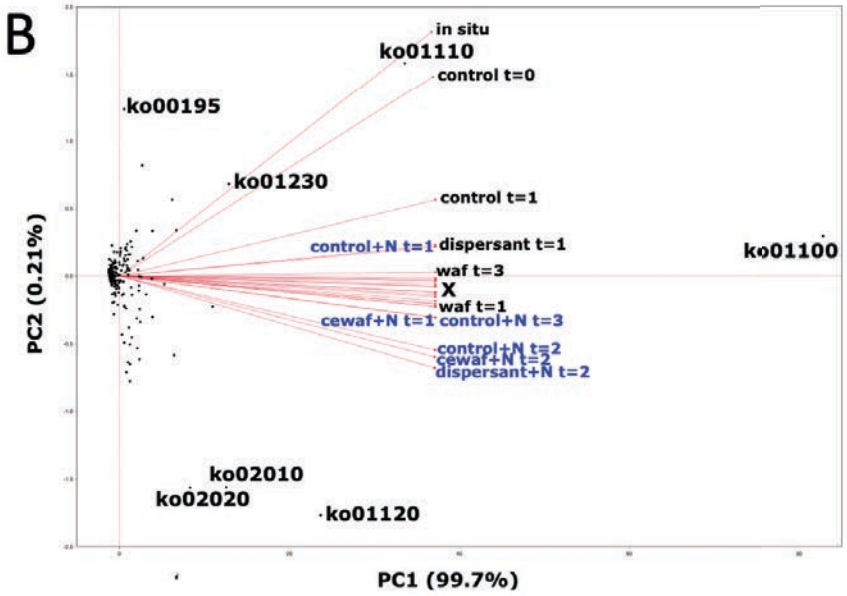
B
in situ
ko01110
control t=0
ko00195
ko01230
control t=1
control+N t=1
dispersant t=1
ko01100
waf t=3
X
waf t=1
cewaf+N t=1
control+N t=3
control+N t=2
cewaf+N t=2
dispersant+N t=2
ko02010
ko02020
ko01120
PC2 (0.21%)
PC1 (99.7%)

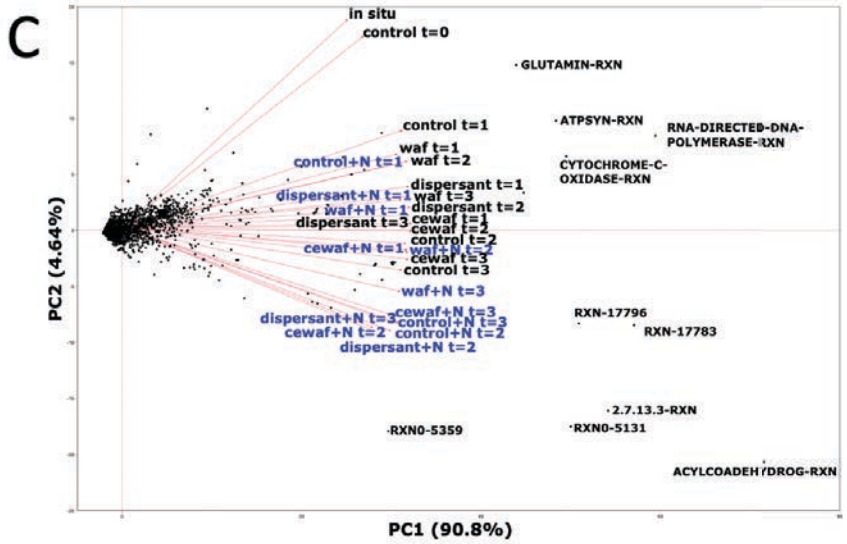
C
in situ
control t=0
GLUTAMIN-RXN
control t=1
ATPSYN-RXN
RNA-DIRECTED-DNA-POLYMERASE-RXN
waf t=1
control+N t=1
waf t=2
CYTOCHROME-C-OXIDASE-RXN
dispersant t=1
dispersant+N t=1
waf t=3
dispersant t=2
waf+N t=1
dispersant t=3
cewaf t=1
cewaf t=2
control t=2
cewaf+N t=1
waf+N t=2
cewaf t=3
control t=3
waf+N t=3
cewaf+N t=3
RXN-17796
dispersant+N t=3
control+N t=3
RXN-17783
cewaf+N t=2
control+N t=2
dispersant+N t=2
2.7.13.3-RXN
RXN0-5359
RXN0-5131
ACYLCOADEHYDROG-RXN
PC2 (4.64%)
PC1 (90.8%)

Figure 4.8: Dimensional analysis of the predicted A) KEGG terms B) KEGG pathways and C) BioCyc reaction profiles predicted from 16S amplicon sequencing data of GC600 incubations across all time points. Loading vectors for each treatment are overlapped on red arrows, and those treatments supplemented with nutrients are highlighted in blue. Symbol “X” in panel B represents the rest of treatments not shown due to close proximity of loading vectors.

Dispersant dilutions in these experiments were higher (1:30000) than those used by Hamdan and Fuller (2011), so at these levels there may have been less inhibitory for these *Marinobacter* ecotypes.

16S rRNA based Functional Metagenomic Prediction

Principal component analysis covered the majority of the variability of the functional profiles for any of the treatments and incubation sites (>95%) (Figures 4.7 and 4.8). All treatments showed a strong collinearity through the principal component 1 (PC1), possibly associated to a linear codependence in the prediction algorithm with respect to the 16S abundance matrix. For all the treatments and sites, we observed co-clustering of nutrient amended treatments towards the negative axis of PC2, specially for the KEGG pathways. However, the explained variability for KEGG pathways was the smallest of the dimensional analysis. On the other hand, BioCyc reaction profiles and KEGG terms for the GC600 site, nutrient and non-nutrient amended treatments were less distinguishable as separate clusters, although the explained variability was higher (~5%). This observation indicates the trade-off of clustering performance (i.e., nutrients-versus-non-nutrients treatments) against the efficiency to capture the variability of the system.

Some functional features were common across treatments and sites towards the in-situ and control time-zero libraries. For instance, ko01100 (metabolic pathways), ko01110 (biosynthesis of secondary metabolites), GLUTAMIN-RXN (EC: 3.5.1.2/3.5.1.38, glutaminase/asparaginase) and ATPSYN-RXN (E.C: 7.1.2.2, ATP synthesis) were commonly observed near the in-situ and control time-zero libraries. We hypothesize that these functional features resembled what the in-situ and control time-zero libraries looked like. We would also

expect these features to be the most perturbed under the exposure to any amendment of the experiment. In contrast, the features K02051 (NitT/TauT family transport system), ko02020 (two component systems), ko02010 (ABC transporters), ACYLCOADEHYDROG-RXN (E.C. 1.3.8.-, Fatty acid β-oxidation) clustered near the nutrient amended treatments. These results are expected and consistent with active microbial communities utilizing nutrient resources while fatty acid β-oxidation could be occurring.

3.4 Conclusions

Nutrients were most depleted in $WAF^{+nutrient}$ amendments in comparison to the other nutrient amendment treatments after the first week incubation, showing that the oil addition alone led to the highest rates of nutrient assimilation by the microbial community. However, this trend was not accompanied by consistently elevated rates of bacterial production or hydrocarbon oxidation or by a specific shift in community composition across sites. For example, OC26 $WAF^{+nutrient}$ incubations at Timepoint 1 was elevated in *Marinobacter* while GC600 $WAF^{+nutrient}$ incubations Timepoint 1 was elevated in *Flavobacteriales*, though nutrient drawdown trends were similar. This difference could be due to the fact that the GC600 microbial community was exposed to oil regularly, and the *Flavobacteriales* may have been primed to respond to that treatment.

Additionally, even though nutrients in nutrient amended treatments were not drastically depleted after a week of exposure to Control, Corexit, and CEWAF, only 32 hours after adding bulk crude oil, all treatments showed evidence of nutrient depletion. This further indicates that exposure to the hydrocarbon suite characteristic of WAFs results in dramatic increase in cellular ammonium (and to a lesser extent TDN, and phosphate) demand.

It is important to note that, because nutrient amendments were only made at the start of the initial exposure period, communities were exposed to the bulk crude oil with differing levels of nutrients remaining. Different nutrient uptake kinetics could have affected potential hydrocarbon oxidation rates in varying ways. Unlike marine derived organic matter, bulk crude oil (or Corexit) does not contribute significantly to N and P concentrations. Ambient water nutrient availability therefore can limit oil degradation in marine systems (Leahy and Colwell, 1990). This dynamic may have influenced community response and potential hydrocarbon oxidation rates of samples as the incubation progressed, and also driven microbial dynamics during the DWH oil spill.

Nutrient additions altered microbial community composition and potential hydrocarbon oxidation rates. This trend has implications for designing future dispersant and oil impact studies. A lot of the previous work on this topic evaluated oil degradation rates and the effect of dispersants on those rates in the presence of added nutrients (Campo et al., 2013; Techtmann et al., 2017; Zahed et al., 2011). As demonstrated here, differences in nutrient availability shifts the community structure, and impacts the potential hydrocarbon oxidation rates. Conducting dispersant investigations solely under nutrient replete conditions is not be representative the natural environment. Nutrient availability, it is critical to evaluate dispersant inhibition/stimulation effects in nutrient conditions that reflect these *in situ* concentrations when developing national and regional contingency plans of the future.

The microbial communities across the experiment showed the influence of nutrients to the exposure of each amendment. OC26 was strongly characterized by the colonization of *Marinobacter* across the nutrient supplemented experiments, except for the WAF only, where *Alteromonas* increased. Similarly, for the GC600 incubations, *Marinobacter* was also a common

microbial driver in presence of nutrients, however *Sulfitobacter pontiacus* succeded to grow in carbon amended without nutrient treatments. *Flavobacteriales* responded quickly to WAF+Nutrients treatment. Finally, the functional metagenomic estimation based on 16S rRNA gene sequencing provided insights of activation of ABC-transporters, two-component sensors and fatty acid β-oxidation processes for nutrient-amended treatments.

Data Availability

All scripts and links to public repositories for raw sequencing data and supplementary data are found on Github (https://github.com/biotemon/Shepard)

3.5 Supplementary Material

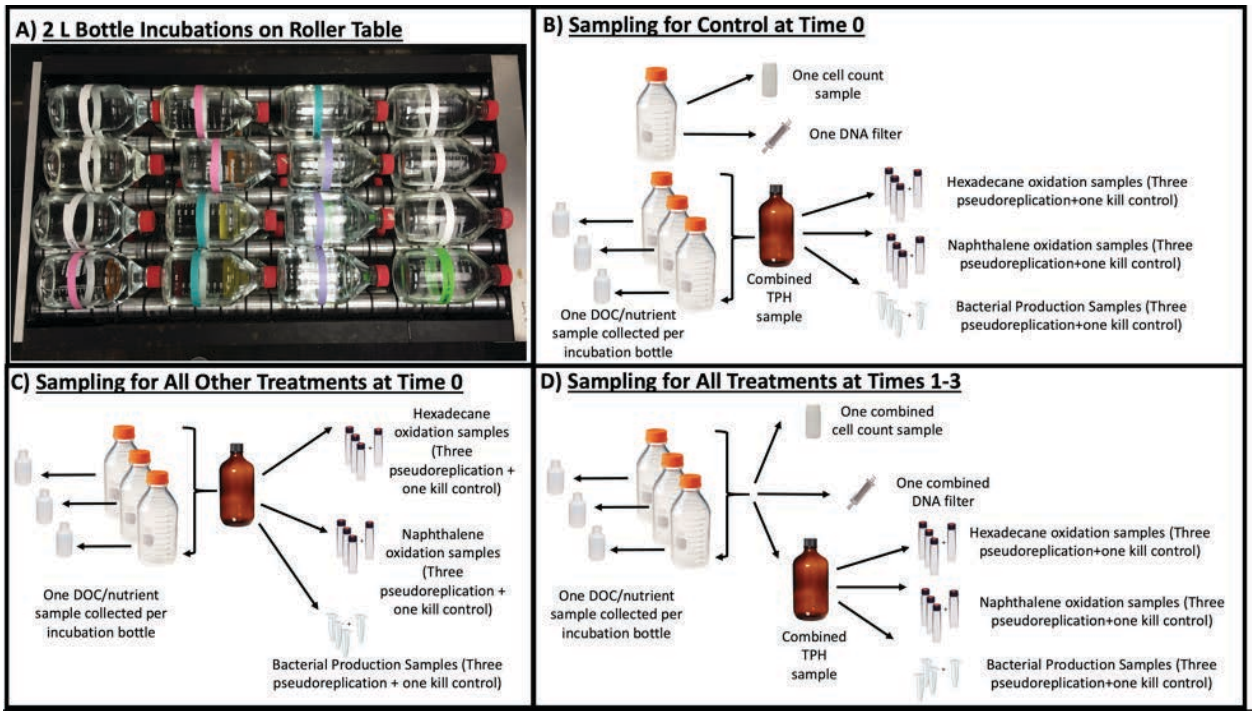

Figure S3.1: a) 2 L bottle incubations on roller table maintained at 24 ºC in the dark, b) samples collected from control incubation bottles at time-zero, c) samples collected from all other treatments (Corexit±nutrients, WAF±nutrients, CEWAF±nutrients) at time-zero, d) samples collected from all treatments at time-one-time-three. time-three sampling was only conducted on GC600 samples. Hexadecane and naphthalene oxidation rates were not collected in Taylor incubations.

3.6 References

Altschul, S.F., Madden, T.L., Schäffer, A.A., Zhang, J., Zhang, Z., Miller, W., Lipman, D.J., 1997. Gapped BLAST and PSI-BLAST: a new generation of protein database search programs. Nucl. Acids Res. 25, 3389–3402. https://doi.org/10.1093/nar/25.17.3389

Andrews, S., 2010. A quality control tool for high throughput sequence data.

Bendschneider, Kenneth, Robinson, Rex J, 1952. A new spectrophotometric method for the determination of nitrite in sea water. J. Mar. Res. 2, 87–96.

Bolger, A.M., Lohse, M., Usadel, B., 2014. Trimmomatic: a flexible trimmer for Illumina sequence data. Bioinformatics 30, 2114–2120. https://doi.org/10.1093/bioinformatics/btu170

Brakstad, O.G., Lødeng, A.G.G., 2005. Microbial Diversity during Biodegradation of Crude Oil in Seawater from the North Sea. Microb Ecol 49, 94–103. https://doi.org/10.1007/s00248-003-0225-6

Braman, R.S., Hendrix, S.A., 1989. Nanogram nitrite and nitrate determination in environmental and biological materials by Vanadium(III) reduction with chemiluminescence detection. Anal. Chem. 61, 2715–2718. https://doi.org/10.1021/ac00199a007

Campo, P., Venosa, A.D., Suidan, M.T., 2013. Biodegradability of Corexit 9500 and Dispersed South Louisiana Crude Oil at 5 and 25 °C. Environ. Sci. Technol. 47, 1960–1967. https://doi.org/10.1021/es303881h

Caporaso, J.G., Kuczynski, J., Stombaugh, J., Bittinger, K., Bushman, F.D., Costello, E.K., Fierer, N., Peña, A.G., Goodrich, J.K., Gordon, J.I., Huttley, G.A., Kelley, S.T., Knights, D., Koenig, J.E., Ley, R.E., Lozupone, C.A., McDonald, D., Muegge, B.D., Pirrung, M., Reeder, J., Sevinsky, J.R., Turnbaugh, P.J., Walters, W.A., Widmann, J., Yatsunenko, T.,

Zaneveld, J., Knight, R., 2010. QIIME allows analysis of high-throughput community sequencing data. Nature methods 7, 335–6. https://doi.org/10.1038/nmeth.f.303

Cardona, Y., Bracco, A., Villareal, T.A., Subramaniam, A., Weber, S.C., Montoya, J.P., 2016. Highly variable nutrient concentrations in the Northern Gulf of Mexico. Deep Sea Research Part II: Topical Studies in Oceanography 129, 20–30. https://doi.org/10.1016/j.dsr2.2016.04.010

Carrero-Colón, M., Nakatsu, C.H., Konopka, A., 2006. Effect of Nutrient Periodicity on Microbial Community Dynamics. Appl. Environ. Microbiol. 72, 3175–3183. https://doi.org/10.1128/AEM.72.5.3175-3183.2006

Clarke, K., Gorley, R., 2006. PRIMER v6: User Manual/Tutorial. Plymouth, UK.

Committee on the Evaluation of the Use of Chemical Dispersants in Oil Spill Response, Ocean Studies Board, Board on Environmental Studies and Toxicology, Division on Earth and Life Studies, National Academies of Sciences, Engineering, and Medicine, 2020. The Use of Dispersants in Marine Oil Spill Response. National Academies Press, Washington, D.C. https://doi.org/10.17226/25161

De Wit, P., Pespeni, M.H., Ladner, J.T., Barshis, D.J., Seneca, F., Jaris, H., Therkildsen, N.O., Morikawa, M., Palumbi, S.R., 2012. The simple fool's guide to population genomics via RNA-Seq: an introduction to high-throughput sequencing data analysis. Mol Ecol Resour 12, 1058–1067. https://doi.org/10.1111/1755-0998.12003

Edwards, B.R., Reddy, C.M., Camilli, R., Carmichael, C.A., Longnecker, K., Van Mooy, B.A.S., 2011. Rapid microbial respiration of oil from the *Deepwater Horizon* spill in offshore surface waters of the Gulf of Mexico. Environ. Res. Lett. 6, 035301. https://doi.org/10.1088/1748-9326/6/3/035301

Gertler, C., Gerdts, G., Timmis, K.N., Yakimov, M.M., Golyshin, P.N., 2009. Populations of heavy fuel oil-degrading marine microbial community in presence of oil sorbent materials. Journal of Applied Microbiology 107, 590–605. https://doi.org/10.1111/j.1365-2672.2009.04245.x

Ghoul, M., Mitri, S., 2016. The Ecology and Evolution of Microbial Competition. Trends in Microbiology 24, 833–845. https://doi.org/10.1016/j.tim.2016.06.011

Hamdan, L., Fulmer, P., 2011. Effects of COREXIT® EC9500A on bacteria from a beach oiled by the Deepwater Horizon spill. Aquat. Microb. Ecol. 63, 101–109. https://doi.org/10.3354/ame01482

Harrison, S., 2017. Lessons from the Taylor Energy oil spill: history, seasonality, and nutrient limitation. University of Georgia, Athens, GA, USA.

Hasan, N.A., Young, B.A., Minard-Smith, A.T., Saeed, K., Li, H., Heizer, E.M., McMillan, N.J., Isom, R., Abdullah, A.S., Bornman, D.M., Faith, S.A., Choi, S.Y., Dickens, M.L., Cebula, T.A., Colwell, R.R., 2014. Microbial Community Profiling of Human Saliva Using Shotgun Metagenomic Sequencing. PLoS ONE 9, e97699. https://doi.org/10.1371/journal.pone.0097699

Huang, Y., Gilna, P., Li, W., 2009. Identification of ribosomal RNA genes in metagenomic fragments. Bioinformatics 25, 1338–1340. https://doi.org/10.1093/bioinformatics/btp161

Hyatt, D., Chen, G.-L., LoCascio, P.F., Land, M.L., Larimer, F.W., Hauser, L.J., 2010. Prodigal: prokaryotic gene recognition and translation initiation site identification. BMC Bioinformatics 11, 1–11. https://doi.org/10.1186/1471-2105-11-119

Johansen, C., Macelloni, L., Natter, M., Silva, M., Woosley, M., Woolsey, A., Diercks, A.R., Hill, J., Viso, R., Marty, E., Lobodin, V.V., Shedd, W., Joye, S.B., MacDonald, I.R.,

2020. Hydrocarbon migration pathway and methane budget for a Gulf of Mexico natural seep site: Green Canyon 600. Earth and Planetary Science Letters 545, 116411. https://doi.org/10.1016/j.epsl.2020.116411

Joye, S., Kleindienst, S., Peña-Montenegro, T.D., 2018. SnapShot: Microbial Hydrocarbon Bioremediation. Cell 172, 1336-1336.e1. https://doi.org/10.1016/j.cell.2018.02.059

Joye, S., Kostka, J.E., 2020. Microbial Genomics of the Global Ocean System: Report on an American Academy of Microbiology (Academy), The American Geophysical Union (AGU), and The Gulf of Mexico Research Initiative (GoMRI) Colloquium held on 9 and 10 April 2019. American Society for Microbiology. https://doi.org/10.1128/AAMCol.Apr.2019

Joye, S.B., 2020. The Geology and Biogeochemistry of Hydrocarbon Seeps. Annu. Rev. Earth Planet. Sci. 48, 205–231. https://doi.org/10.1146/annurev-earth-063016-020052

Joye, S.B., Teske, A.P., Kostka, J.E., 2014. Microbial Dynamics Following the Macondo Oil Well Blowout across Gulf of Mexico Environments. BioScience 64, 766–777. https://doi.org/10.1093/biosci/biu121

Kirchman, D., 2001. Measuring bacterial biomass production and growth rates from leucine incorporation in natural aquatic environments, in: Methods in Microbiology. Elsevier, pp. 227–237. https://doi.org/10.1016/S0580-9517(01)30047-8

Kleindienst, S., Grim, S., Sogin, M., Bracco, A., Crespo-Medina, M., Joye, S.B., 2016. Diverse, rare microbial taxa responded to the Deepwater Horizon deep-sea hydrocarbon plume. ISME J 10, 400–415. https://doi.org/10.1038/ismej.2015.121

Kleindienst, S., Paul, J.H., Joye, S.B., 2015a. Using dispersants after oil spills: impacts on the composition and activity of microbial communities. Nat Rev Microbiol 13, 388–396. https://doi.org/10.1038/nrmicro3452

Kleindienst, S., Seidel, M., Ziervogel, K., Grim, S., Loftis, K., Harrison, S., Malkin, S.Y., Perkins, M.J., Field, J., Sogin, M.L., Dittmar, T., Passow, U., Medeiros, P.M., Joye, S.B., 2015b. Chemical dispersants can suppress the activity of natural oil-degrading microorganisms. Proceedings of the National Academy of Sciences 112, 14900–14905. https://doi.org/10.1073/pnas.1507380112

Kostka, J.E., Prakash, O., Overholt, W.A., Green, S.J., Freyer, G., Canion, A., Delgardio, J., Norton, N., Hazen, T.C., Huettel, M., 2011. Hydrocarbon-Degrading Bacteria and the Bacterial Community Response in Gulf of Mexico Beach Sands Impacted by the Deepwater Horizon Oil Spill. Appl. Environ. Microbiol. 77, 7962–7974. https://doi.org/10.1128/AEM.05402-11

Li, D., Liu, C.-M., Luo, R., Sadakane, K., Lam, T.-W., 2015. MEGAHIT: an ultra-fast single-node solution for large and complex metagenomics assembly via succinct de Bruijn graph. Bioinformatics 31, 1674–1676. https://doi.org/10.1093/bioinformatics/btv033

Liu, Z., Liu, J., 2013. Evaluating bacterial community structures in oil collected from the sea surface and sediment in the northern Gulf of Mexico after the *Deepwater Horizon* oil spill. MicrobiologyOpen 2, 492–504. https://doi.org/10.1002/mbo3.89

Malkin, S.Y., Saxton, M.A., Harrison, S., Sweet, J., Passow, U., Joye, S.B., 2021. Remarkable variability in microbial hydrocarbon oxidation rates in offshore surface waters of the Gulf of Mexico. Journal of Marine Science and Engineering. https://doi.org/in revision

Mas-Lladó, M., Piña-Villalonga, J.M., Brunet-Galmés, I., Nogales, B., Bosch, R., 2014. Draft Genome Sequences of Two Isolates of the Roseobacter Group, Sulfitobacter sp. Strains 3SOLIMAR09 and 1FIGIMAR09, from Harbors of Mallorca Island (Mediterranean Sea). Genome Announcements 2, e00350-14, 2/3/e00350-14. https://doi.org/10.1128/genomeA.00350-14

McFarlin, K.M., Prince, R.C., Perkins, R., Leigh, M.B., 2014. Biodegradation of Dispersed Oil in Arctic Seawater at -1°C. PLoS ONE 9, e84297. https://doi.org/10.1371/journal.pone.0084297

Miller, C.S., Baker, B.J., Thomas, B.C., Singer, S.W., Banfield, J.F., 2011. EMIRGE: reconstruction of full-length ribosomal genes from microbial community short read sequencing data. Genome Biology 12, R44. https://doi.org/10.1186/gb-2011-12-5-r44

Narayan, N.R., Weinmaier, T., Laserna-Mendieta, E.J., Claesson, M.J., Shanahan, F., Dabbagh, K., Iwai, S., DeSantis, T.Z., 2020. Piphillin predicts metagenomic composition and dynamics from DADA2-corrected 16S rDNA sequences. BMC Genomics 21, 56. https://doi.org/10.1186/s12864-019-6427-1

Ni, B., Colin, R., Link, H., Endres, R.G., Sourjik, V., 2020. Growth-rate dependent resource investment in bacterial motile behavior quantitatively follows potential benefit of chemotaxis. Proc Natl Acad Sci USA 117, 595–601. https://doi.org/10.1073/pnas.1910849117

Parada, A.E., Needham, D.M., Fuhrman, J.A., 2016. Every base matters: assessing small subunit rRNA primers for marine microbiomes with mock communities, time series and global field samples: Primers for marine microbiome studies. Environ Microbiol 18, 1403–1414. https://doi.org/10.1111/1462-2920.13023

Parks, D.H., Tyson, G.W., Hugenholtz, P., Beiko, R.G., 2014. STAMP: statistical analysis of taxonomic and functional profiles. Bioinformatics 30, 3123–3124. https://doi.org/10.1093/bioinformatics/btu494

Peña-Montenegro, T.D., Kleindienst, S., Allen, A.E., Eren, A.M., McCrow, J.P., Sánchez-Calderón, J.D., Arnold, J., Joye, S.B., 2020. *Colwellia* and *Marinobacter* metapangenomes reveal species-specific responses to oil and dispersant exposure in deepsea microbial communities (preprint). Microbiology. https://doi.org/10.1101/2020.09.28.317438

Place, B.J., Perkins, M.J., Sinclair, E., Barsamian, A.L., Blakemore, P.R., Field, J.A., 2016. Trace analysis of surfactants in Corexit oil dispersant formulations and seawater. Deep Sea Research Part II: Topical Studies in Oceanography 129, 273–281. https://doi.org/10.1016/j.dsr2.2014.01.015

Pomeroy, L.R., Sheldon, J.E., Sheldon, W.M., Peters, F., 1995. Limits to growth and respiration of bacterioplankton in the Gulf of Mexico. Marine Ecology Progress Series 117, 259–268.

Quast, C., Pruesse, E., Yilmaz, P., Gerken, J., Schweer, T., Yarza, P., Peplies, J., Glöckner, F.O., 2012. The SILVA ribosomal RNA gene database project: improved data processing and web-based tools. Nucleic Acids Research 41, D590–D596. https://doi.org/10.1093/nar/gks1219

Redmond, M.C., Valentine, D.L., 2012. Natural gas and temperature structured a microbial community response to the Deepwater Horizon oil spill. Proceedings of the National Academy of Sciences 109, 20292–20297. https://doi.org/10.1073/pnas.1108756108

Ryther, J.H., Dunstan, W.M., 1971. Nitrogen, Phosphorus, and Eutrophication in the Coastal Marine Environment. Science 171, 1008–1013. https://doi.org/10.1126/science.171.3975.1008

Salinas-Martínez, A., de los Santos-Córdova, M., Soto-Cruz, O., Delgado, E., Pérez-Andrade, H., Háuad-Marroquín, L.A., Medrano-Roldán, H., 2008. Development of a bioremediation process by biostimulation of native microbial consortium through the heap leaching technique. Journal of Environmental Management 88, 115–119. https://doi.org/10.1016/j.jenvman.2007.01.038

Seidel, M., Kleindienst, S., Dittmar, T., Joye, S.B., Medeiros, P.M., 2016. Biodegradation of crude oil and dispersants in deep seawater from the Gulf of Mexico: Insights from ultra-high resolution mass spectrometry. Deep Sea Research Part II: Topical Studies in Oceanography 129, 108–118. https://doi.org/10.1016/j.dsr2.2015.05.012

Sexton, D.J., Schuster, M., 2017. Nutrient limitation determines the fitness of cheaters in bacterial siderophore cooperation. Nat Commun 8, 230. https://doi.org/10.1038/s41467-017-00222-2

Shepard, C.G., 2019. Nutrient availability modulates the effects of Corexit 9500A on oil biodegradation. University of Georgia, Athens, GA, USA.

Sibert, R., Harrison, S., Joye, S.B., 2016. Protocols for Radiotracer Estimation of Primary Hydrocarbon Oxidation in Oxygenated Seawater, in: McGenity, T.J., Timmis, K.N., Nogales, B. (Eds.), Hydrocarbon and Lipid Microbiology Protocols, Springer Protocols Handbooks. Springer Berlin Heidelberg, Berlin, Heidelberg, pp. 263–276. https://doi.org/10.1007/8623_2016_227

Smith, D.C., Farooq, A., 1992. A simple, economical method for measuring bacterial protein synthesis rates in seawater using 3H-leucine. Mar. Microb. Food Webs 6, 107–114.

Solórzano, L., 1969. Determination of ammonia in natural waters by phenolhypochlorite method. Limnol. Oceanogr. 14, 799–801. https://doi.org/10.4319/lo.1969.14.5.0799

Solórzano, L., Sharp, J.H., 1980. Determination of total dissolved phosphorus and particulate phosphorus in natural waters1. Limnol. Oceanogr. 25, 754–758. https://doi.org/10.4319/lo.1980.25.4.0754

Techtmann, S.M., Zhuang, M., Campo, P., Holder, E., Elk, M., Hazen, T.C., Conmy, R., Santo Domingo, J.W., 2017. Corexit 9500 enhances oil biodegradation and changes active bacterial community structure of oil-enriched microcosms. Appl Environ Microbiol 83, e03462-16, e03462-16. https://doi.org/10.1128/AEM.03462-16

Tully, B., 2015. Detecting 16S rRNA Gene Fragments from a Metagenome to Assemble Full-Length 16S Sequences v1. https://doi.org/10.17504/protocols.io.d7u9nv

Warr, L.N., Friese, A., Schwarz, F., Schauer, F., Portier, R.J., Basirico, L.M., Olson, G.M., 2013. Bioremediating Oil Spills in Nutrient Poor Ocean Waters Using Fertilized Clay Mineral Flakes: Some Experimental Constraints. Biotechnology Research International 2013, 1–9. https://doi.org/10.1155/2013/704806

Yu, S., Li, S., Tang, Y., Wu, X., 2011. Succession of bacterial community along with the removal of heavy crude oil pollutants by multiple biostimulation treatments in the Yellow River Delta, China. Journal of Environmental Sciences 23, 1533–1543. https://doi.org/10.1016/S1001-0742(10)60585-2

Zahed, M.A., Aziz, H.A., Isa, M.H., Mohajeri, L., Mohajeri, S., Kutty, S.R.M., 2011. Kinetic modeling and half life study on bioremediation of crude oil dispersed by Corexit 9500.

Journal of Hazardous Materials 185, 1027–1031. https://doi.org/10.1016/j.jhazmat.2010.10.009

Zhu, W., Lomsadze, A., Borodovsky, M., 2010. Ab initio gene identification in metagenomic sequences. Nucleic Acids Research 38, e132–e132. https://doi.org/10.1093/nar/gkq275

Zhuang, G., Peña-Montenegro, T.D., Montgomery, A., Hunter, K.S., Joye, S.B., 2018. Microbial metabolism of methanol and methylamine in the Gulf of Mexico: insight into marine carbon and nitrogen cycling. Environ Microbiol 20, 4543–4554. https://doi.org/10.1111/1462-2920.14406

CHAPTER 5

CONCLUSIONS AND FUTURE RESEARCH

4.1 Major Outcomes

The Deepwater Horizon oil spill was a tragic mark in history of the Gulf of Mexico. This study is part of a huge collective effort to understand better the underlying mechanisms by which the ocean endured to abrupt and unprecedented exposure to oil and dispersants. In the rise of application of massive sequencing of nucleic acids, we explored approaches to better understand the complexity of the microbial world and their surrounding responses. The main conclusions of this study are summarized in the following paragraphs.

Environmental perturbations through the lens of DEM-pangenomes

The creating of DEM-pangenomes (**Chapter 2)** allowed us to explore distinct ecotypes thriving under complex oil-infused conditions. The DEM-pangenome approach provides valuable insight to the complex interactions between the microbial communities and their surrounding environment that occur in response to perturbation. This study confirmed the hypothesis of Goyal (2018) that accessory genome components promote response and adaptability in microbial populations.

Chapter 2 stemmed from the work of Kleindienst et al., (2015) that aimed to mimic the observed geochemistry reported in the DWH oil spill, including conditions under the exposure of oil, dispersants and nutrients. The application of DEM-pangenomes allowed identify a complex

suite of responses in *Colwellia* and *Marinobacter*, including unique aspects of their metabolic capabilities that explained treatment-specific abundance. Two very contrasting roles became evident for the two major microbial drivers of the Kleindienst et al. study. *Colwellia* exhibited an opportunistic response to organic carbon enrichment, while *Marinobacter* displayed a well-tuned response to oil pollution. Genomic and transcriptomic plasticity promoted the success of one versus the other across the treatment regime and underscores the role of generalist vs. specialist components of marine microbiomes, revealing how and why specific organisms respond to particular conditions through employment of metabolic cassettes associated with core versus accessory pangenomes.

Environmental perturbations through the lens of biosynthetic activities

In **Chapter 3** we explored the application and interpretation of LRD scores in the context of environmental perturbations. Our study provided valuable insights in the biological role of members of the microbial community based on the LRD score. This score is able to provide an quantifiable estimate to distinguish those microorganisms that are replicating faster than what they would synthesize fundamental biomolecules. Or vice versa, the biosynthetic rate is considerably larger than their replication rate. In this way, we were able to identify microorganisms that probably depended on difficult to digest molecules, which may have reduced their biosynthetic rate. For instance, in the LRD Group-I, with LRD>5, likely contained highly active microorganisms given the extreme enrichment of transcription read counts over 16S rRNA gene read counts. Methylotrophs (i.e., *Methylophaga, Methylobacter*) and native hydrocarbon degraders (i.e., *Bermanella,* and *Parvibaculum*) were affiliated with this group, consistent with previous reports of active indigenous oil degraders including members of these

genera (see Chapter 3). Methylophaga was also stimulated by the by-products of high molecular weight dissolved organic matter metabolism in seawater, suggesting that they are important components of aerobic microbial associations that play key roles in organic carbon turnover

In contrast, members of LRD Group-III were poorly adapted for the experimental conditions, relative to members of LRD Group-I and LRD Group-II. LRD Group-III included members of the family *Oceanospirillaceae,* such as *Amphritea, Pseudospirillum,* and *Balneatrix*, hydrocarbon degraders, including *Oleiphilus, Porticoccus, Cycloclasticus, Rhodobacteraceae, Rhodobiaceae,* and *Alteromonadaceae*, and members of *Flavobacteria, Bacteroidetes, Bdellovibrionaceae* and *Spongibacter* (see Chapter 3). Many hydrocarbon degraders are slow-growing in nature and membership in LRD Group-III could reflect time-sensitive, adaptive responses that occur in different groups of hydrocarbon degrading bacteria over longer time scales. This pattern may also reflect specific niche-adaptation strategies in hydrocarbon degrading microbial communities.

Environmental perturbations through the lens of viruses and phages

In Chapter 3, we also explored the role of megaviruses and jumbophages in a Gulf of Mexico microcosm setting under the exposure to oil and dispersants. Megaviruses are important regulators of the ciliate and flagellate populations that impart top-down control on microbial populations. As such, an intriguing possibility is that the stimulation of megaviruses in response to oil exposure could relax predation and allow populations of oil degraders to bloom in the absence of predation. We found that the majority of viral DE genes were upregulated in all of the amended treatments, WAF, dispersant, and CEWAF with and without nutrients. However, the viral repertoire completely shifted after the addition of nutrients. The inherent stress imposed on

the microbial community through nutrient limitation appears to have led to a more substantial viral-induced stress response in the CEWAF treatment, compared to the CEWAF+nutrient treatment. In conclusion, the absence of nutrients could have triggered stress-responses in the microbial communities, with a collateral effect on the activation of viral communities.

Environmental perturbations through the lens of differential exposure regimes

The evidence in the previous chapter not only suggested the potential role of nutrients but also the timing of exposure were essential for the microbial communities to find a niche and respond accordingly. **Chapter 4** builds on the work of Shepard (2019) and aimed to identify trends in the microbial succession and potential microbial responses to the subsequential exposure of WAF cocktails followed by bulk oil amendment. The results provided insights of microbial colonizers adapting to nutrients (i.e. *Marinobacter*), or the lack thereof (i.e. *Sulfitobacter*). The experiment provided valuable insights given the complex trends of utilization of nitrogen and carbon. In particular, the nutrient drawdown observations paired with significant microbial community shifts.

Finally, in Chapter 4 explored the functional metagenomic fingerprinting of the microbial communities in the experiment based on 16S amplicon sequencing data. Although further confirmation is needed, we were able to identify important ABC-transport, two-component systems and fatty acid β-oxidation signatures associated with treatments supplemented with nutrients.

4.2 Future research considerations

Several questions remain to be solved in future research endeavors. To mention some of them:

- Further exploration for the role of *Kordia* would be extremely interesting and valuable. Our results suggest that *Kordia* is able to outgrow other microbial competitors under dispersant exposure.
- More controlled experiments providing mechanistic insights of the regulation of Megaviruses and Jumbophages in microbial communities could help understand how interactive factors (nutrients vs. organic exposure) stimulate these important components of the mobilome. This is also linked with the very real challenge of maintaining microbial isolates stable in laboratory so we could perform adequate viral-host tests.
- The DEM-pangenome approach has tremendous promise for advancing the knowledge of how specific microorganisms respond to environmental perturbation, which is clearly a key challenge of the Anthropocene age.

4.3 References

Goyal, A. (2018). Metabolic adaptations underlying genome flexibility in prokaryotes. *PLOS Genetics*, *14*(10), e1007763. https://doi.org/10.1371/journal.pgen.1007763

Kleindienst, S., Seidel, M., Ziervogel, K., Grim, S., Loftis, K., Harrison, S., … Joye, S. B. (2015). Chemical dispersants can suppress the activity of natural oil-degrading microorganisms. *Proceedings of the National Academy of Sciences*, *112*(48), 14900–14905. https://doi.org/10.1073/pnas.1507380112

Shepard, C. G. (2019). *Nutrient availability modulates the effects of Corexit 9500A on oil biodegradation* (University of Georgia). University of Georgia, Athens, GA, USA. Retrieved from https://getd.libs.uga.edu/pdfs/shepard_cathrine_g_201908_ms.pdf